

A STUDY OF THE VIBRATIONAL CHARACTERISTICS  
OF TWO MULTISTORY BUILDINGS

Thesis by  
Douglas Allen Foutch

In Partial Fulfillment of the Requirements  
for the Degree of  
Doctor of Philosophy

California Institute of Technology  
Pasadena, California

1977

(Submitted September 20, 1976)

## ACKNOWLEDGMENTS

The author wishes to express his gratitude to his advisor, Professor P. C. Jennings, for his guidance and for his helpful suggestions provided throughout this investigation. The assistance provided by Professor G. W. Housner in obtaining permission for the tests of the Ralph M. Parsons Company World Headquarters building, and by Professor C. D. Babcock in providing suggestions regarding instrumentation is greatly appreciated.

The financial support provided by the California Institute of Technology in the form of teaching and research assistantships is appreciated. The partial support of this investigation by a grant from the National Science Foundation is acknowledged.

The author expresses his thanks to the Ralph M. Parsons Company for granting permission to test their World Headquarters building.

The assistance provided by Mr. Raul Relles in maintaining the instrumentation system and in conducting the tests is greatly appreciated. Gratitude is also extended to Mr. Albert Ting and Mr. Marty Cohen who provided assistance in conducting the tests and reducing data. The help of Mr. Donald Laird and the Mechanical Engineering Shop is also acknowledged.

Sincere thanks are given to Mrs. Henriette Wymar for her skillful typing of the manuscript.

The author extends his heartfelt appreciation to his wife,

Margaret. Without her love, her patience and her understanding, the completion of this goal would not have been possible.

## ABSTRACT

Forced vibration tests and associated analysis of two multistory buildings are described. In one case, the dynamic properties of the building measured during the tests are compared to those predicted by simple analytical models. A three-dimensional finite element model of the second building was constructed for the purpose of evaluating the accuracy of this type of analysis for predicting the observed dynamic properties of the structure.

Forced vibration tests were performed on Millikan Library, a nine-story reinforced concrete shear wall building. Measurements of three-dimensional motions of approximately 50 points on each of six floors (including the basement) were taken for excitation in the N-S and E-W directions. The results revealed a complex interaction between lateral and vertical load carrying systems in both directions. The results also suggest that a significant change in the foundation response of the structure occurred in the stiffer N-S direction during the San Fernando earthquake. This phenomenon was investigated through the use of two analytical models of the building which included the effects of soil-structure interaction.

The Ralph M. Parsons World Headquarters building, a twelve-story steel frame structure, was also tested. The natural frequencies, three-dimensional mode shapes, and damping coefficients of nine modes of vibration were determined. Other features of this investigation included the study of nonlinearities associated with increasing levels of response and the measurement of strain in one of the columns of the

structure during forced excitation. The dynamic characteristics of the building determined by these tests are compared to those predicted by a finite element model of the structure. The properties of primarily translational modes are predicted reasonably well; but adequate predictions of torsional motions were not obtained. The comparison between measured and predicted strains suggests that estimates of stress obtained from finite element analyses of buildings should be within 25 percent of those experienced by the structure for a known excitation.

## TABLE OF CONTENTS

<u>Part</u>	<u>Title</u>	<u>Page</u>
Acknowledgments		ii
Abstract		iv
Chapter I	Introduction	1
Chapter II	Instrumentation and Data Reduction Procedures for Full-Scale Tests of Multistory Buildings	8
2.1	Motion Sensing Transducers	8
2.2	Signal Conditioning and Recording	10
2.3	Force Generating Systems	13
Chapter III	Three-Dimensional Deformation of a Nine-Story Reinforced Concrete Building During Forced Excitation	20
3.1	Description of the Building and Experimental Procedures	20
3.2	Presentation and Discussion of Results	23
3.3	Conclusions	35
Chapter IV	The Use of Simple Models as an Aid to Interpreting Experimental Results	37
4.1	An Euler Beam Model of the Millikan Library Building	38
4.2	A Lumped Parameter Model of the Millikan Library Building	44
4.3	An Additional Investigation of the Observed Changes in the Dynamic Characteristics of the Millikan Library Building	56
4.4	Conclusions	58

<u>Part</u>	<u>Title</u>	<u>Page</u>
Chapter V	Forced Vibration Tests of the Ralph M. Parsons Company World Headquarters Building	61
5.1	Description of the Building	61
5.2	Preliminary Tests	69
5.3	Natural Frequencies, Mode Shapes and Damping	78
5.4	Three-Dimensional Motion of Three Floors and the Surrounding Ground	93
5.5	Measurement of Strain in the Moment Resisting Frame	119
5.6	Investigation of Apparent Nonlinearities in the Dynamic Response of the Parsons Building	125
5.7	A Study of the Response of the Parsons Building to Ambient Excitation	136
5.8	Conclusions	147
Chapter VI	Dynamic Characteristics of the Parsons Building Predicted by a Finite Element Model	151
6.1	Description of the Model	151
6.2	Computed Natural Frequencies and Mode Shapes for the Model of the Parsons Building	158
6.3	Comparison of Measured and Computed Responses	169
6.4	Conclusions	174
Chapter VII	Summary and Conclusions	176
References		

<u>Part</u>	<u>Title</u>	<u>Page</u>
Appendix A	Enlarged Figures Showing Floor Deformations Measured During Forced Vibration Tests of Millikan Library	192

## CHAPTER I

## Introduction

The analysis of stress and deformation in structures such as buildings, bridges and dams is often accomplished by constructing and analyzing a mathematical model of the structure. These models are based on the behavior of individual members such as beams, columns, plates and walls and on the assumed combined behavior of these elements as a structural system. Consequently, the reliability of these analyses is largely dependent on the engineer's ability to model complex structural systems. To improve this reliability, engineers have performed numerous experiments to determine the elastic and post-yield behavior of individual elements as well as a more limited number of tests on full-scale structures. As a result, much is known about the static and dynamic behavior of structural components; but the knowledge of the behavior of complete structures is in a less advanced state.

In the past 15 years the tools for modeling and analysis that are available to the structural engineer have increased rapidly. This is due to the expanding technology of digital computers, coupled with the advancement of the state-of-the-art of the finite element method of analyzing structures. One consequence of this rapid development of tools for analysis, however, is that the experimental verification of assumptions commonly used in applying these methods to structures has lagged behind their application in engineering decision making.

Although extensive experimental programs have been performed to determine the behavior of structural components, only a small number of studies have been undertaken to test the assumptions regarding the behavior and interaction of these components when they are combined to form a structural system. Several studies of the dynamic behavior of planar models of structural systems have been completed using shake tables in recent years. Since these tests are performed in a laboratory, a high degree of control is maintained over the loadings applied to these models and a large number of detailed measurements may be taken. Much of our knowledge of the dynamic post-yield behavior of structures is the direct result of these tests. While these tests have provided valuable information, they are limited by the size and composition of test specimens that can be accommodated. The test structures do not contain the so-called nonstructural members which may play a significant role in the overall behavior of a real structure; they do not possess the three-dimensional dynamic characteristics of a real structure, which may be critical for understanding its behavior during dynamic excitations; nor do they rest on a deformable foundation which may also influence the behavior of the system. These properties may only be studied through field tests of full-scale structures.

The need for full-scale testing has long been recognized and vibration studies have been performed on multistory buildings in the United States for over 40 years.<sup>10</sup> The earliest of these studies depended on the environmental forces such as wind and microseismic

waves to induce motion in multistory buildings. This method of testing has also been used in recent years,<sup>17, 60, 64, 67</sup> as well, because it is easily implemented and because the development of the fast Fourier transform greatly facilitated the analyses of the recorded motions. The scope of these tests is limited, however, since the investigator has no control of the magnitude, duration, or frequency content of the exciting forces.

In the mid-1930's, forced vibration generators were developed to give investigators more control over the forces applied to the structure being tested.<sup>3, 4, 6</sup> These generators provided for the first detailed studies of the dynamic properties such as natural frequencies, mode shapes and damping. However, due to the lack of a good speed control system for the shakers, results of some of these earlier studies were misleading.

The development of a vibration generation system with adequate speed control was undertaken in the early 1960's. Since its development, most investigators have studied in detail the dynamic characteristics of such structures as dams,<sup>37, 57</sup> nuclear reactors<sup>30, 46, 47, 58</sup> and multistory buildings.<sup>7, 13, 14, 34, 49, 53, 54, 59</sup> As would be expected, many of these experiments were performed in conjunction with analytical studies of the structures being tested.

Even though these tests were performed with the idea of verifying mathematical models of the structures, many of the investigations were limited in scope because of the simplicity of the analytical models that were employed. In the analysis of multistory buildings, for example,

it is common practice to use planar idealizations of the structure to analyze its response to dynamic excitations. Consequently, many of the previous tests of multistory buildings investigated only the unilateral mode shapes and associated frequencies of vibration. Whereas this particular assumption is satisfactory for a limited number of buildings, it certainly is not realistic for many others.

To advance the state of the art in this field, an extensive series of forced vibration tests of two multistory buildings has been conducted by this investigator over the past three years. One purpose of these studies was to broaden the scope of the full-scale forced vibration tests. This goal was accomplished through the development of new experimental procedures and through the improved deployment and orientation of the motion-sensing transducers. Also, the use of an improved instrumentation system was an integral part of the testing program. Results of these studies revealed that much more information may be obtained about the three-dimensional dynamic behavior of multistory buildings than has been sought in previous tests.

Another purpose of this study was to investigate some of the common assumptions concerning the dynamic behavior of buildings made in their analysis for design. Of particular interest to this investigator was the phenomenon of torsional motions in buildings. The significance of these torsional motions is that larger than expected stresses may be induced in the structural elements at the periphery of the building. Torsional response is usually considered only in an approximate, empirical manner in the design of buildings. In a

nominally symmetric structure, for example, only planar analytical models are derived for the building and torsional response is approximated by applying a static force eccentrically to the structural frame. Torsional motions may be induced in such a structure, however, by purely unilateral excitations. This occurs because of modal coupling and modal interference.

Modal coupling occurs in a single mode when the centers of mass and centers of rigidity of the floors of a building do not coincide. Thus, when inertial loads are applied through the centers of mass, a torque results about the center of rigidity. Thus a mode which is primarily translational can include significant rotational motions as well. Modal interference involves the interaction of two modes whose frequencies of vibration are close together. If a torsional mode has a component of motion in the direction of a translational mode which is being excited, the torsional mode will also be excited if their frequencies lie close together. Also, if a torque is produced by the vibration of the translational mode, the torsional mode will be excited. Consequently, modal interference can occur in symmetrical, as well as nonsymmetrical, structures. These phenomena have been previously studied both experimentally<sup>34</sup> and analytically.<sup>25, 64</sup>

A final goal of this investigation was to establish a procedure whereby the reliability of current modeling practices to predict stresses in structural members for a given excitation could be evaluated. This involved the measurement of strain in a column of a building during forced excitation. Attempts have been made to assess

the reliability of finite element models of structures based on recorded ground motion and on the resulting response of these structures during earthquakes.<sup>56</sup> These studies provided some valuable lessons to designers;<sup>19</sup> but, since they were based only on recorded accelerations, knowledge of the actual stresses in the members was lacking. The knowledge of the member strains for a given configuration of floor displacements is essential if the accuracy of finite element models is to be studied thoroughly.

To summarize, the aims of this investigation were to expand the state-of-the-art of forced vibration testing of full-scale structures, to investigate the adequacy of the assumptions concerning the overall dynamic behavior of multistory buildings which are commonly employed in their analysis for design, and to attempt to assess the reliability of estimates of stresses in structural members predicted by finite element models of the structure.

A brief summary of the contents of each chapter follows:

A description of the instrumentation used for forced vibration tests of structures is presented in Chapter II. This improved instrumentation system greatly facilitated the accomplishment of the detailed measurements taken during these tests.

The results of forced vibration tests of Millikan Library, a nine-story reinforced concrete structure, are presented in Chapter III. Measurements of the three-dimensional deformations of the floor slabs of the building (including the basement) provided insight into the significance of coupling of lateral and vertical load carrying systems and

the significance of soil deformations on the dynamic response of this structure.

A surprising result of the Millikan Library test was the apparent change that occurred in the foundation compliance of the structure as a result of the San Fernando earthquake. In Chapter IV, an Euler beam model with translational and rotational springs at the base is used as an aid to interpreting these results. A simple lumped mass model which accounted for the shear deformations in the structure is also employed in this investigation. Also presented is an analytical procedure emphasizing simplified ideas in mechanics and minimal computational effort which may be employed in the analysis of some multistory buildings.

In Chapter V, results of forced vibration tests of the Parsons building, a twelve-story steel frame building, are presented. Dynamic properties of the building that were studied in detail include natural frequencies, three-dimensional mode shapes and damping; modal coupling and modal interference; apparent nonlinearities associated with increasing levels of response; and strain levels in a column of the structure during forced excitations.

In Chapter VI, a finite element model of the Parsons building is presented and discussed. The analysis is accomplished using SAP IV, a general purpose finite element code used by many engineers. The dynamic properties measured for the building are compared to those predicted by the model; and the difference between the analytical and experimental results are discussed.

## CHAPTER II

Instrumentation and Data Reduction Procedures  
For Full-Scale Tests of Multistory Buildings

A description of the instrumentation and data reduction procedures used during the full-scale tests of the Millikan Library building and the Parsons building is presented in this chapter. The instrumentation and data reduction procedures were similar for both tests with only minor differences which will be pointed out in the text.

2.1 Motion Sensing Transducers

The majority of the measurements taken during the tests utilized up to twelve Model SS-1 Ranger seismometers made by Kinematics of San Gabriel, California, as the motion sensing transducers. The Ranger is a spring-mass system in which a permanent magnet is the seismic mass. The magnet travels within a coil attached to the frame of the seismometer. The changing magnetic flux caused by the motion of the magnet induces a voltage in the coil proportional to the velocity of the mass. The instrument has a nominal natural period of one second. A potentiometer in parallel with the coil provides adjustable damping ranging from nearly zero percent to above critical for the seismometer. The damping was set above critical for all of the forced vibration tests to avoid overdriving the amplifiers.

Due to the difficulty of making absolute calibrations of the velocity sensing Rangers in the field, they were used only to measure

relative motion and phase between points. Two 0.25 g Statham accelerometers with a Brush model 13 4212 02 carrier preamplifier were used to measure absolute motions. The natural frequency of this transducer is about 400 Hz and the damping about 0.7 of critical. Absolute calibration of an accelerometer is easily accomplished by tilting it a known angle in the earth's gravitational field.<sup>38</sup>

The vast majority of the measurements taken during forced vibration tests are used to determine the relative motion between two points. The Ranger seismometers were chosen as the principal transducers for these tests because their high output and their high signal-to-noise ratio facilitates the accurate measurement of both amplitudes and relative phases. Errors of most measurements made with the Rangers are within 3 percent to 6 percent; whereas the error of similar measurements made with a Statham can approach 10 percent or higher.

One difficulty is encountered with the use of the Rangers, however, that is not a problem with the Stathams. Since the natural periods of the Rangers are in the range of measured frequencies and since the natural period and damping is different for each instrument, the transfer functions of the instruments are not identical. Consequently, relative calibrations must be performed at all of the frequencies of interest. To accomplish this the instruments are aligned side by side in the same direction, the building is excited at a known frequency, and then the outputs of all of the Rangers are measured. In this manner the differences in output between transducers for a

particular frequency may be determined. Figure 2.1 shows a typical calibration set-up.

## 2.2 Signal Conditioning and Recording

The signal conditioning system which is used with the Ranger seismometers serves several purposes. A model SC-201 A signal conditioner made by Earth Sciences Division of Teledyne was used during the tests of Millikan Library. This provides amplification of approximately 350,000 as well as independent integration and differentiation of up to four input signals. Consequently, output signals proportional to displacement and acceleration are available. This is a useful feature when taking ambient measurements. The displacement circuit may be used to study the fundamental mode since this signal will accentuate the lower frequencies of the motion. The velocity or acceleration circuits may be used to measure the motion due to higher modes since these will enhance the higher frequencies and diminish the lower frequencies.

Two four-channel Kinometrics model SC-1 signal conditioners were used during the tests of the Parsons building. These are similar to the Teledyne model but have a gain of 100,000. They also provide optional low-pass filters which are continuously adjustable between 1 and 100 Hz. This feature is useful during ambient studies where it can be used to diminish the presence of high-frequency noise in the signal. The SC-201 A signal conditioner is shown in Figure 2.2 and the SC-1 signal conditioners are shown in Figure 2.1.

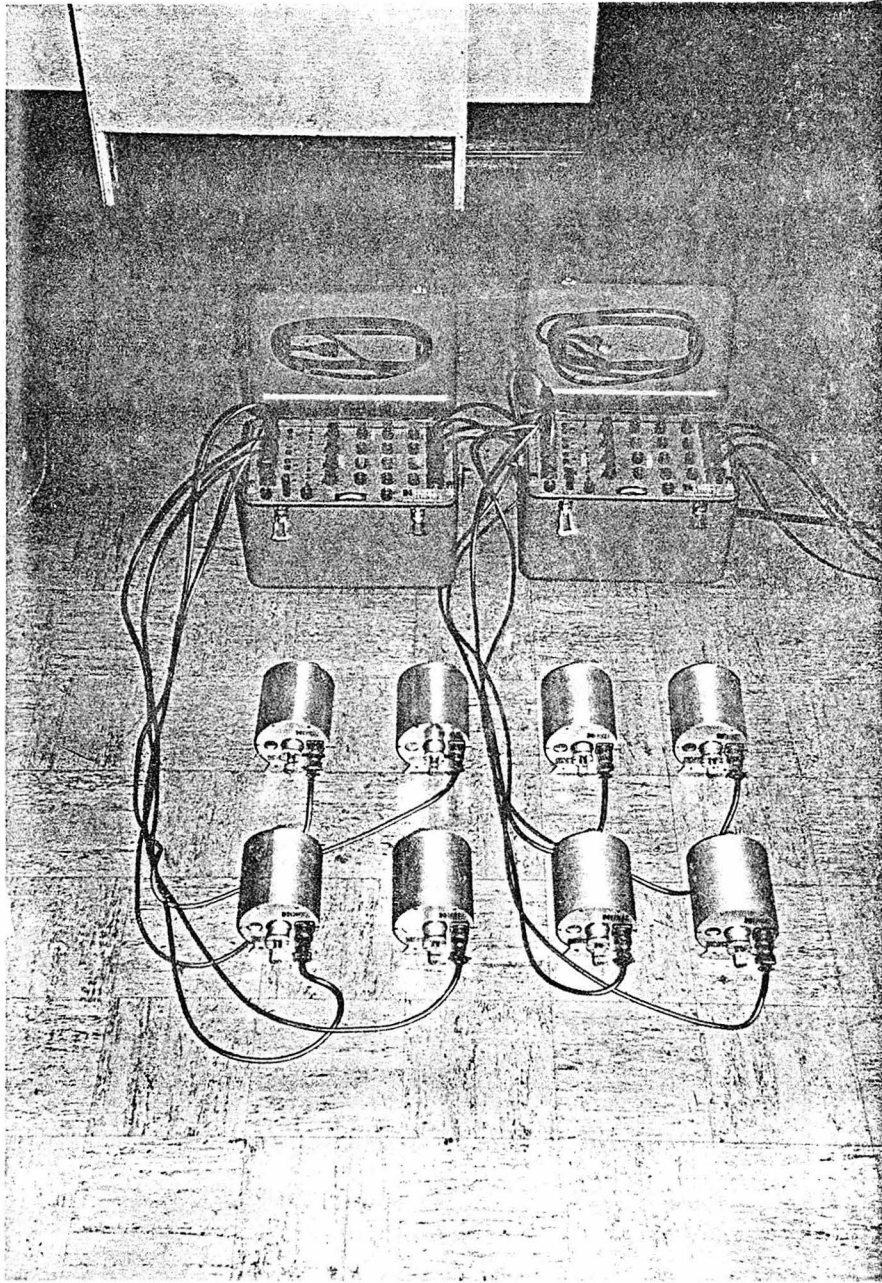


Figure 2.1 Typical calibration set-up for Ranger seismometers.

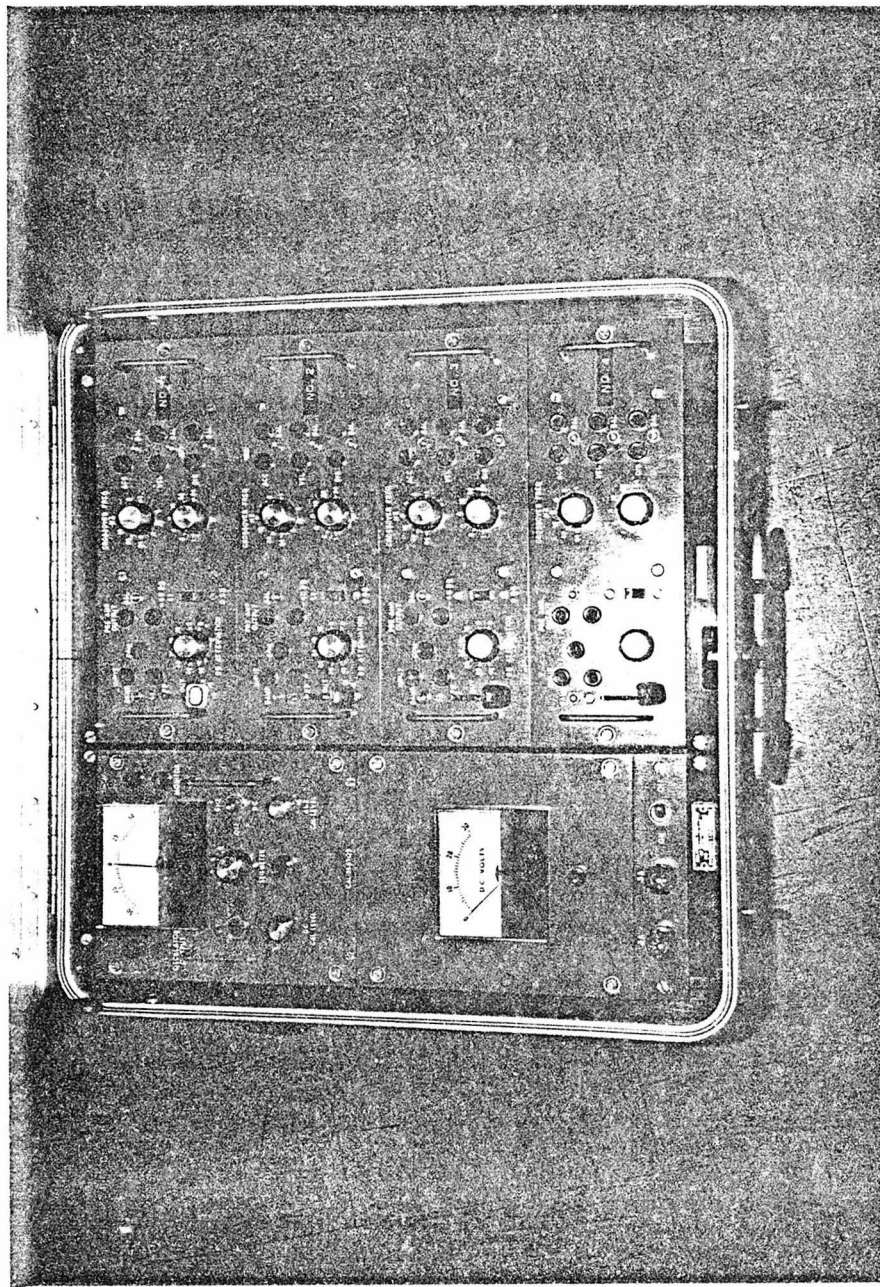


Figure 2.2 SC-201 A Signal conditioner used during Millikan Library tests.

During the Millikan tests, signals from the Rangers were recorded on two Brush Mark 220 two-channel strip chart recorders. The measurements taken during the Parsons tests were recorded on an eight-channel Hewlett-Packard Model 7418A thermal tip recorder equipped with seven 8802 A DC preamplifiers and one 8805 A carrier preamplifier. The latter item was installed for use with a Statham accelerometer. The Hewlett-Packard system was found to be the superior of the two because it provided a cleaner, more readable trace and allowed twice as many simultaneous recordings.

For each measurement, the sensitivities of the recorders were adjusted so that the amplitude of the trace was as large as possible. The resulting double amplitudes may be read to within  $\frac{1}{2}$  of a division. Sample traces from the Hewlett-Packard recorder are shown in Figure 2.3.

During low-level ambient tests, signals from the Ranger seismometers were recorded on two four-channel Hewlett-Packard 3960 instrumentation tape recorders. These tapes were then taken to the lab where the recorded analog signals were digitized using a Kinematics model DDS-101 analog-to-digital converter. Details concerning sampling rate and filtering will be discussed in a later chapter.

### 2.3 Force Generating Systems

The vibration generating system used for the forced vibration tests of Millikan Library was one of the original four units designed and developed approximately 15 years ago at the California Institute of Technology. Briefly, the force generating mechanism consists of

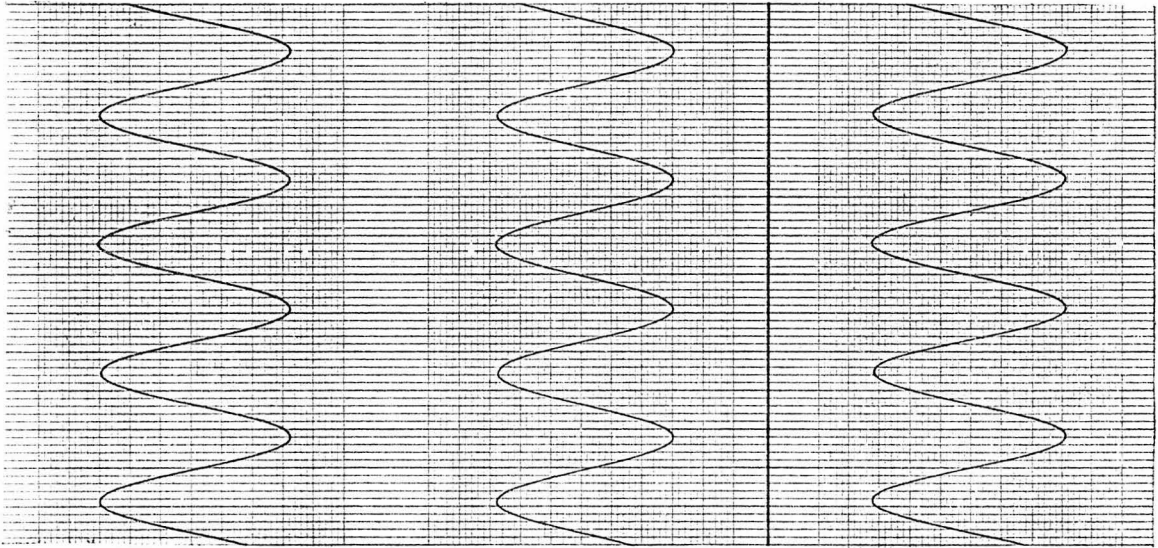


Figure 2.3 Sample traces from Hewlett-Packard recorder made during forced vibration tests of the Parsons building.

counter-rotating baskets which may be loaded with a variable number of lead weights. The resulting sinusoidal force may be aligned in any fixed direction. This was the first design that incorporated an accurate speed control system. The rotational speeds are adjustable to within 0.1 percent. A more detailed description of the system is given by Hudson.<sup>28</sup>

A model VG-1 vibrational generation system designed by Kinometrics was used for tests of the Parsons building. This system has two mechanical shakers which are nearly identical, mechanically, to the ones designed at Caltech. The control consoles, however, are a new design utilizing solid state control circuits. One console is provided for each shaker. The consoles differ only in that one may be used as a master unit in a master-slave set-up. In this case the shakers are run simultaneously at the same frequency. Improved features of this system include: 1) relative ease of operation in the master-slave arrangement; 2) continuous adjustment of the relative phase (accurate to  $\pm 1.25$  degrees) of the forces generated by the two shakers when they are run simultaneously; 3) a  $0^\circ$ - $180^\circ$  switch for easy adjustment of the relative phase between the forces when torsional excitation is required; and 4) digital display of the exciting frequency accurate to  $\pm 0.001$  Hz. Figure 2.4 shows the front panel of the master console of the VG-1 system with the mechanical shaker in the background.

For both vibration generating systems, the force produced is proportional to the square of the exciting frequency. The maximum frequency of about 9.5 HZ is limited by the stress in the shakers.

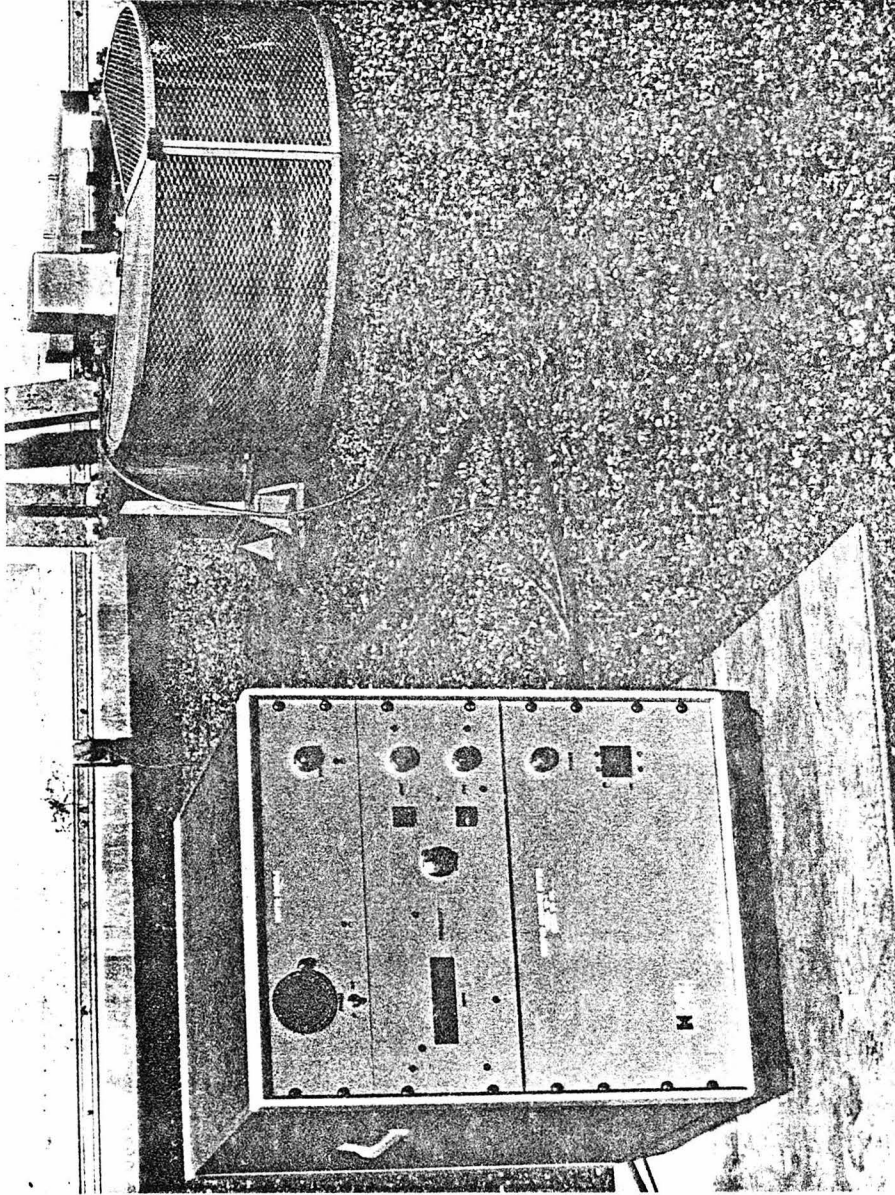


Figure 2.4 Master control console of VG-1 vibration generating system with shaker in the background.

The force generated by each shaker is obtained by the equation

$$\text{FORCE} = 0.102 \times (\text{WR}) \times f^2 \text{ lbs.}, \quad (2.1)$$

where  $f$  is the exciting frequency in Hz, and WR is a constant depending on the combination of weights in the baskets. Table 2.1 lists the values of WR for various combinations of weights and Table 2.2 gives the maximum allowable frequency for these weight combinations.

These tables were taken from the instruction manual for the VG-1 system.<sup>39</sup>

Slight variations in the procedures and some additional specialized instrumentation were required for certain of the Millikan and Parsons tests. These will be discussed, as they occur, in the following chapters.

Table 2.1 - "WR" (Lb-In) for Each Weight Combination

		Small Weights				
		0	S1	S2	S3	S4
Large Weights	0	520	947	1374	1801	2228
	L1	1935	2362	2789	3216	3643
	L2	3350	3777	4204	4631	5058
	L3	4765	5192	5619	6046	6473
	L4	6180	6607	7034	7461	7888

$$\text{FORCE} = 0.102 \times (\text{WR}) \times f^2$$

f = frequency (Hz)

(WR) is in "Lb-In"

FORCE is in "Lb"

S = small weight (center section)

L = large weight (side section)

The number (1, 2, 3, or 4) following "S" or "L" indicates the number of weights of that size placed in each section of that size in each weight bucket.

Table 2.2 - Maximum Frequency (Hz) for Each Weight Combination

		Small Weights				
		0	S1	S2	S3	S4
Large Weights	0	9.7	7.2	6.0	5.2	4.7
	L1	5.0	4.6	4.2	3.9	3.7
	L2	3.8	3.6	3.4	3.3	3.1
	L3	3.2	3.1	3.0	2.8	2.8
	L4	2.8	2.7	2.6	2.6	2.5

S = small weight (center section)

L = large weight (side section)

The number (1, 2, 3, or 4) following "S" or "L" indicates the number of weights of that size placed in each section of that size in each weight bucket.

## CHAPTER III

Three-Dimensional Deformations of a Nine-Story Reinforced  
Concrete Building During Forced Excitations

Forced vibration tests of the nine-story reinforced concrete Millikan Library building were conducted between August and December 1974. The three-dimensional motion of approximately 50 points on each of six floors including the basement and at approximately 100 points on the ground surrounding the building was measured. The purpose of the tests was to ascertain the breadth of information that may be gained about the dynamic behavior of multistory buildings using forced vibration tests. The tests revealed a substantial amount of deformation of the floor slabs and interaction between horizontal and vertical load carrying members. The tests also indicated that the deformation of the soil had significant influence on the response of the building in the stiffer N-S direction. Results of these tests were reported in abbreviated form in reference 4.

3.1 Description of the Building and Experimental Procedures

The Robert A. Millikan Memorial Library is a nine-story reinforced concrete building located on the campus of the California Institute of Technology in Pasadena, California. Since its completion in 1966, the building has experienced three earthquakes (Borrego Mountain, 1968; Lytle Creek, 1970; and San Fernando, 1971) which were recorded by strong motion accelerographs located in the basement and on the roof of the structure. During and following its

construction, several tests and analyses have also been performed on the building.<sup>14,32,35,44,64,65</sup> The collection of all of these tests and analyses provides a valuable case study of a multistory building that has been subjected to dynamic loads of varying types and intensities.

The library building is  $69 \times 75$  feet in plan and stands 144 feet above grade and 158 feet above the basement level. This includes an enclosed roof on which elevator and air handling equipment are located. The majority of the lateral loads in the transverse (N-S) direction are resisted by 12-inch reinforced concrete walls of the central core which houses two elevators and an emergency stairway. The foundation system is composed of a central pad 32 feet wide by 4 feet deep that extends between the east and west curved shear walls. In addition to this, continuous foundation beams 10 feet wide by 2 feet deep run east-west beneath the columns at the north and south ends of the building. These are connected to the central pad by stepped beams. Plan and section views of the foundation system are shown in Figure 3.1(a). Plan and section views of the structural system are shown in Figures 3.1(b) and 3.1(c), respectively. A more detailed description of the building may be found in reference 44.

One vibration generator was mounted on the roof at point A in Figure 3.1(b). With the baskets of the shaker loaded to capacity, the building was shaken at resonance in either the N-S or E-W direction.

The maximum force applied in the N-S direction was approximately 2930 pounds which produced a peak acceleration of about 1.4% g on the roof. In the E-W direction, a maximum response of the roof of 0.9% g was produced by a 1180 pound exiting force.

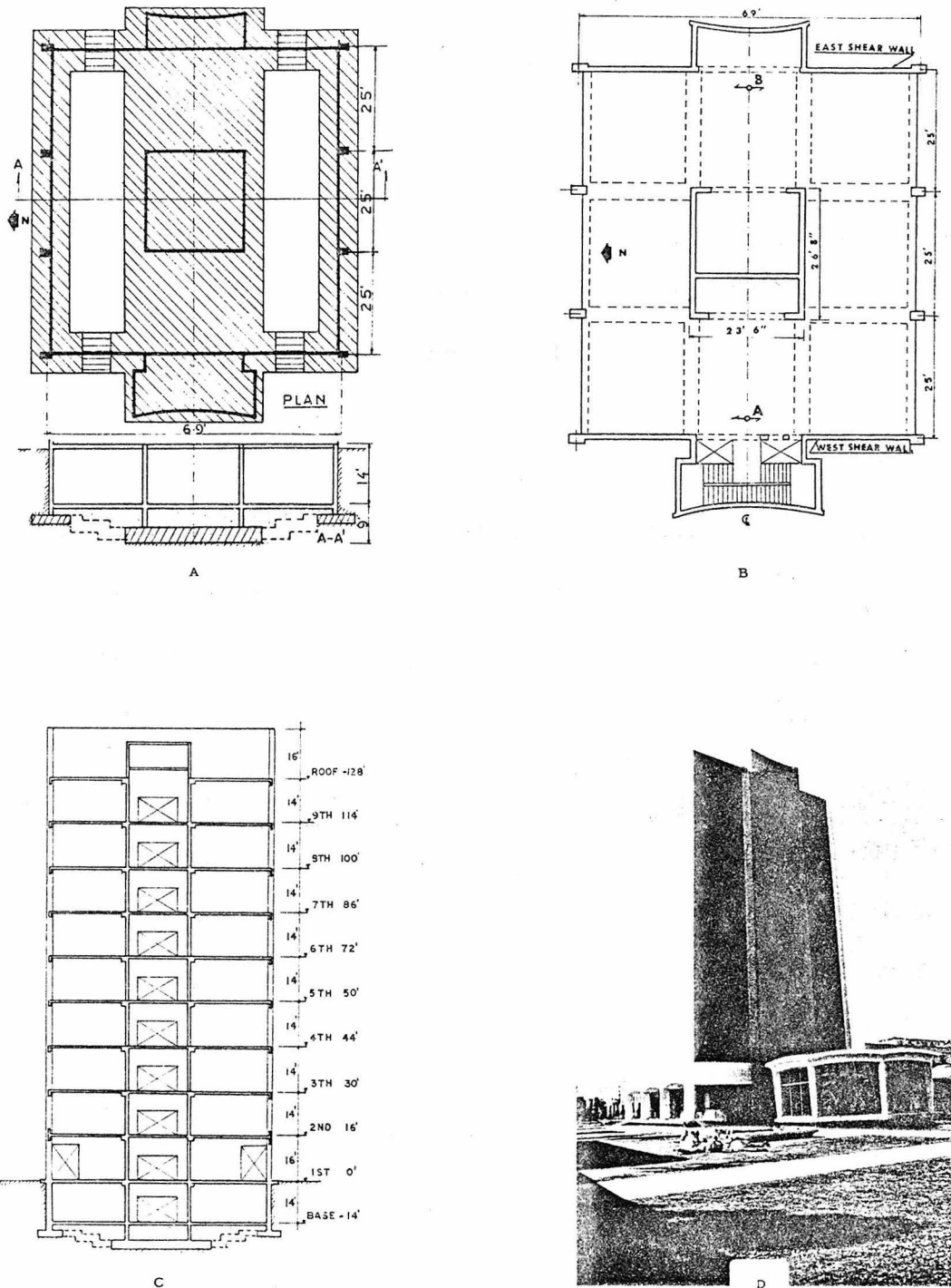


Figure 3.1 Millikan Library Building: (a) foundation plan and N-S section; (b) typical floor plan; (c) a N-S section view; (d) view of building looking Northwest.

One Ranger seismometer was placed in the basement of the building at a reference point located at the center of the north face of the central core wall where it remained throughout all the tests. This point was chosen to facilitate the matching of the test results with measurements taken in the basement and on the surrounding ground by other investigators.<sup>14</sup> Three Rangers were mounted on an aluminum plate in such a way that three orthogonal components of motion at a point could be more easily measured. This package of transducers was then moved from point to point to measure the three-dimensional motion during steady state response. The transducer package as well as the signal conditioner and recorder discussed in Chapter II are shown in Figure 3.2

### 3.2 Presentation and Discussion of Results

During the forced excitation, the building oscillates between two extreme positions. As the building oscillates, the floor slabs undergo translational and rotational in-plane motions and various points on the floor also move vertically due to bending deformations in the slab. Consequently, at one of the extreme positions of the building, the displacement of a particular joint on a floor slab may be composed of three components of motion.

The three-dimensional motions of the basement, second, fourth, sixth and eighth floors and also the roof at one of their maximum positions are shown in Figure 3.3 for shaking in the N-S direction at the resonant frequency of 1.76 Hz. For each of these figures the light grid represents the undeformed position of the points on each

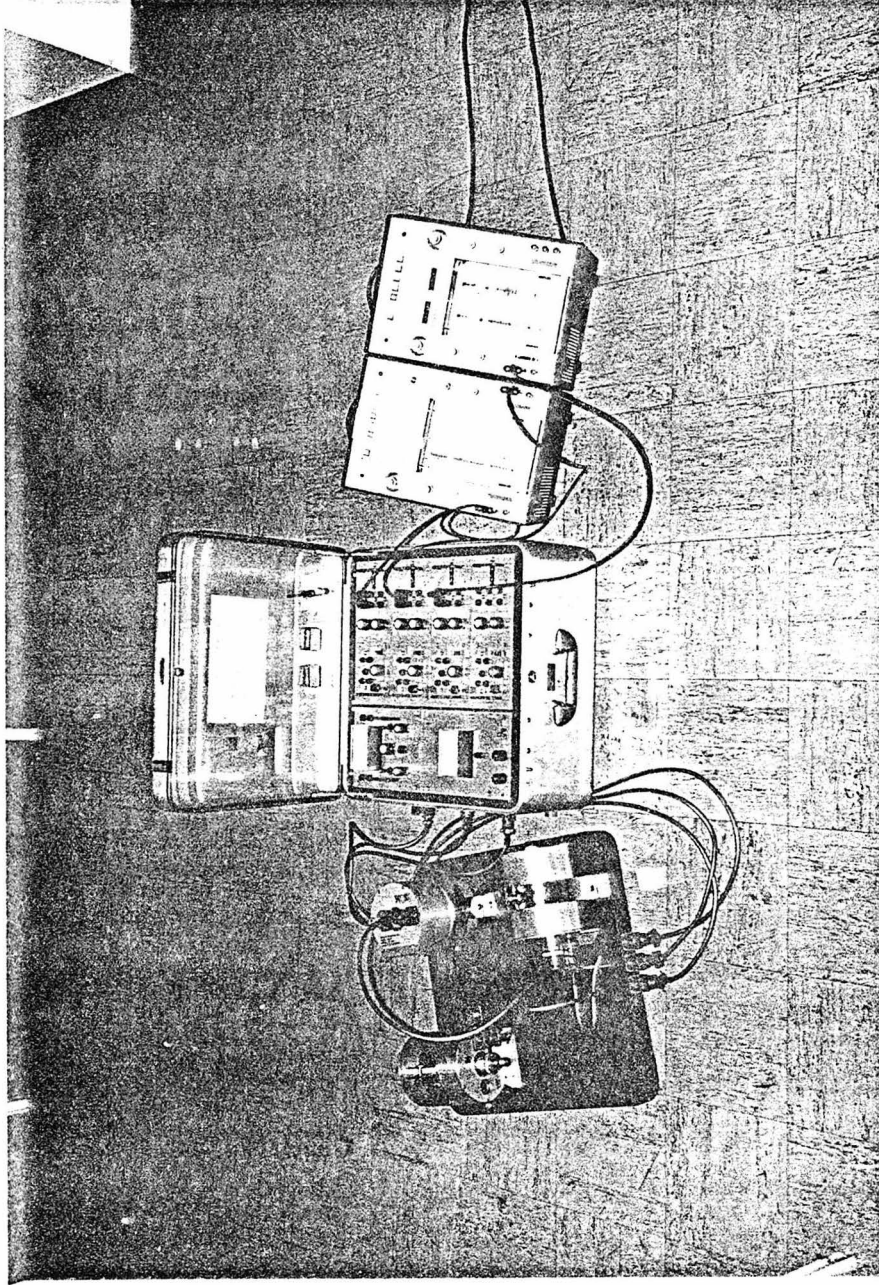


Figure 3.2 Instrumentation package and recorders used for the Millikan Library tests.

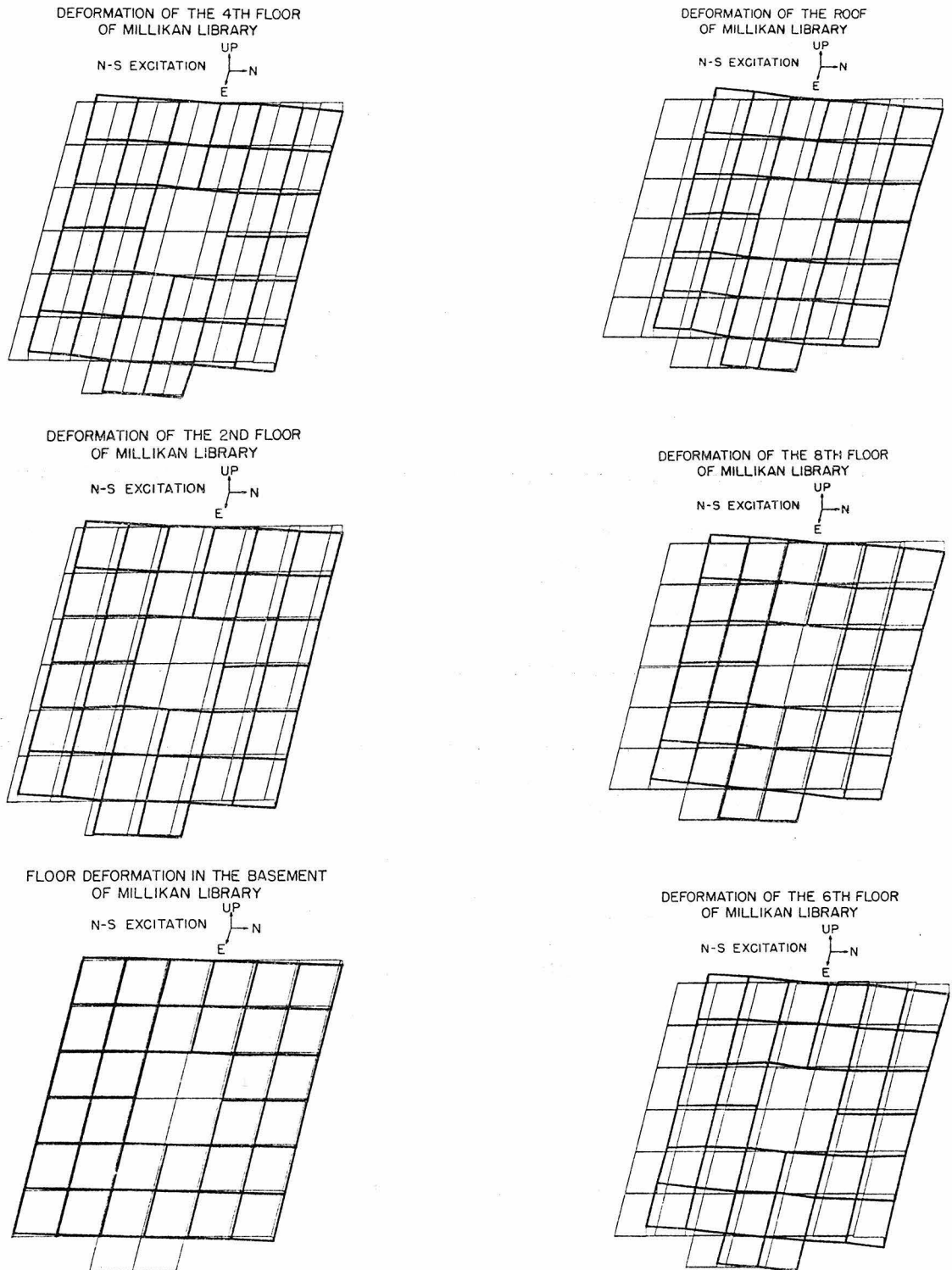


Figure 3.3 Floor deformations during N-S excitation.

floor, and the heavy lines connect the points at their maximum deformed position. In addition, each displaced point is connected to its undisplaced position by three light lines representing the three components of displacement. Clearly, the displacements are drawn to a much different scale than the structure. An enlarged view of each of these figures is shown in Appendix A.

The characteristics of the motion of the structure for shaking in the N-S direction are dominated by the behavior of the shear walls at the east and west ends of the building. Figure 3.4 shows an enlarged view of the deformations for the eighth floor. Notice that the edges of the slab at the east and west ends of the building moved nearly as straight lines as the structure deformed. This indicates that, although the channel-shaped section joining the two straight portions of wall (see Figure 1a) experienced some shearing-type deformations, the overall behavior of the wall assemblage was more like that of a single Euler beam than two beams acting independently. A simple analysis based on the section properties of the shear wall indicate that approximately 25% of the total deformation of the roof was due to shear deformation. The bending-type behavior was even more evident for the west shear wall where the stairs acted as a bracing element resisting shear deformation. This would be an important consideration for the designer attempting to estimate the stresses in each wall element.

The bending behavior of the walls produced vertical motion of the slab which reached a maximum at the ends of the walls. This maximum vertical motion was approximately 24% of the horizontal

DEFORMATION OF THE 8TH FLOOR  
OF MILLIKAN LIBRARY

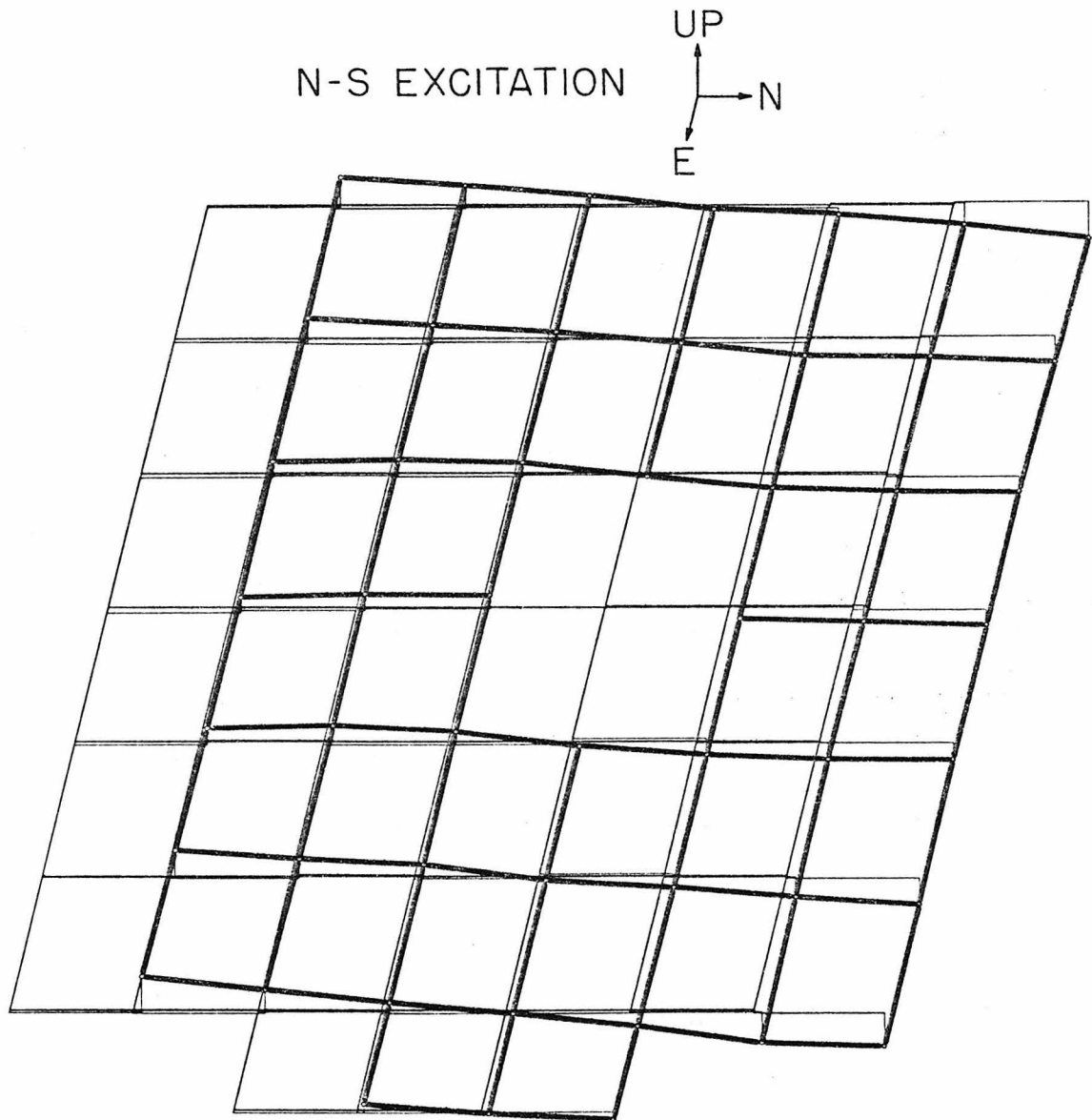


Figure 3.4

motion of the roof. The columns at the north and south edges of the slab acted as rigid elements in the vertical direction, thus resisting the vertical motion of the slab caused by the bending of the walls. This produced bending in the slab as well as the edge beams connecting the wall to the column. Consequently, if one ignored the interaction of the vertical and horizontal load-carrying systems in the design model, conservative estimates of the stresses in the wall would result; but nonconservative estimates of the stresses in the column, in the slab and in the edge beam would arise for this building.

The behavior of a section of the building along the west shear wall is shown in Figure 3.5. Again, the bending-type behavior of the wall section is demonstrated. Notice also the amount of deformation of the soil that takes place at the basement level. The translation of the base of the building was about 4 percent as large as the horizontal roof translation, while the maximum vertical motion, which again occurred at the corners of the shear wall, was twice as great as the horizontal motion.

The importance of the foundation deformation during forced vibration is illustrated in Figure 3.6. Using the average rotation of the basement slab, rocking of the structure accounts for 25 percent of the roof motion. This amount added to the four percent contribution due to translation indicates that almost 30 percent of the roof motion is attributable to foundation compliance. This is a surprisingly high contribution and differs significantly from results reported by Jennings and Kuroiwa in 1968.<sup>34,44</sup> Their results indicated that

DEFORMATION OF SECTION ALONG WEST  
SHEAR WALL OF MILLIKAN LIBRARY  
N-S EXCITATION

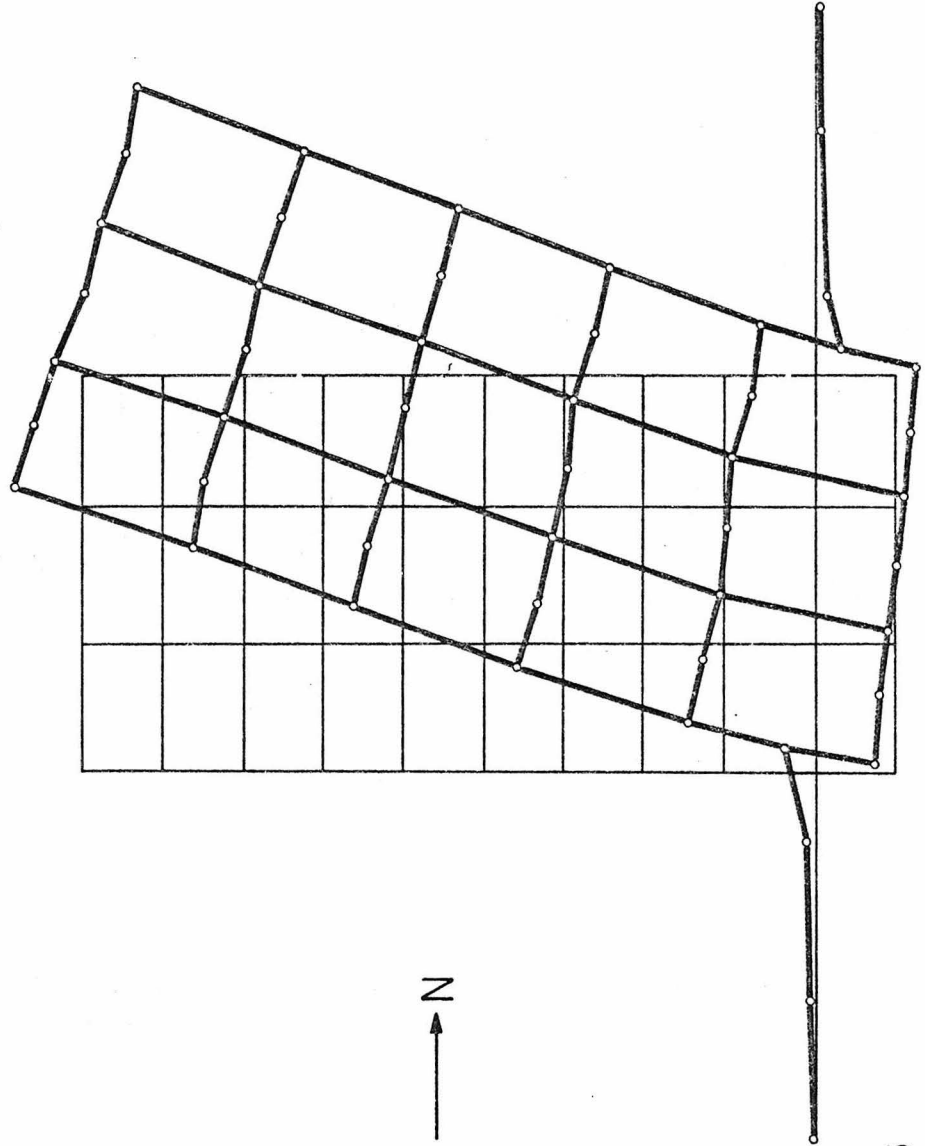


Figure 3.5

# CONTRIBUTION OF FOUNDATION DEFORMATION TO ROOF MOTION FOR N-S SHAKING

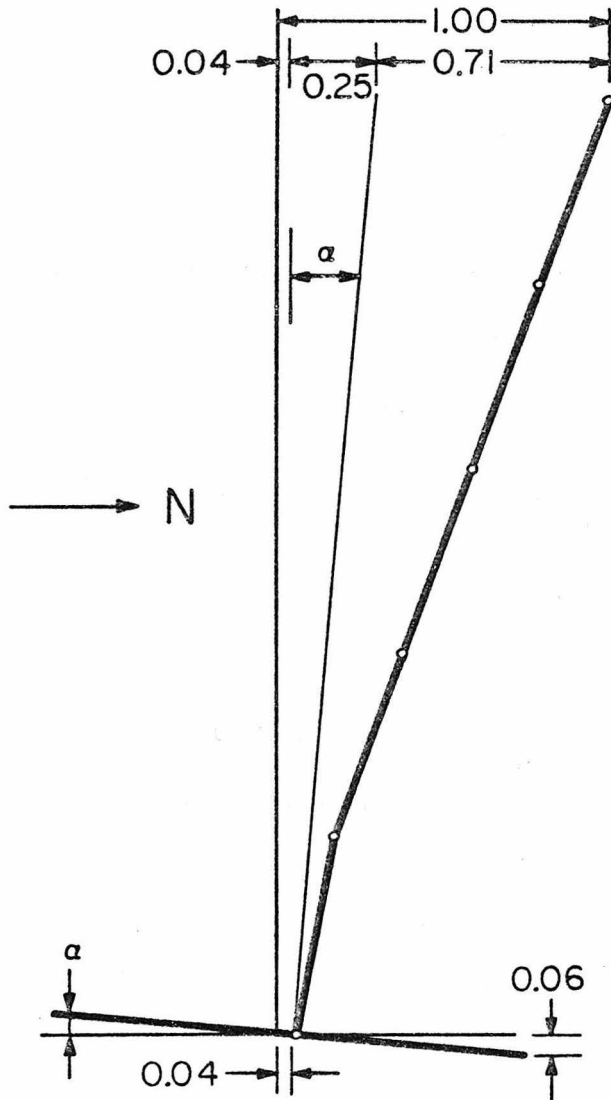


Figure 3.6

the soil deformation contributed less than 3 percent to the roof motion. Possible reasons for this difference are considered in Chapter IV.

The three-dimensional floor deformations for the basement, the second, fourth, sixth and eighth floors and the roof for shaking in the E-W direction at the resonant frequency of 1.21 Hz are shown in Figure 3.7; and Figure 3.8 is an enlarged view of the deformations of the eighth floor. The figures indicate that the building behaved quite differently in the E-W direction when compared to the N-S response. There was little vertical motion of the slab around the perimeter of the building, but there was a substantial amount at the east and west ends of the central core wall. Consequently, there was considerable deformation in the slabs. This result occurred because of the different types of load resisting elements in the system. The central core behaved like a bending beam, while the columns and the east and west shear walls acted as rigid elements in the vertical direction. A section through the center of the core wall is shown in Figure 3.9. This indicates a behavior similar to that expected for shear wall-frame interaction. In this case the central core is the shear wall and the east and west shear walls, acting in their weak directions, behave as the frame elements.

Figure 3.9 also indicates that there was only a small amount of basement translation which measured 2 percent of the horizontal roof motion. Due to the shear wall-frame pattern of deformation in the E-W direction, it is difficult to define a meaningful average rotational component for the base motion. One possible definition would be to use the average maximum vertical motion of the points

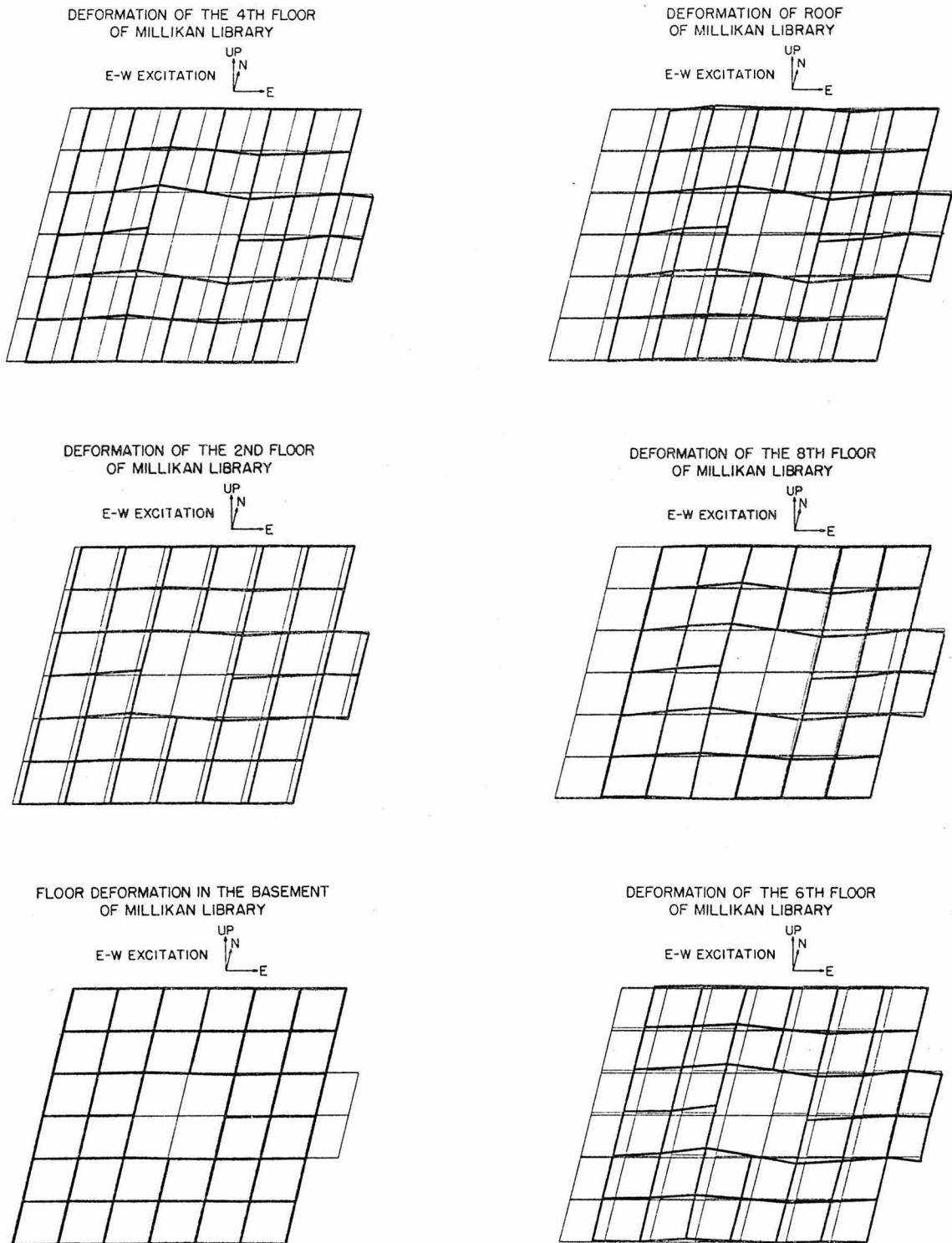


Figure 3.7 Floor deformations during E-W excitations.

DEFORMATION OF THE 8TH FLOOR  
OF MILLIKAN LIBRARY



E-W EXCITATION

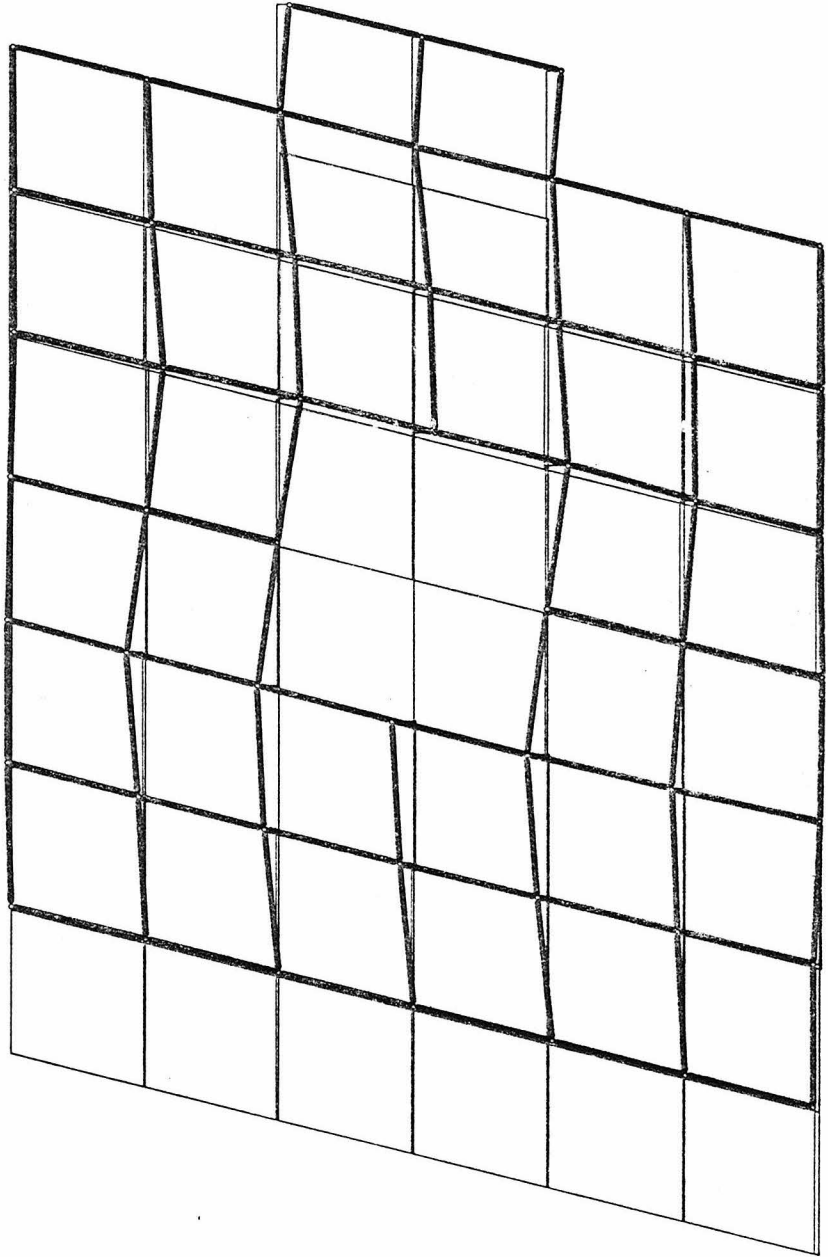


Figure 3.8

DEFORMATION OF SECTION THROUGH CENTERLINE  
OF ELEVATOR CORE OF MILLIKAN LIBRARY  
E-W EXCITATION

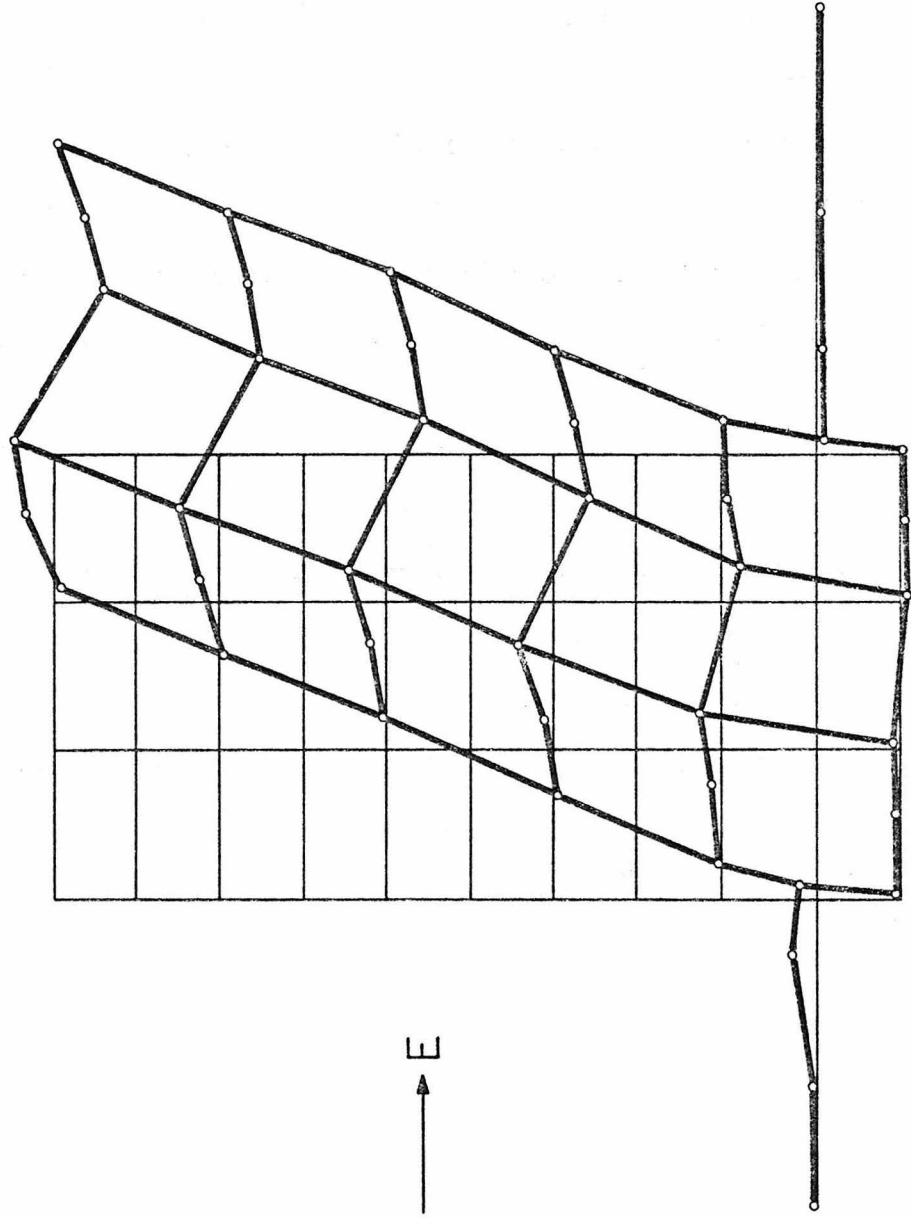


Figure 3.9

at the extreme east or west edges of the slab divided by the distance from the center of the slab to the extreme edge. For this definition, the average vertical motion at the edge of the slab is 1.6 percent as large as the horizontal roof motion. Thus, rotation of the base would cause roughly 6 percent of the roof motion. Again, these are larger values than those reported by Jennings and Kuroiwa, but the foundation motions for vibration in the E-W direction will have considerably less important effects on the dynamic behavior of the building than those for the N-S direction.

### 3.3 Conclusions

The results presented in this chapter give a clear insight into the nature and degree of the interaction that can occur between the lateral and vertical load carrying systems of a complicated structure. This type of detailed information would be very valuable for analytical studies of the building utilizing sophisticated finite-element models. Consequently, even though the information obtained is for low levels of excitation, this study has shown that very useful information may be obtained concerning the interaction of the various elements of a complex dynamic system. In fact, forced vibration tests are the only reliable means of obtaining this type of information for full-scale structures at the present time.

These tests also revealed that soil-structure interaction has a significant effect on the dynamic response of the Millikan Library building. This effect is most pronounced in the stiffer N-S direction.

Effects of this foundation compliance will be considered in more detail in Chapter IV.

Finally, the results indicated that the dynamic behavior and distribution of stresses in a real structure may be quite different than a simple one-dimensional model (a planar model with one degree of freedom per floor) would predict. In particular, out-of-plane deformation of floor systems may induce significant stresses in other members of the structural system even though in-plane deformations are negligible. In the case of Millikan Library, this effect significantly contributed to the interaction of the shear walls and other elements of the structural system.

## CHAPTER IV

The Use of Simple Models as an Aid to  
Interpreting Experimental Results

In this chapter the results of the tests of Millikan Library are interpreted through the use of simple analytical models. In the first analysis, the library structure and foundation system are modeled as an Euler beam with a translational and a rotational spring at the base. This model was used to investigate the differences in the fundamental period of vibration and the mode shape in the N-S direction as measured before and after the San Fernando earthquake. In the second analysis, an engineering model of the building in the N-S direction is constructed. The model is derived from the geometric and material properties of the building and the supporting soil. The emphasis is on simplified computations which are easily accomplished in an engineering design office. The dynamic characteristics are compared to those demonstrated by the building during forced vibration tests and during the San Fernando earthquake. In the third analysis, a lumped-mass model of the building which includes the effects of shear deformation is constructed to investigate the apparent changes in the vibrational characteristics of the structure that were mentioned above. The results of this analysis are compared to those based on the Euler beam model; and conclusions are drawn regarding the dependency of the results on the characteristics of the particular model.

#### 4.1 An Euler Beam Model of the Millikan Library Building

A surprising result of the Millikan Library tests was the large amount of soil-structure interaction that was present during vibration in the N-S direction. The results revealed that approximately 29 percent of the roof translation during steady-state vibration was the result of translation and rocking at the foundation level. The largest contributor was the rocking mode which caused 25% of the roof translation. These results differed from those reported by Jennings and Kuroiwa.<sup>32</sup> They determined that less than 3 percent of the roof motion was the result of foundation compliance and that the rocking at the base level contributed less than 1 percent. Since the original tests were performed before the San Fernando earthquake of 1971 and those reported in this paper were completed afterwards, and since the acceleration levels in the building reached 45% g at the top during the earthquake with 20% g at the base, it was believed that the differences could be attributed to a change in the foundation resistance that was the result of the earthquake.

In addition to these observed changes in the foundation motion, a lengthening of the fundamental period by 11 percent was also observed. The natural frequency of the first mode in the N-S direction was determined by Kuroiwa to be 1.97 Hz and by this investigator to be 1.76 Hz for similar exciting forces. (During the earthquake the natural frequency was approximately 1.6 Hz.) The permanent decrease in the natural frequency is consistent with possible softening of the foundation stiffness. It was not clear, however, whether the amount of change

observed in the frequency of vibration was consistent with the observed change in the mode shape. In particular, it seemed that the natural frequency might be more sensitive to large changes in the base rotational component of the mode shape than the building demonstrated. This suggested that larger than expected experimental error could possibly have occurred during the initial measurements. This could be the result of the low signal-to-noise ratio that would be expected for the accelerometers used to measure these extremely low levels of motion at the foundation level, or of some other difficulty that occurred in the two sets of experiments. Part of the difference may be explained by the fact that the measurements of rocking made by Kuroiwa were made at the point of minimum vertical motion of the base. The average rotation of the base as determined by this investigator was about 50 percent greater than the minimum. For purposes of comparison, the rotational component of Kuroiwa's mode shape was adjusted accordingly from that which he reported.

In order to determine if the change in the natural frequency of vibration was quantitatively consistent with the changes in the mode shape, two simple models of the building-foundation system were constructed. Since the test results indicated that the behavior of the structure in the N-S direction was dominated by the bending characteristics of the shear walls at the east and west ends of the building, an Euler cantilever beam was chosen to model the building behavior. A translational and a rotational spring were included at the base to model the effects of the foundation deformation. Figure 4.1 shows a sketch of

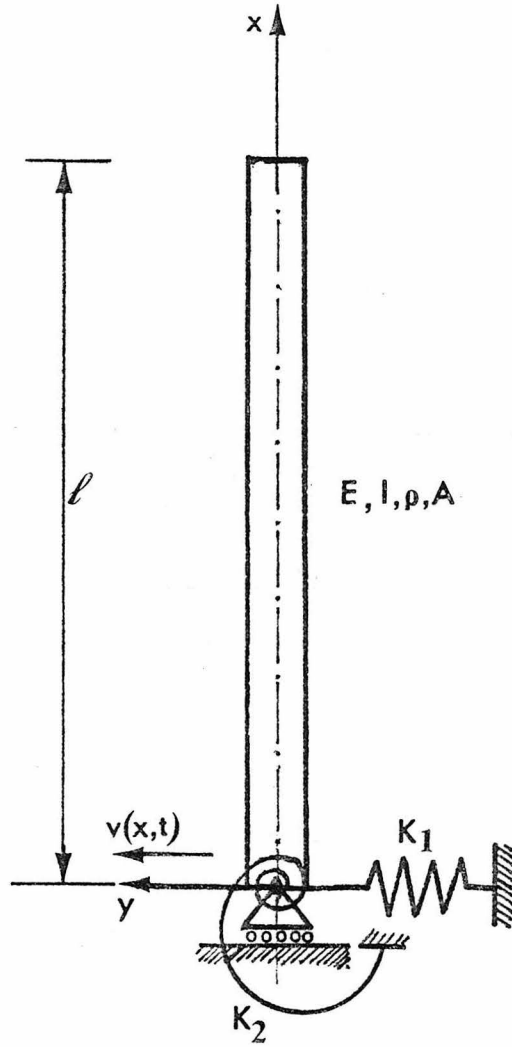


Figure 4.1 An Euler beam model of the Millikan Library building with a translational spring and a rotational spring at the base.

the model. A second model which includes the effects of shear deformations in the structure is presented in section 4.3.

From Timoshenko,<sup>62</sup> the differential equation of the vibrating beam may be written

$$\frac{\partial^4 v(x)}{\partial x^4} = \frac{1}{a^2} \frac{\partial^4 v(x)}{\partial t^2} \quad (4.1)$$

where

$$a^2 = \frac{EI}{\rho A} = \frac{EI}{\mu} . \quad (4.2)$$

In equation (4.2), E is the modulus of elasticity; I is the moment of inertia of the beam;  $\rho$  is the density of the material; A is the cross sectional area of the beam; and  $\mu$  is the mass per unit length of the beam. The method used for solving equation (4.1) is separation of variables which leads to the well known characteristic function

$$X(x) = C_1 \sin(kx) + C_2 \cos(kx) + C_3 \sinh(kx) + C_4 \cosh(kx) , \quad (4.3)$$

where

$$k^2 = \frac{\omega}{a} . \quad (4.4)$$

In (4.4),  $\omega$  is the characteristic frequency of vibration in radians per second.

The boundary conditions for the beam shown in Figure 4.1 are<sup>62</sup>

$$\begin{aligned}
C_1 E I k^3 - C_2 k_1 - C_3 E I k^3 - C_4 k_1 &= 0 \\
-C_1 k_2 - C_2 E I k - C_3 k_2 + C_4 E I k &= 0 \\
-C_1 \cos(k\ell) + C_2 \sin(k\ell) + C_3 \cosh(k\ell) + C_4 \sinh(k\ell) &= 0 \\
-C_1 \sin(k\ell) - C_2 \cos(k\ell) + C_3 \sinh(k\ell) + C_4 \cosh(k\ell) &= 0 .
\end{aligned} \tag{4.5}$$

In matrix form, these equations may be written

$$\det \begin{vmatrix} E I k^3 & -k_1 & -E I k^3 & -k_1 \\ -k_2 & -E I k & -k_2 & E I k \\ -\cos(k\ell) & \sin(k\ell) & \cosh(k\ell) & \sinh(k\ell) \\ -\sin(k\ell) & -\cos(k\ell) & \sinh(k\ell) & \cosh(k\ell) \end{vmatrix} = 0 . \tag{4.6}$$

Expanding this equation and substituting  $\alpha = k\ell$  yields the following frequency equation, in  $\alpha$ , for the Euler cantilever beam with a rotational and a translational spring at the base:

$$\begin{aligned}
&\left(\frac{E I}{\ell^2}\right)^2 [\cos(\alpha) \cosh(\alpha) - 1] \alpha^4 + \frac{E I k_2}{\ell^3} [\sin(\alpha) \cosh(\alpha) - \cos(\alpha) \sinh(\alpha)] \alpha^3 \\
&+ \frac{E I k_1}{\ell} [\sin(\alpha) \cosh(\alpha) - \cos(\alpha) \sinh(\alpha)] \alpha + k_1 k_2 [-1 - \cos(\alpha) \cosh(\alpha)] = 0 .
\end{aligned} \tag{4.7}$$

As a simple check on equation (4.7), one can observe the effect of letting  $k_1$ , the translational spring constant, and  $k_2$ , the rotational spring constant, approach infinity. This should lead to the standard frequency equation for the cantilever beam with fixed end conditions.

Dividing equation (4.7) by  $k_1 k_2$  and letting  $k_1$  and  $k_2$  approach infinity yields

$$\cos(\alpha) \cosh(\alpha) = -1 \quad (4.8)$$

which is the expected result.

The first step of this investigation was to construct a model of the building in the N-S direction that would closely match the dynamic characteristics measured by Kuroiwa. To obtain a realistic value for EI, the total weight of the building was assumed to be distributed over the height of the building (142 ft.) Using the resulting value for  $\mu$  ( $\mu g = 1.97 \times 10^5$  lb/ft.), the frequency equation of the fixed-free cantilever beam was solved for EI, assuming a frequency of vibration of about 2.00 Hz. This resulted in an initial estimate of  $EI = 3.177 \times 10^{13}$  lb-ft.<sup>2</sup> Values of  $k_1$  and  $k_2$  were then found so that the natural frequency and mode shape of the model would match those measured for the building before the San Fernando earthquake. A slight adjustment in the initial estimate of EI was also required.

Starting with this model which represented very closely the dynamic properties of the structure measured before the earthquake, EI was held constant and the values of  $k_1$  and  $k_2$  were adjusted until the mode shape reported in this thesis was obtained. This included an iterative scheme whereby equation (4.7) was solved for certain values of  $k_1$  and  $k_2$ ; the resulting frequency was then substituted into equation (4.3) and the mode shape was computed and normalized to equal 1.0 at the top ( $x = \ell$ ); the values of base translation and base rotation were then compared to the measured values and the spring constants were

modified in the appropriate direction. This procedure was continued until the author's measured values of base translation and rotation were closely approximated.

The results of this investigation are shown in Figure 4.2. The initial slight adjustment in EI so that Kuroiwa's results could be matched resulted in a fixed-base frequency of 2.02 Hz. The frequency of vibration that was then obtained after adjusting  $k_1$  and  $k_2$  until the predicted mode shape matched the most recently measured one was 1.65 Hz. This result is in good agreement with the value of 1.76 Hz that was measured by this investigator, considering the simplicity of the model. The resulting frequency is about 6 percent lower than the measured value.

The results of this initial investigation suggest that the observed change in the frequency of vibration is consistent with the apparent change in the mode shape. A more thorough discussion of these results will be given in section 4.3 where they are compared to those based on a model that includes the effects of shear deformation in the building.

#### 4.2 A Lumped Parameter Model of the Millikan Library Building

Due to economical considerations, a building the size of Millikan Library would not normally be analyzed for design using a sophisticated finite element analysis. More likely, the design of the structure to resist earthquake forces would be accomplished by approximating the dynamic forces by means of a static analysis using some equivalent static forces obtained from the Building Code. Another approach which the design engineer could adopt which would approximate the dynamic

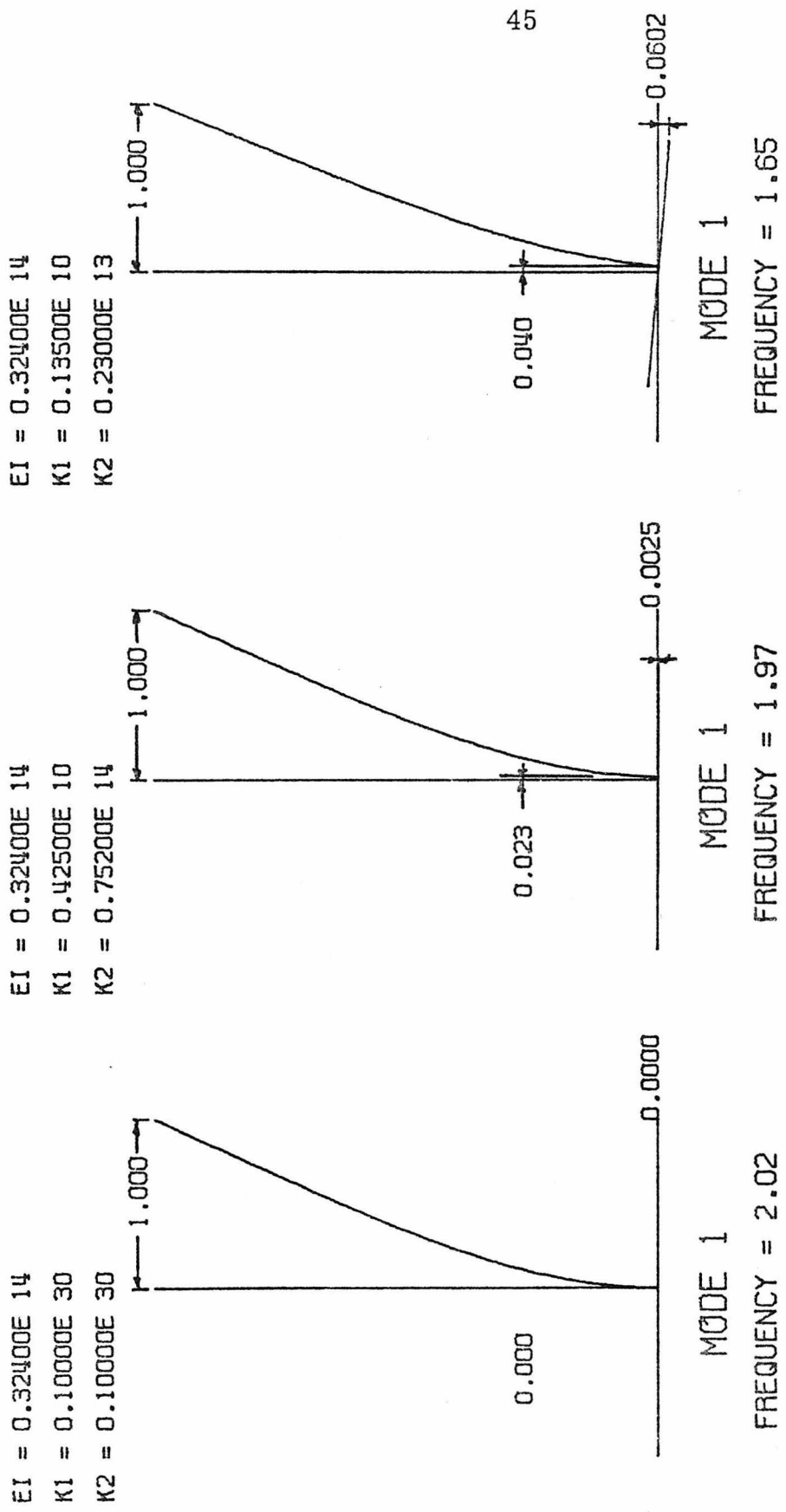
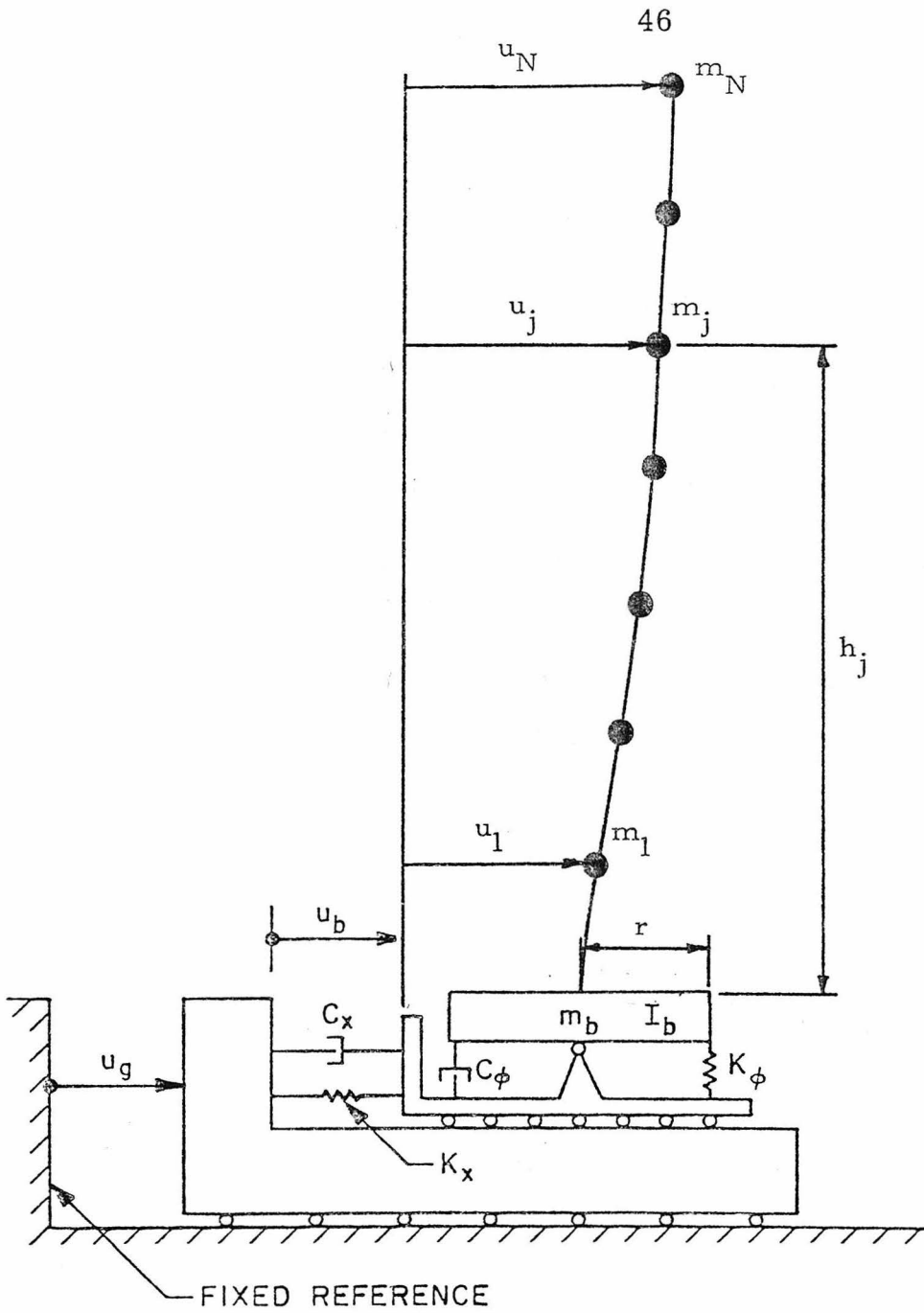


Figure 4.2 Results of analysis using an Euler beam model of the Millikan Library building. (a) Fixed base model; (b) rotational and translational springs added to base, to match mode shape and frequency determined by Kuroiwa; (c) base springs adjusted to match mode shape measured by Foutch.



## SOIL-STRUCTURE INTERACTION MODEL

Figure 4.3 Lumped-mass model of Millikan Library.

behavior of a building more realistically would be to construct a simple lumped-mass model of the building based on the physical properties of the structural members. The effects of soil-structure interaction may even be included with little additional effort.

To demonstrate the procedure that could be followed in a simplified dynamic analysis of a building and to determine how accurate the results of this approach might be, a lumped-mass model of the Millikan Library building in the N-S direction was constructed. The effects of shear deformation in the walls of the building and the effects of soil-structure interaction were included in the model.

A schematic of the dynamic model of the building is shown in Figure 4.3. The equations of motion for this system may be written

$$M \ddot{\underline{u}}^S + C \dot{\underline{u}}^S + K \underline{u}^S + M(\underline{h} \ddot{\phi} + \ddot{u}_g + \dot{u}_b) = 0$$

$$\sum_{j=1}^n m_j (\ddot{u}_j^S + h_j \ddot{\phi} + \ddot{u}_g + \dot{u}_b) + m_b (\ddot{u}_g + \dot{u}_b) + C_x \dot{u}_b + K_x u_b = 0 \quad (4.9)$$

$$\sum_{j=1}^n m_j h_j (\ddot{u}_j^S + h_j \ddot{\phi} + \ddot{u}_g + \dot{u}_b) + I_t \ddot{\phi} + C_\phi r^2 \dot{\phi} + K_\phi r^2 \phi = 0 ,$$

where,

$u_g$  = acceleration of the ground

$u_b$  = the relative translation between the base of the structure and the fixed reference.

$\underline{u}^S$  = a vector of horizontal displacements of the floors relative to the base.

- $u_j^S$  = the horizontal displacement of floor j relative to the base.  
 $\underline{h}$  = a vector of floor heights above the base.  
 $h_j$  = the height of floor j above the base.  
 $\phi$  = the rotation of the base.  
 $I_t$  = the sum of the centroidal moments of inertia of the floors and base masses.  
 $K$  = the fixed base stiffness matrix of the model.  
 $C_\phi$  = the foundation rotational damping coefficient.  
 $K_\phi$  = the foundation rotational spring constant.  
 $C_x$  = the foundation translational damping coefficient.  
 $K_x$  = the foundation translational spring constant.  
 $M$  = the fixed base mass matrix of the structure.

Neglecting the damping terms, this may be written in matrix form

$$M^* \ddot{\underline{u}} + K^* \ddot{\underline{u}} = -\underline{m} \ddot{\underline{u}}_g \quad (4.10)$$

where,



and,

$$\underline{m} = \left\{ \begin{array}{c} m_1 \\ \cdot \\ \cdot \\ \cdot \\ m_n \\ m_b \\ \sum_{j=1}^n h_j m_j \end{array} \right\} \cdot \quad (4.13)$$

In these equations  $K_x$  is equivalent to the translational spring,  $k_1$ , of the previous model and  $r^2 K_\phi$  is equivalent to the rotational spring,  $k_2$ .

The numerical values used in these equations for the model of the library building were derived using the geometric and material properties of the east shear wall (see Figure 3.1) and of the foundation material. The weights of the floors used in the model were as follows:<sup>32</sup> roof,  $2.6 \times 10^6$  lbs.; floors 9-3,  $1.95 \times 10^6$  lbs.; floor 2,  $2.433 \times 10^6$  lbs.; floor 1,  $2.28 \times 10^6$  lbs.; and the base weight is approximately  $7.0 \times 10^6$  lbs. The moment of inertia of the east shear wall was computed to be  $3.32 \times 10^4$  ft.<sup>4</sup>. This value was then doubled so that the total mass of the building could be used. In this way, results could be more easily compared to those of the previous section. Young's modulus for 4000 psi concrete is approximately<sup>1</sup>  $3.6 \times 10^6$  psi =  $5.18 \times 10^8$  lbs./ft.<sup>2</sup>. The resulting value for EI was  $3.44 \times 10^{13}$  lbs.-ft.<sup>2</sup>

A common practice of determining the equivalent springs to model the foundation compliance of a structure is based on the exact solution

of a rigid disk on a half space. Veletsos<sup>66</sup> gives the following equations for determining the equivalent springs:

$$K_x = \alpha_x K \quad (4.14)$$

$$K_\phi = \alpha_\phi K \quad (4.15)$$

where

$$K = \frac{8}{2 - \nu} Gr \quad (4.16)$$

and

$\nu$  = Poisson's ratio

$r$  = radius of foundation base.

The parameters  $\alpha_x$  and  $\alpha_\phi$  depend on the frequency of excitation, the radius of the base and the shear wave velocity of the foundation material. For Millikan Library,  $\alpha_x$  and  $\alpha_\phi$  are approximately equal to 1.0 and 0.85 respectively. The shear modulus of the foundation was estimated from the approximate shear wave velocity of the soil immediately under the building by the relation  $C_s = \sqrt{G/\rho}$ , where  $C_s$  is the shear wave velocity and  $\rho$  is the mass density of the material. Using the values 1650 ft./sec. for the shear wave velocity,<sup>68</sup> 110 lbs./ft.<sup>3</sup> for the weight density, and 41 feet for the radius of the equivalent circular base resulted in the following values for the base springs:

$$K_x = 1.8 \times 10^9 \text{ lb./ft.}$$

$$r^2 K_\phi = 2.7 \times 10^{12} \text{ ft.-lb./rad}$$

These values were increased by 22 percent for  $K_x$  and by 28 percent for  $r^2K_\phi$  to account for imbeddment.<sup>43</sup> The final values used in this analysis were  $K_x = 2.2 \times 10^9$  lb./ft. and  $r^2K_\phi = 3.5 \times 10^{12}$  ft.-lb./rad..

The dimensions of the east shear wall of Millikan Library indicate that approximately 20-25 percent of the deflection of the roof due to lateral loading may be contributed by shear deformations. The model of the building should reflect this contribution. The plane stress solution for the displacement of the centerline of a rectangular cantilever beam with a concentrated load applied at the end is<sup>27</sup>

$$v(x) = \frac{P(3l-x)x^2}{6EI} + \frac{Pc^2x}{2GI} \quad (4.17)$$

The first term of this expression represents the part of the total displacement due to bending and the second term represents the contribution due to shear deformation.

The flexibility matrix was determined for the fixed base model by applying a unit load independently at each floor level and computing the resulting floor displacements at each floor level using equation (4.17). The resulting flexibility matrix was then inverted to obtain the stiffness matrix,  $K$ , of the fixed-base model.

The procedure as discussed so far has been based on simple ideas in mechanics. The numerical computations required could have been completed in the design office without the use of a digital computer. In order to remain consistent with this approach, the natural frequency of the model was computed using Rayleigh's Quotient which for this system may be written

$$R = \frac{\psi^T K^* \psi}{\psi^T M^* \psi} = \left( \frac{f_n}{2\pi} \right)^2 \quad (4.18)$$

In equation (4.18),  $\psi$  represents the approximate mode shape for the first mode of the model.  $\psi$  was obtained by applying loads at each floor level which were equal to the weight of the floor and computing the resulting displacements. Using this procedure, the normalized computed displacements are usually very close to the exact mode shape of the system. The resulting natural frequencies are expected to be within 1-2 percent of the exact values. Error in the predicted natural frequency for the fixed base condition was less than 1 percent.

Using the stiffness and mass matrices of the fixed base model, eigenvalues were computed which revealed that the first natural frequency was 1.89 Hz. When the translation and rotation of the base are included in the model the natural frequency dropped to 1.66 Hz. The fact that this value is smaller than either of the test results may be potentially due to the added stiffness of the building (contributed by the core wall and the columns) which was not included in the model. This was partially offset, however, by the omission of the effect of holes in the shear wall at the first floor level [see Figure 3.1 (d)]. The resulting mode shape is shown in Figure 4.4.

It is interesting to note that the natural frequency of this model is actually quite close to the one at which the building vibrated during the San Fernando earthquake. Assuming that the mode shape measured after the event is representative of the one during the earthquake, the mode shape predicted by the model is also representative of the actual

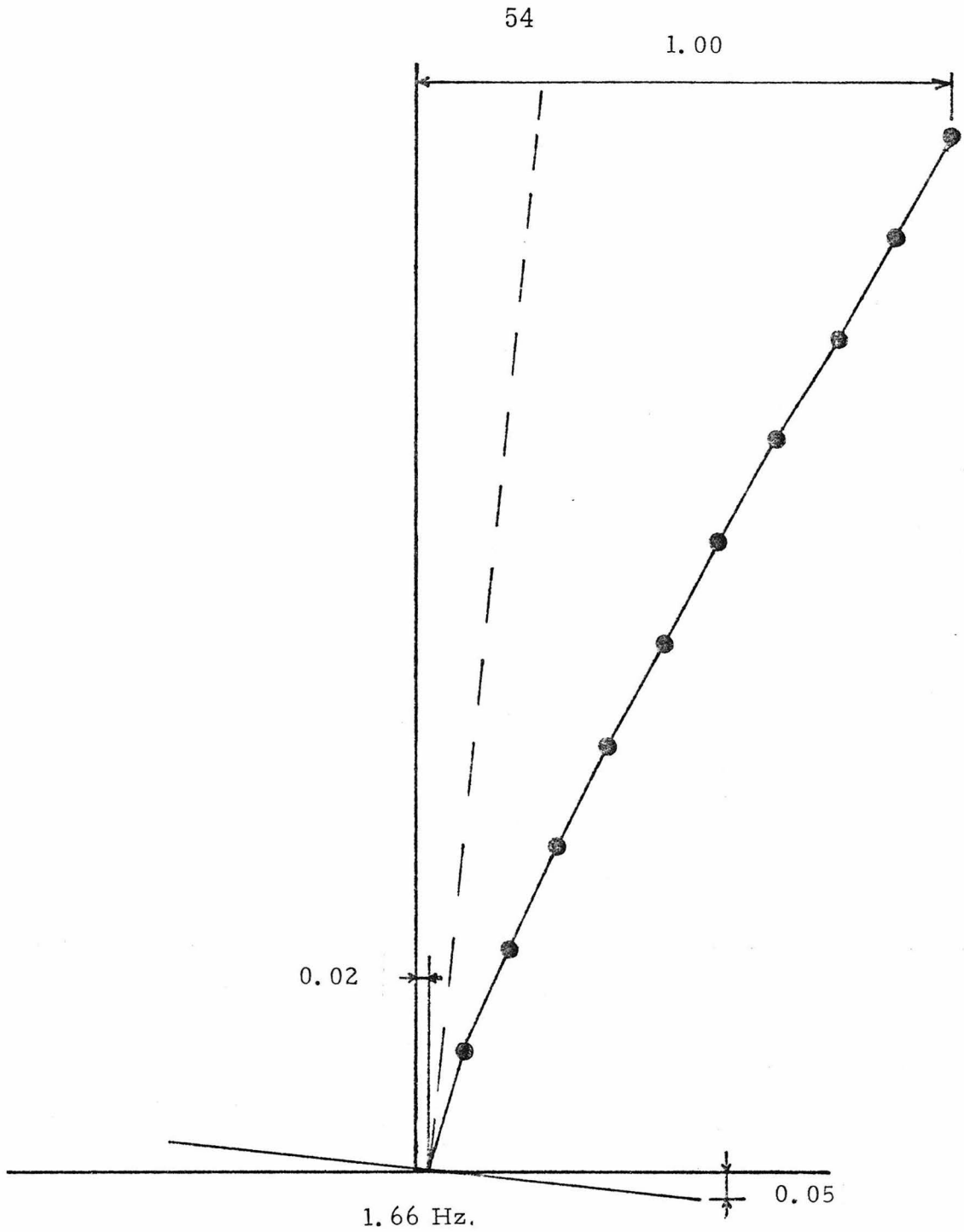


Figure 4.4 Mode shape and frequency of the fundamental N-S mode of the Millikan Library building resulting from a lumped-mass model of the structures based on physical properties of the structure and supporting soil.

structure. The model actually portrays a slightly stiffer foundation than the measured quantities indicate. If the foundation springs were adjusted to match the test conditions, the resulting frequency of the model would be nearly identical to natural frequency of the building during the earthquake. Even without this adjustment the predicted frequency is only about 4 percent in error. This is quite good considering the simplicity of the model and indicates the usefulness of this type of analysis in engineering practice.

#### 4.3 An Additional Investigation of the Observed Changes in the Dynamic Characteristics of the Millikan Library Building

In section 4.1, an analysis of the Millikan Library building was presented which was based on an Euler beam model of the structure with springs included at the base to simulate the effects of soil-structure interaction. The results of the analysis indicated that the change in the natural frequency of vibration of the structure determined by forced vibration tests conducted before and after the San Fernando earthquake were consistent with the observed changes in the mode shape of the building. However, only bending deformations in the structure are assumed when an Euler beam model is used.

An additional analysis was conducted to determine if the results of section 4.1 are dependent upon the model chosen to investigate the observed phenomenon. The model chosen for the investigation was identical to the lumped-mass model that was described in section 4.2. Consequently, the model is more representative of the actual structure since shear deformations in the walls are included in the analysis.

Also, the masses are lumped at discrete points which is also the approximate case for a multistory building.

The procedure used in this analysis was identical to that described in section 4.1. Values of  $EI$ ,  $k_1$  and  $k_2$  were found so that the dynamic characteristics of the model closely approximated those measured by Kuroiwa. The foundation spring constants,  $k_1$  and  $k_2$ , were then adjusted until the mode shape measured after the earthquake was obtained for the model. The resulting natural frequency could then be compared to the measured post-earthquake value.

Several observations may be made based on the results of this analysis which are presented in Figure 4.5. First, the final natural frequency that resulted when the mode shape that matched the present condition of the building was obtained was 1.68 Hz. This is quite close to the measured value of 1.76 Hz, the difference being only 4.5%. The results of this analysis and those of the previous section indicate that the observed changes in the natural frequency of vibration of the building are compatible with the measured changes in the foundation compliance. Consequently, unusually large experimental error appears unlikely as a possible cause of the difference in the mode shape measured in the two tests; it appears most probable that a significant change in the behavior of the foundation in the N-S direction occurred as a result of the San Fernando earthquake. The change in the translation and rocking compliances of the base indicated by these measurements implies that a substantial loss of rotational and translational stiffness occurred. This is thought not to be the result of a change in the material properties of the supporting soil, however, since the

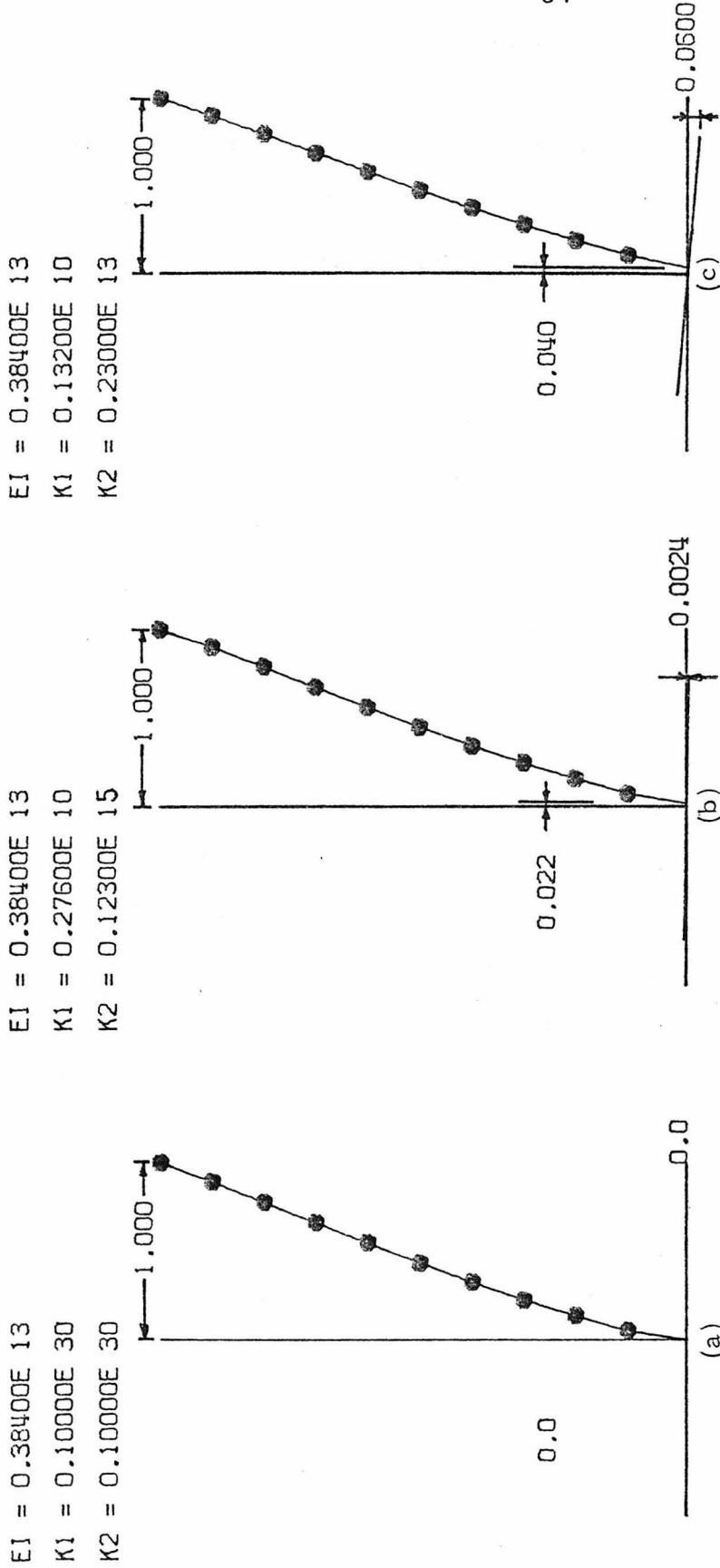


Figure 4.5 Results of analysis using a lumped-mass model of the Millikan Library building: (a) fixed-base model; (b) rotational and translational springs added to base to match mode shape and frequency determined by Kuroiwa; (c) base springs adjusted to match mode shape measured by Foutch.

approximate analysis based on the properties of the soil resulted in a mode shape that was quite close to that measured after the earthquake. It seems more likely that the loss in stiffness was the result of the fracture of some brittle elements that connect the building to adjacent structures at the foundation level.

In comparing the results of the analysis based on the Euler beam model with those presented in this section note that the value of  $EI$  required to match the test results was about 20% higher for the model that allowed shear deformation. This reflects the fact that the beam that includes shear deflection is basically softer than one that only allows bending deflections. Consequently, to achieve nearly equal frequencies of vibration for the two models, a higher value of  $EI$  for the beam including shear deformations was needed. Another point of interest lies in the comparison of the foundation spring constants required for each model to match the present mode shape of the building. They are nearly identical for both models. In the case where Kuroiwa's results were matched, however, the base spring constants for the Euler beam were substantially larger. Since a greater change was required for the foundation springs of the Euler beam model to approximate the change in the building after the earthquake, this indicates that this model is less sensitive to changes in the foundation compliance than the model which allows shear deformation.

A final comparison of the results of this analysis is shown in Figure 4.6. This shows various measured and computed mode shapes with the base translation and base rotation components removed. Consequently, one may observe which model best represents the structural deformation of the building. As expected, the figure indicates that the model including shear deformation is more representative of the deformation of the actual building.

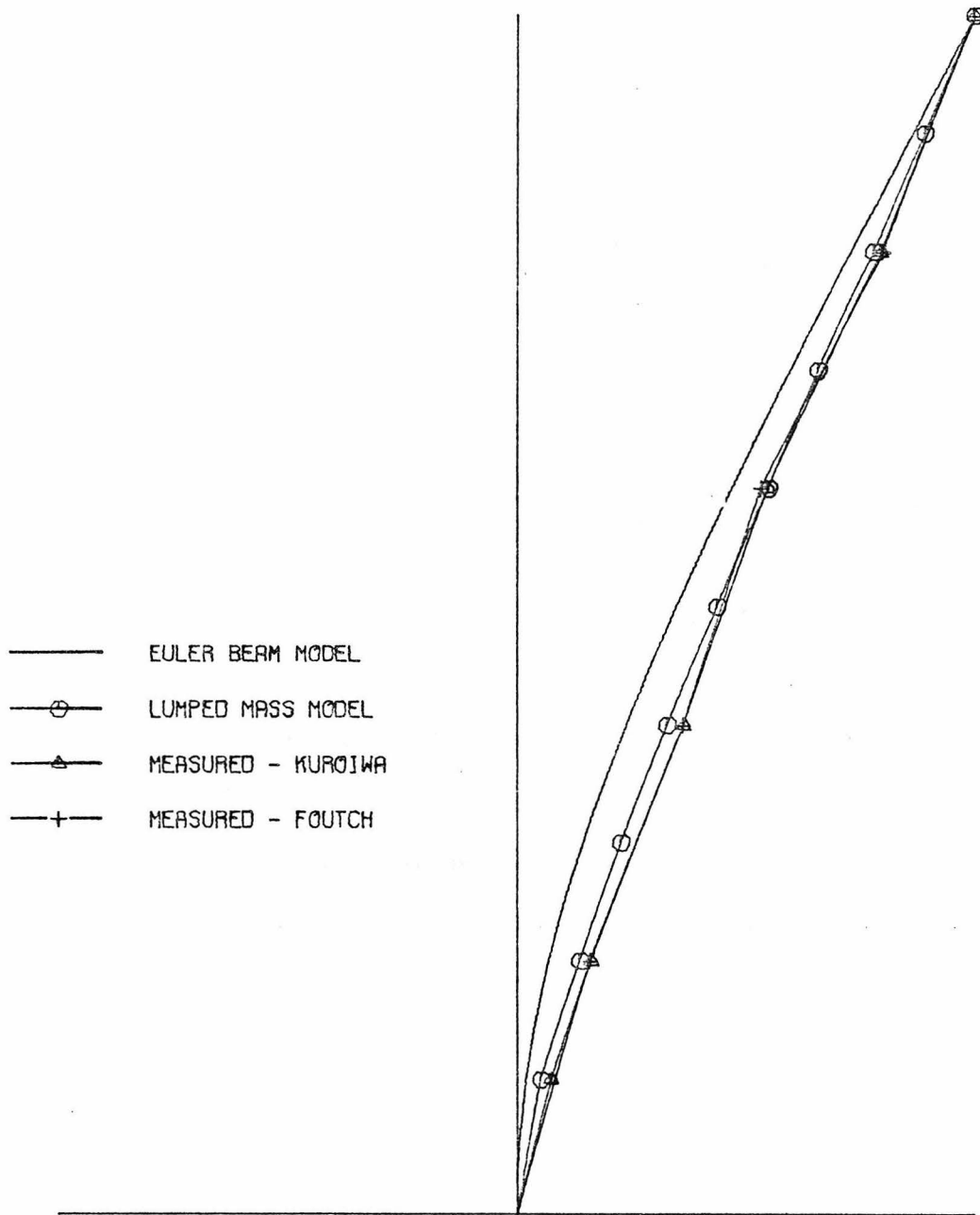


Figure 4.6 Measured and computed mode shapes of Millikan Library after earthquake with effects of base translation and rotation removed.

#### 4.4 Conclusions

The analysis presented in this chapter indicated that simple analytical models may be extremely useful in interpreting unexpected experimental results. These models may often be employed with little computational effort.

The results of this analysis indicated the strong probability that a change in the foundation compliance of the Millikan Library building occurred during the San Fernando earthquake. For a given excitation, the measured motion at the basement level was twice as great in translation and approximately 25 times greater in rotation after the earthquake than before the event, although the deformations in the building were similar. If changes in the foundation compliances are responsible for the observed differences in the mode shapes, then it seems likely that the substantial loss of stiffness must be the result of failure of brittle elements adjacent to the building foundation, rather than changes in the soil conditions.

The lumped parameter model of the Millikan Library building derived using elementary mechanics indicated that good estimates of the dynamic characteristics of real structures may be obtained in an engineering design office without the use of large digital computers. The effects of soil-structure interaction may also be included with little additional effort. Therefore, the dynamic effects of earthquakes on many structures may be more realistically approximated using this type of analysis as opposed to one based on equivalent static loads, without the penalty of increased cost or complexity.

## CHAPTER V

Forced Vibration Tests of the Ralph M. Parsons Company  
World Headquarters Building

Forced vibration tests of the twelve-story steel framed Ralph M. Parsons Company World Headquarters building were conducted between August 1975 and May 1976. Dynamic characteristics of the structure that were studied in detail include natural frequencies, mode shapes and damping values for nine modes of vibration, non-linearity associated with increasing levels of response, modal interference and modal coupling. In addition to these, strain was measured in one of the columns of the structure during forced excitation.

5.1 Description of the Building

The Ralph M. Parsons Company World Headquarters is a steel framed structure located in downtown Pasadena, California. The east elevation of the complex is shown in Figure 5.1 and a plan view of the headquarters is shown in Figure 5.2. As indicated in Figure 5.2, the headquarters is composed of three buildings. Two identical four-story satellite structures are located to the northeast and northwest of the main building. The main structure has a large four-story portion at the south end and a twelve story tower that is roughly octagonal in shape on the north side. The dashed lines in Figure 5.2 indicate where the tower intersects the lower portion of the main

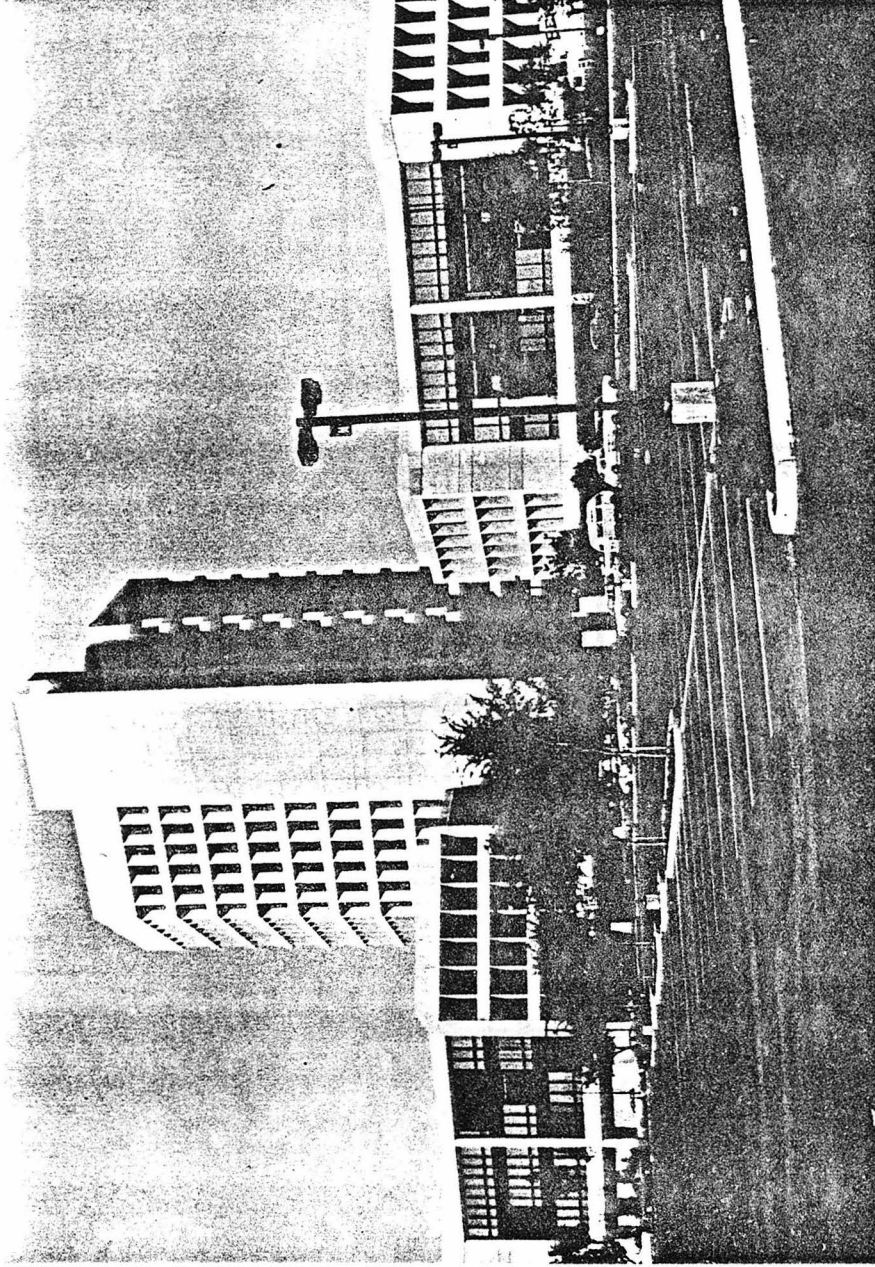


Figure 5.1 East elevation view of Ralph M. Parsons Company World Headquarters Complex.

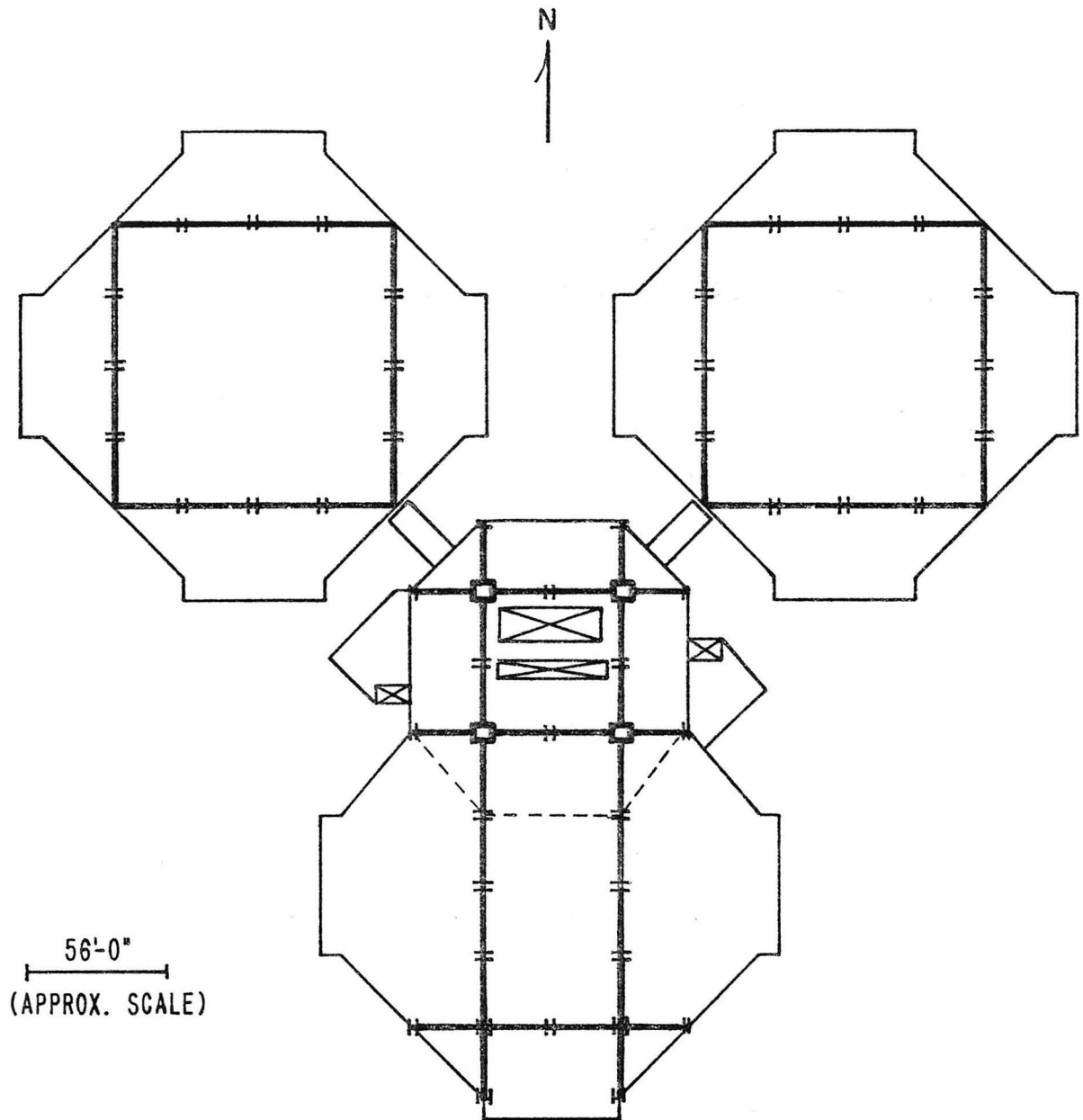


Figure 5.2 Plan view of the Ralph M. Parsons Company World Headquarters Complex.

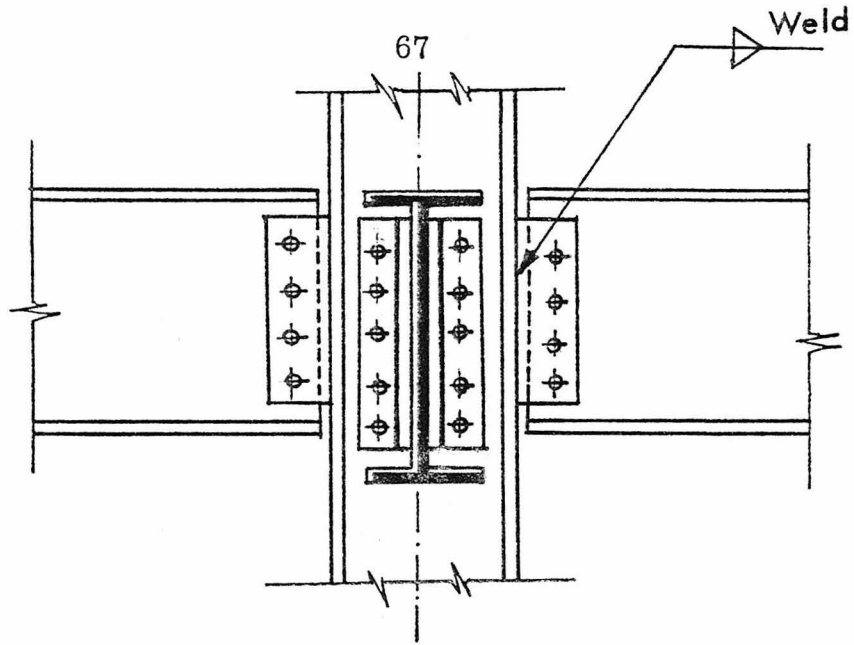
structure. Separation joints are provided at the satellite end of the walkway joining the central building to the satellite structures. This separation joint is 2 inches wide at the second floor level and 5 inches wide at the third, fourth and fifth floor levels.

The lateral loads are resisted by full moment resisting steel frames shown as heavy lines in Figure 5.2. The girders of all other frames (not shown in Figure 5.2) were designed only to resist shear and they carry only gravity loads. Figure 5.3 shows a plan view of the framing system of the main building. Again, the heavy lines indicate the moment resisting frames. Secondary girders that resist gravity loads are not shown. Also shown in Figure 5.3 is a numbering of the column lines which will be referred to in future sections of this thesis. Figure 5.4 shows a section along one of the N-S moment resisting frames. The circles represent hinge, or shear connections. Typical details for the moment resisting and shear connections are shown in Figure 5.5

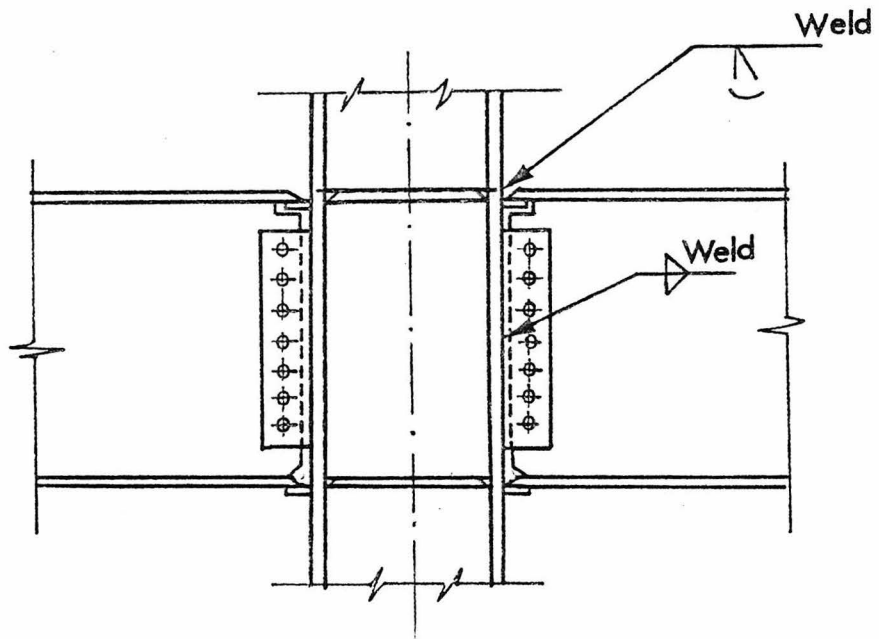
The foundation system is composed of individual spread footings with pedestals beneath each column. The bottoms of the footings beneath the tower columns of the moment resisting frames are 14 feet below the finished floor levels of the first floor and those beneath the columns of the four story portion are 7 feet down. Grade beams are also provided along the column lines of the moment resisting frames. These measure 5 feet by 3 feet beneath the tower and 3 feet by 2 feet 3 inches for the others. Typical foundation details are shown in Figure 5.6.





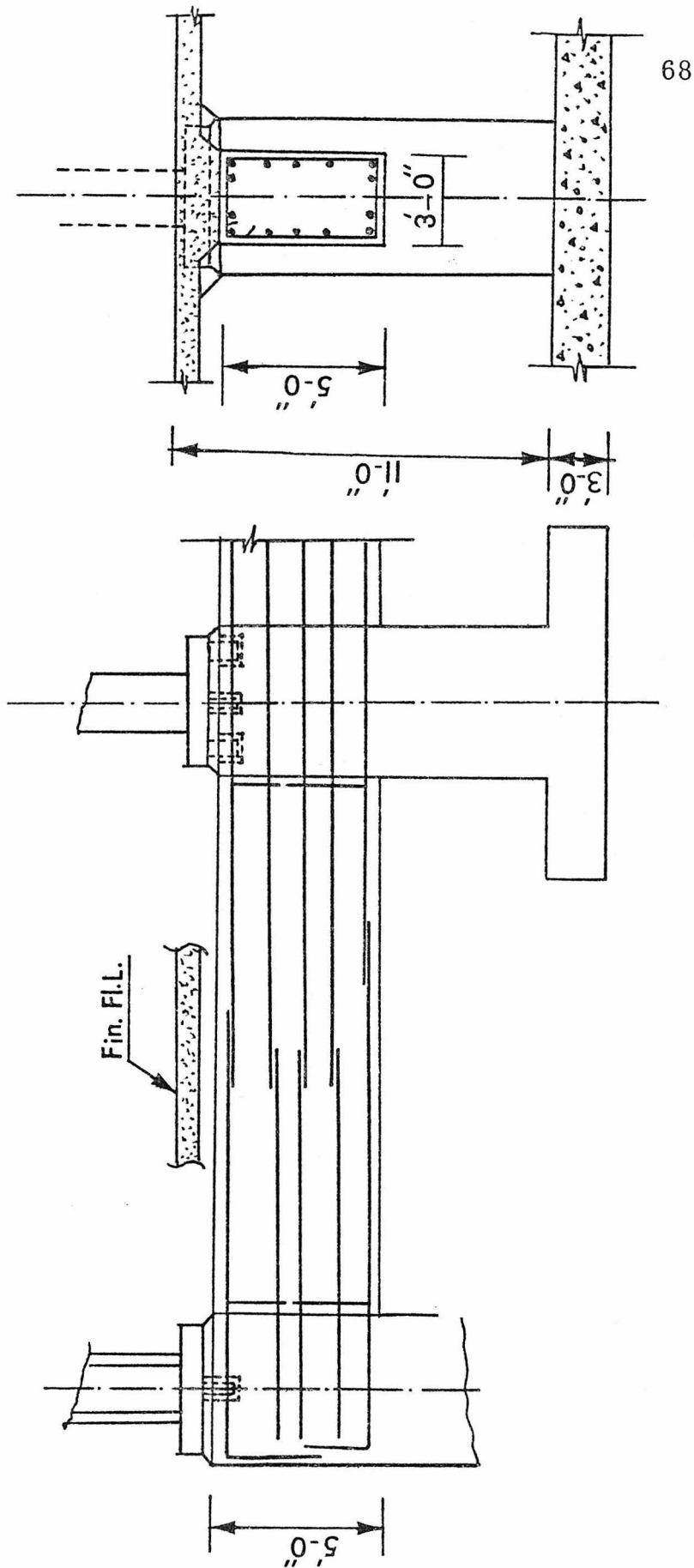


**TYPICAL. SHEAR CONNECTION**



**TYPICAL MOMENT CONNECTION**

Figure 5.5 Typical connection details for the framing system of the Parsons building.



TYPICAL FOUNDATION DETAIL

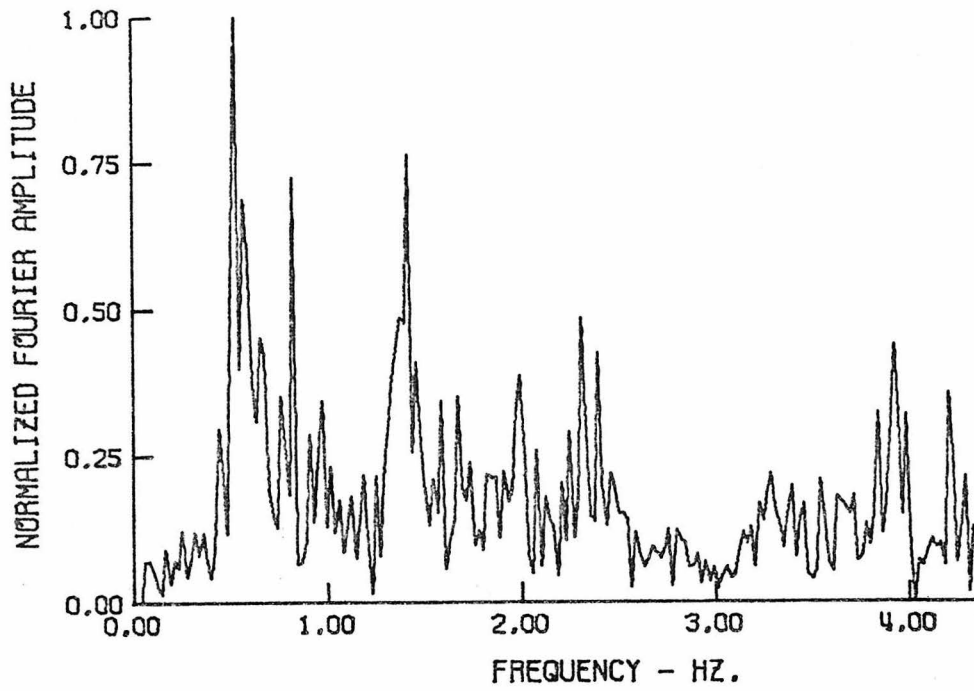
Figure 5.6

## 5.2 Preliminary Tests

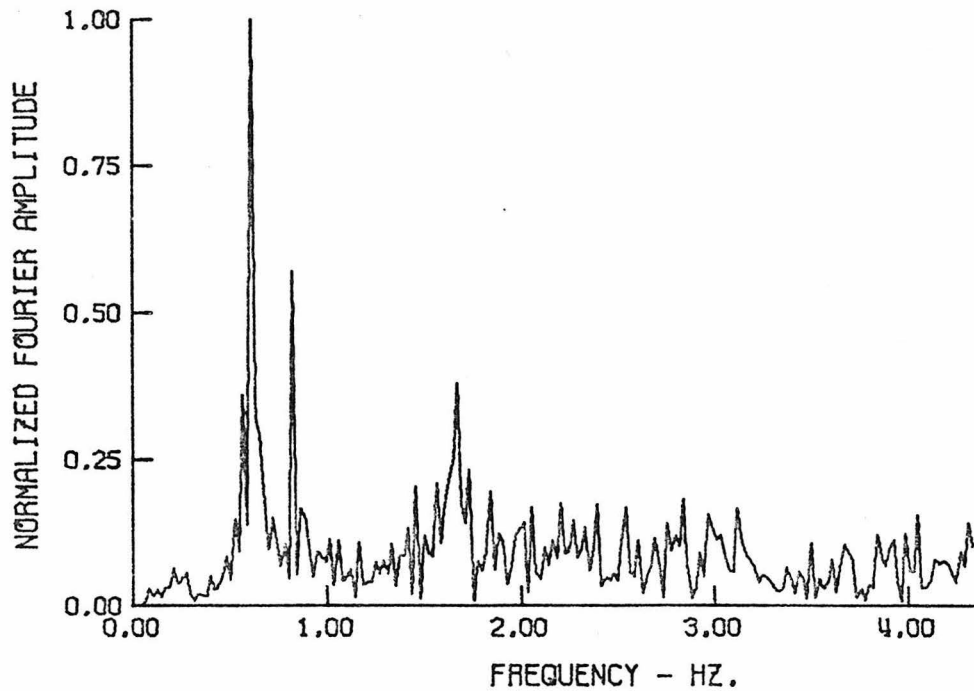
Preliminary tests of the Parsons building began in August 1975. At this time, ambient measurements were taken on the roof of the tower. Fourier amplitude spectra of the velocity response measured in the N-S and E-W directions at the geometric center of the roof are shown in Figure 5.7 (a) and (b), respectively. These tests served two purposes. The ambient tests provided a quick means of identifying the first three natural frequencies in each of the three principal directions (N-S, E-W and torsion). This information facilitated the frequency sweeps using forced excitation which tended to be laborious and time-consuming. Also, ambient tests were performed so that this type of testing could be evaluated as a possible replacement for forced vibration testing. This aspect of ambient testing will be discussed in more detail in a subsequent section of this chapter.

The approximate natural frequencies obtained from the preliminary ambient tests are listed in Table 5.1. Natural frequencies for E-W and torsional modes were somewhat difficult to identify due to coupling of these two types of modes. A degree of success was achieved by adding the responses of two points at the north and south edges of the slab to enhance E-W motion and subtracting the signals to emphasize torsional motions. Before calculation of Fourier spectra, all signals were low-pass analog filtered with a cutoff frequency of 12.5 Hz to remove high frequency noise, and sampled at 50 samples per second.

Modal interference and modal coupling should be redefined at



(a)



(b)

Figure 5.7 Fourier amplitude spectrum of velocity proportional response of roof during ambient excitation: (a) N-S response, (b) E-W response.

Table 5.1 - Natural Frequencies Estimated from Preliminary Ambient Tests

Mode	Frequency (Hz.)	Period (Sec.)
N-S 1	0.549	1.82
N-S 2	1.42	0.70
N-S 3	2.32	0.43
N-S 4	3.30	0.30
N-S 5	4.85	0.21
E-W 1	0.623	1.61
E-W 2	1.70	0.59
E-W 3	2.89	0.35
Tors. 1	0.647	1.55
Tors. 2	1.6 ?	0.63 ?
Tors. 3	2.23-2.25	0.45-0.44

this time since these terms are used extensively throughout this chapter. Modal interference occurs when two modes of vibration lie close to each other in the frequency domain. When this happens, the response of the structure about one natural frequency is influenced by components of motion of the other mode. Consequently, a pure mode is not excited in this case. Modal coupling, on the other hand, occurs when the centers of mass and rigidity do not coincide. This leads to both translational and rotational components of motion in a given mode of vibration. These ideas were discussed more extensively in the introduction to this thesis.

The next stage of the testing program involved preliminary frequency sweeps using forced excitation. The locations of the shakers on the roof plan are shown in Figure 5.8. For these tests the building was excited at a specific frequency until steady-state response of the structure was attained, at which time the responses of several points on the roof were recorded. The frequency of excitation was then increased and the process repeated. The results of these tests are shown in Figures 5.9, 5.10 and 5.11 for excitation in the N-S, E-W and torsional directions, respectively. Discontinuities in these curves result when changes were made in the weight combinations used in the shakers. The particular weight combination used for each segment of the curves is indicated on the figure. Since the Rangers were used as the motion sensing transducers, no absolute calibration was made. Therefore, for these tests, the magnitude of the double-amplitude of the response was normalized

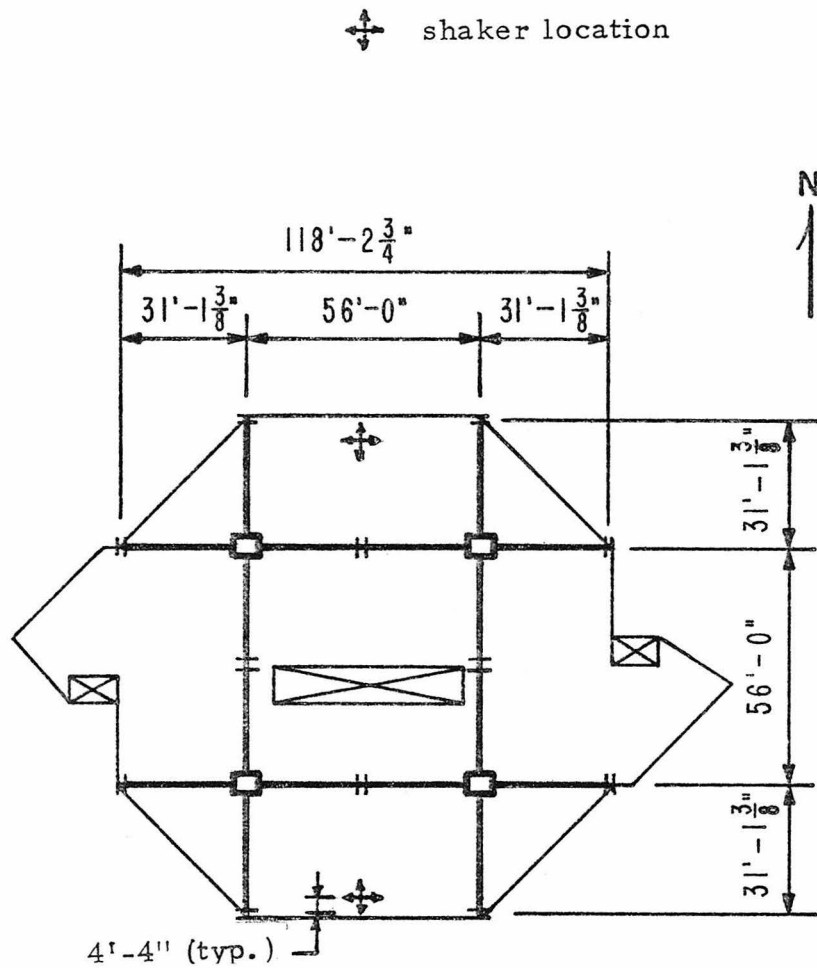


Figure 5.8 Typical tower floor plan with the location of the shakers indicated for the roof.

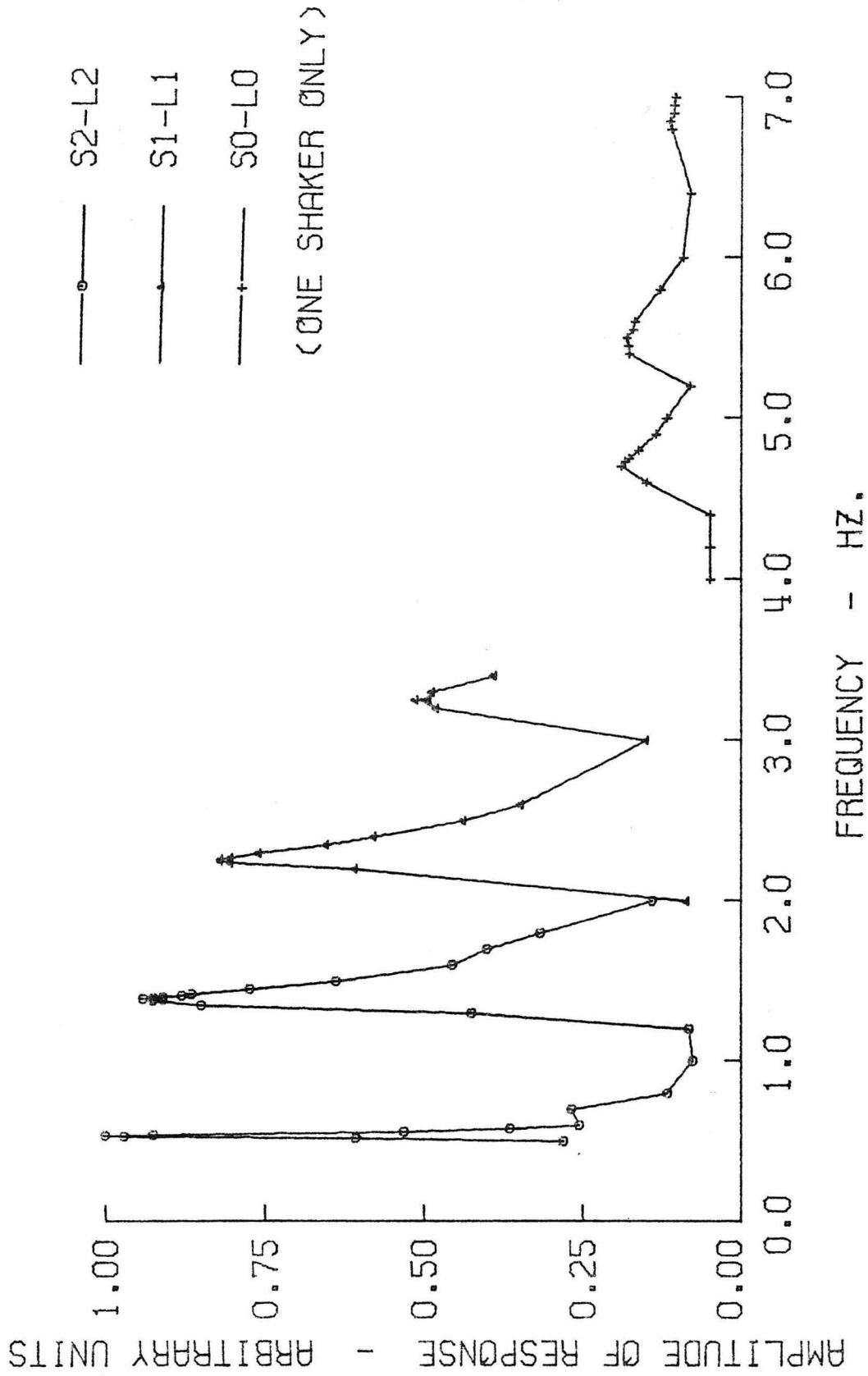


Figure 5.9 Preliminary frequency sweep for N-S excitation. Displacement proportional response of center of roof.

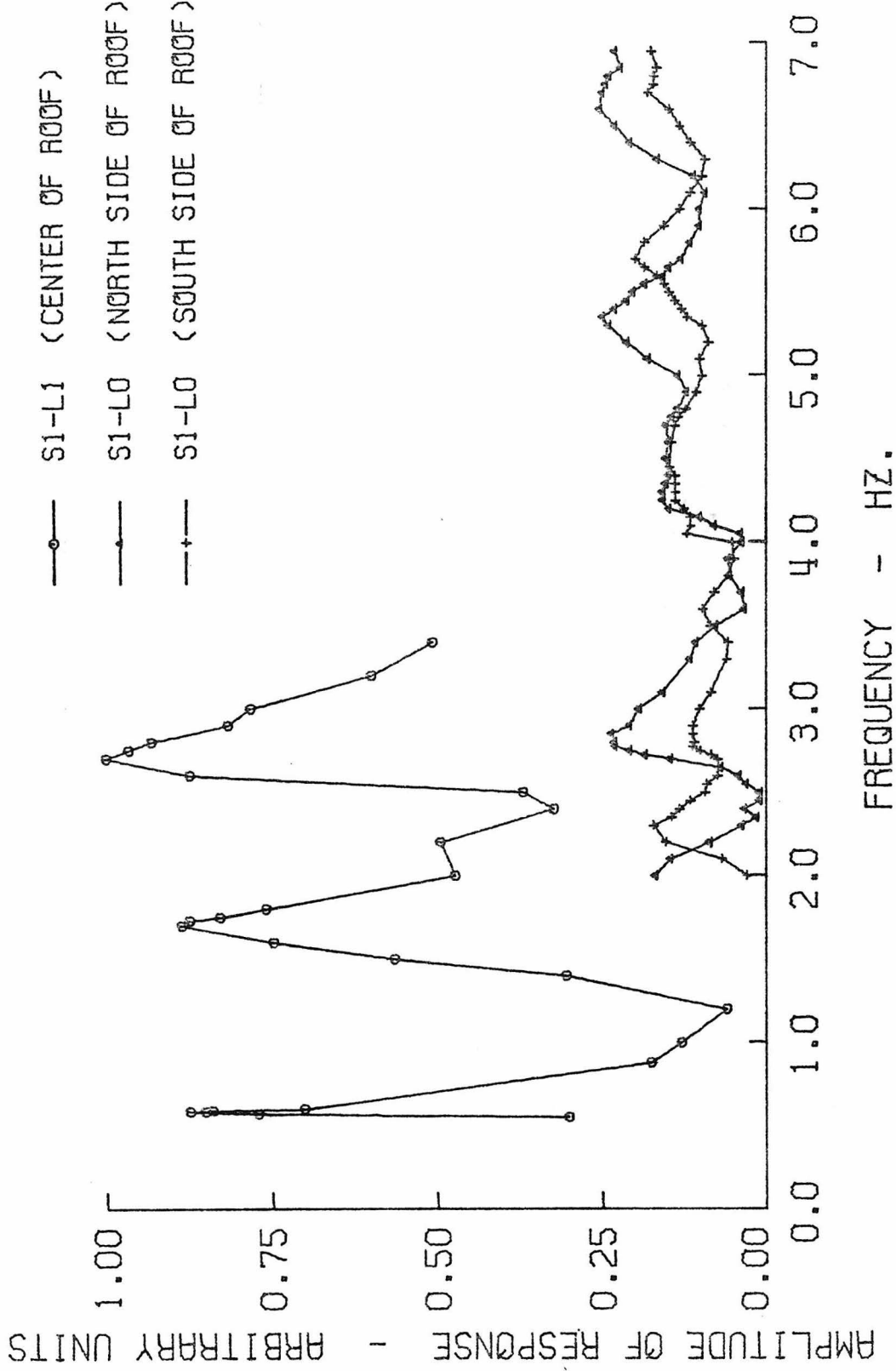


Figure 5.10 Preliminary frequency sweep for E-W excitation. Displacement proportional response of center of roof or north and south edges of roof.

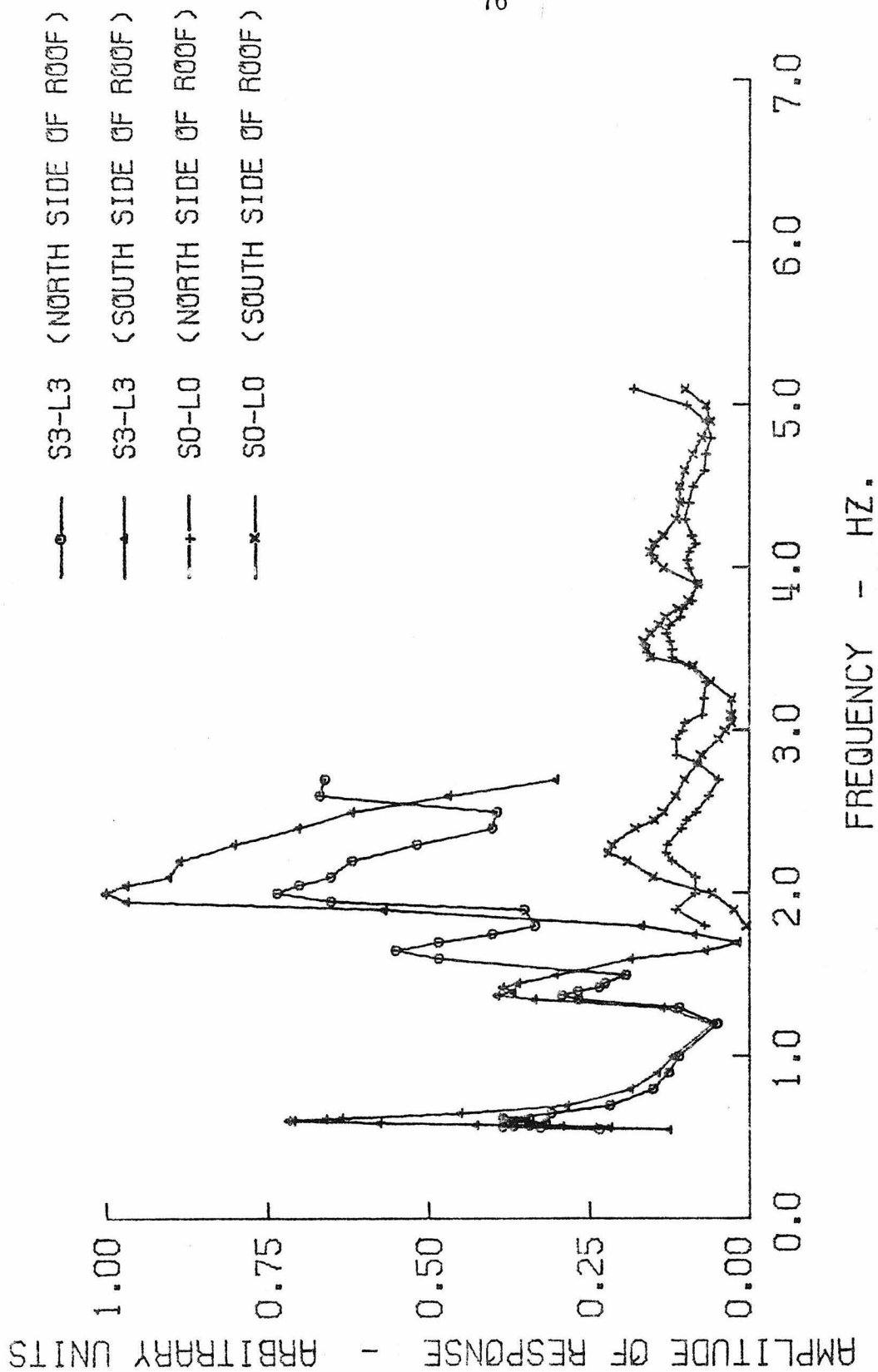


Figure 5.11 Preliminary frequency sweeps for torsional excitation. Displacement proportional E-W response of north and south edges of roof.

(divided by the largest response obtained) and then plotted versus frequency.

It is clear from Figure 5.9 that the first four natural frequencies in the N-S direction are rather well defined. This was not the case for the E-W and torsional frequencies, however.

For the E-W excitation shown in Figure 5.10, the second and third peaks for the S3-L3 force level appear quite broad. This can be indicative of modal interference, which can complicate the determination of damping using methods which rely on the width of the resonance curve. The results for the S1-L0 excitation on the same figure also reveal some interesting points. For this case the response of the north edge and the south edge of the roof are shown. Notice that at about 2 Hz the north side of the slab responds with a relatively high amplitude but the response of the south edge is quite small. This frequency corresponds to the third torsional resonance frequency which is being excited by E-W excitation. At about 2.3 Hz the opposite effect is present. The south edge of the roof has a large response but the north edge hardly moves. This frequency corresponds to the third N-S resonance frequency. In both of these cases the responses of the north and south edges were about  $90^\circ$  out of phase with each other. Both edges achieved a local maximum at the third E-W natural frequency of about 2.7 Hz and the responses were in phase. This indicates the importance of having more than one instrument on the roof when frequency sweeps are being conducted. Similar phenomena are clearly evident in the torsional frequency sweeps as

can be seen in Figure 5.11.

The natural frequencies determined from the preliminary frequency sweeps are listed in Table 5.2. These may be compared with the results from the ambient tests listed in Table 5.1. As would be expected, the N-S frequencies agree reasonably well considering the difference in the amplitudes of the response.

The E-W and torsional frequencies do not correspond very closely, however. The ambient values are consistently 5-10 percent higher than those obtained during the preliminary frequency sweeps. Since the level of response was 5-10 times larger during the forced tests, these differences are consistent with the nonlinear characteristics of the building which will be discussed in a subsequent section of this chapter. It is not clear, however, why this same phenomenon was not present in the N-S results. A more thorough evaluation of the ambient tests will be given in the last section of this chapter.

### 5.3 Natural Frequencies, Mode Shapes and Damping

As mentioned in the previous section, the presence of modal interference adds to the difficulty of determining accurate estimates of natural frequencies, mode shapes and damping. This problem arises because a pure mode may not be excited by applying a forcing function at the roof of a building. It was shown by Jennings<sup>34</sup> that this problem can often be overcome by measuring the 90° out-of-phase part of the total response of a given floor.

The total response of the  $i^{\text{th}}$  mass for an  $m r \omega^2 \cdot \sin(\omega t)$  excitation applied at the  $n^{\text{th}}$  level can be written<sup>24</sup>

Table 5.2 - Natural Frequencies Estimated from Preliminary  
Frequency Sweeps

Mode	Frequency (Hz.)	Period (Sec.)
N-S 1	0.535	1.87
N-S 2	1.39	0.72
N-S 3	2.26	0.44
N-S 4	3.25	0.31
N-S 5	4.70	0.21
E-W 1	0.581	1.72
E-W 2	1.58-1.70	0.69-0.64
E-W 3	2.58-2.80	0.39-0.36
E-W 4	4.2 -4.5	0.24-0.22
Tors. 1	0.605	1.65
Tors. 2	1.38	0.73
Tors. 3	2.0 -2.25	0.50-0.44

$$\ddot{x}_i = - \sum_{j=1}^n \frac{\phi_{ij} \phi_{nj} m r \omega^2 \frac{\omega^2}{\omega_j^2}}{\left(1 - \frac{\omega^2}{\omega_j^2}\right)^2 + (2\zeta_j \frac{\omega}{\omega_j})^2} \left[ \left(1 - \frac{\omega^2}{\omega_j^2}\right) \sin(\omega t) - (2\zeta_j \frac{\omega}{\omega_j}) \cos(\omega t) \right]. \quad (5.1)$$

Equation (5.1) indicates that there is a component of the response in phase with the force as well as a component  $90^\circ$  out-of-phase with it. Near the resonant frequency of the  $k^{\text{th}}$  mode, the contribution to the  $90^\circ$ -out-of-phase component of the response,  $\ddot{x}_i$ , from the  $j^{\text{th}}$  mode when  $j \neq k$  is minimal.<sup>34</sup> Consequently,

$$\ddot{x}_i \cong + \frac{\phi_{ik} \phi_{nk} m r \omega^2 \frac{\omega^2}{\omega_k^2}}{\left(1 - \frac{\omega^2}{\omega_k^2}\right)^2 + (2\zeta_k \frac{\omega}{\omega_k})^2} \left[ 2\zeta_k \frac{\omega}{\omega_k} \cos(\omega t) \right]. \quad (5.2)$$

Following Hoerner and Jennings<sup>24</sup>, let  $\omega = \omega_k(1 + \alpha \zeta_k)$ . Substituting this expression into equation (5.2) gives

$$\left| \ddot{x}_i \right| = \frac{\phi_{ik} \phi_{nk} \omega_k^2 (1 + \alpha \zeta_k)^4 \cdot 2\zeta_k (1 + \alpha \zeta_k)}{\left[ 1 - (1 - \alpha \zeta_k)^2 \right]^2 + 4\zeta_k^2 (1 + \alpha \zeta_k)^2}. \quad (5.3)$$

This expression achieves its maximum value

$$\left| \ddot{x}_i \right|_{\max} = \frac{\phi_{ik} \phi_{nk} m r \omega_k^2}{2\zeta_k} \quad (5.4)$$

where  $\omega = \omega_k$  or  $\alpha = 0$ .

Expanding (5.3) and simplifying yields

$$|\ddot{\bar{x}}_i| \cong \frac{2K[\alpha^5 \zeta_k^5 + 5\alpha^4 \zeta_k^4 + 10\alpha^3 \zeta_k^3 + 10\alpha^2 \zeta_k^2 + 5\alpha \zeta_k + 1]}{\zeta_k[(\alpha^2 + 4)(\alpha \zeta_k)^2 + 4(\alpha^2 + 2)(\alpha \zeta_k) + 4(\alpha^2 + 1)]} \quad (5.5)$$

where  $K = \phi_{ik} \phi_{nk} m r \omega_k^2$ . Jennings, et al.<sup>34</sup> used only the zeroth order terms in  $\zeta_k$ , or,

$$|\ddot{\bar{x}}_i| \cong \frac{K}{2\zeta_k(\alpha^2 + 1)} \quad (5.6)$$

Thus, for  $\alpha = \pm 1$

$$|\ddot{\bar{x}}_i| \cong \frac{K}{4\zeta_k} = \frac{1}{2} |\ddot{\bar{x}}_i|_{\max} \quad (5.7)$$

This states that the bandwidth of the resonance curve for

$|\ddot{\bar{x}}_i| = \frac{1}{2} |\ddot{\bar{x}}_i|_{\max}$  is  $2\zeta_k$ . This gives a method for measuring  $\zeta_k$ .

Using only the zeroth order term in  $\zeta_k$ , however, suggests that the  $90^\circ$  out-of-phase response curve should be symmetric about the resonant frequency. Figure 5.12 is a plot of the total response and the  $90^\circ$  out-of-phase component of the response of the fourth floor for N-S excitation around the third resonant frequency in that direction. The curve is clearly not symmetric about  $\omega_3$ . To determine if this amount of asymmetry should be expected and to verify if this method of determining damping is acceptable when it is present, one higher order of  $\zeta_k$  was retained in equation (5.5).

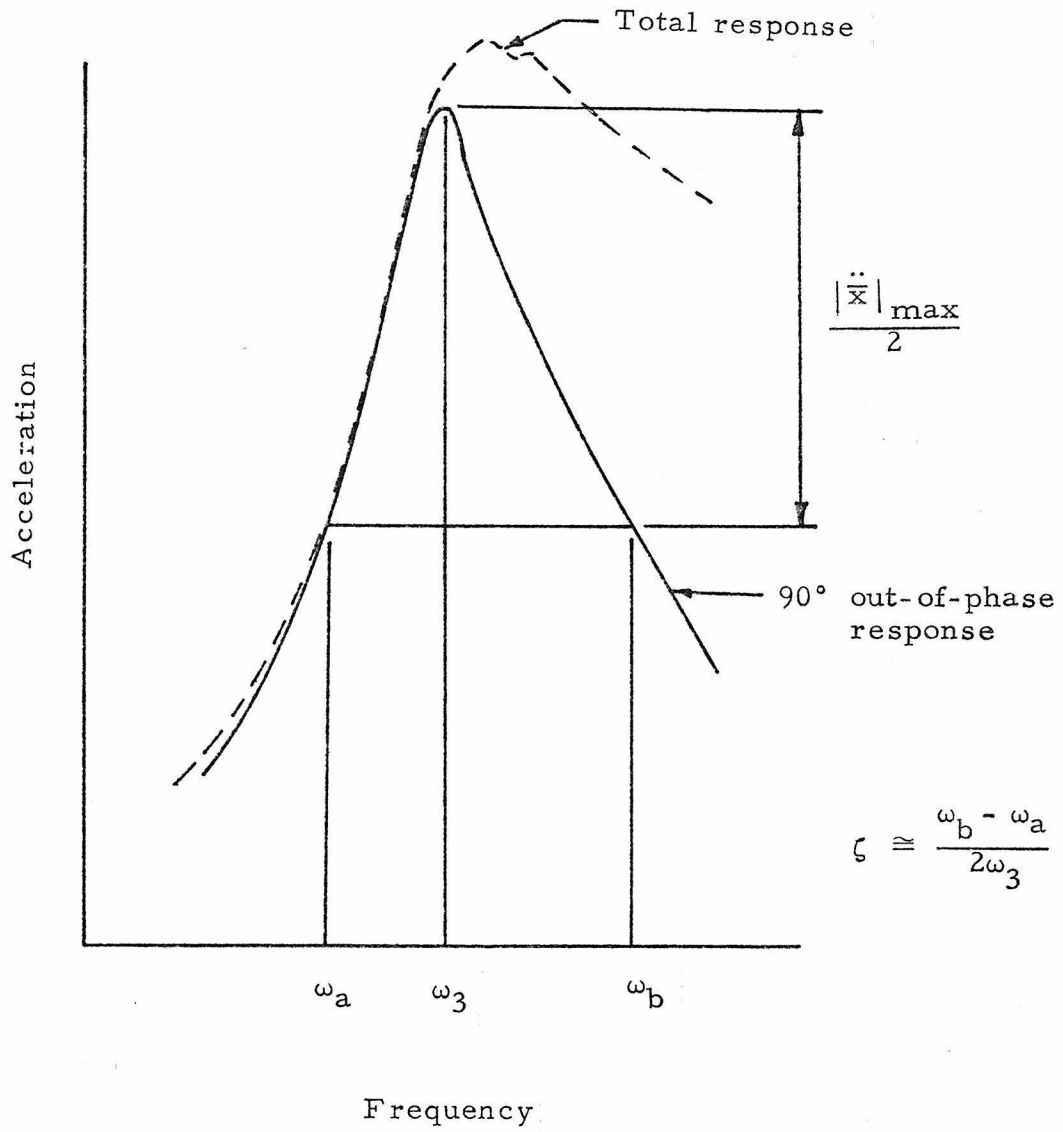


Figure 5.12 Determination of damping from out-of-phase component of acceleration. Third N-S resonant frequency.

To first order in  $\zeta_k$

$$|\ddot{x}_i| \cong \frac{K(1 + 5\alpha\zeta_k)}{2\zeta_k[(\alpha^2 + 2)\alpha\zeta_k + (\alpha^2 + 1)]} . \quad (5.8)$$

Solving this equation for  $|\ddot{x}_i| = \frac{1}{2}|\ddot{x}_i|_{\max}$  yields

$$\zeta_k \alpha^3 + \alpha^2 - 8\alpha\zeta_k - 1 = 0 . \quad (5.9)$$

Solutions for this equation for various values of damping are given in Table 5.3 along with values of the bandwidth and the amount of asymmetry to be expected for each case. These results indicate that the total bandwidth is quite stable even though the asymmetry increases quite rapidly with damping. For Figure 5.12 the value of  $\frac{\omega_b - \omega_k}{\omega_k - \omega_a}$  was about 1.5. This is somewhat higher than one would expect from Table 5.3 since the damping was only 4.1 percent of critical. This additional skewness could probably be explained using higher order terms in  $\zeta$  in equation (5.5).

Utilizing the procedure discussed above, the 90° out-of-phase components of the responses of the various floors were used to determine the natural frequencies, mode shapes and damping for the first nine modes of vibration of the Parsons building. The results included values for three modes each in the N-S, E-W and torsional directions. It was decided that the majority of the testing time would be devoted to studying in detail these nine modes since these would contribute the most to the total response of the building during an

Table 5.3 - Solutions to Equation (5.8)

$\zeta$	$\alpha$	bandwidth ( $\omega_b - \omega_a$ )	asymmetry ( $\omega_b - \omega_k$ )/( $\omega_k - \omega_a$ )
0.01	1.035 -0.965	2.000 $\zeta$	1.073
0.02	1.071 -0.931	2.002 $\zeta$	1.092
0.03	1.107 -0.898	2.005 $\zeta$	1.233
0.04	1.143 -0.865	2.008 $\zeta$	1.321
0.05	1.185 -0.834	2.019 $\zeta$	1.421
0.06	1.215 -0.803	2.018 $\zeta$	1.513

earthquake.<sup>50</sup>

The natural frequencies and damping values for these nine modes are listed in Table 5.4. Two items may be noted in this table. First, the building is somewhat more flexible than might be expected. The rule of thumb commonly employed is that the fundamental period of a steel-framed structure is about  $0.1 N$  where  $N$  is the number of stories. The fundamental period of the Parsons building is 1.91 seconds and  $0.1 N$  is 1.2 seconds. Secondly, the damping values are somewhat higher than are usually encountered for these low levels of excitation. It would be interesting to see if these trends are continued for earthquake excitations.

Due to the high in-plane rigidity of floor slab systems found in most multistory buildings, only small and insignificant in-plane deformations usually occur as a building vibrates. Consequently, only three dynamic degrees of freedom per floor (two translational and one rotational) are usually needed to describe adequately the dynamic behavior of the structure. This was also the case for the Parsons building. Consequently, two translational components and one rotational component of motion for each floor were determined for nine modes of vibration for the Parsons building. The three-dimensional motion of the structure when vibrating in a few selected modes was measured and is reported later in this chapter.

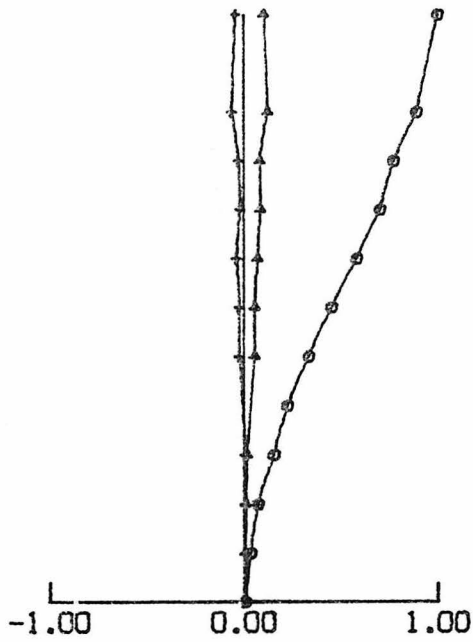
The  $\underline{x}$ ,  $\underline{y}$  and  $\underline{R\theta}$  components of the first nine modes of vibration are shown numbered in order of increasing frequency in Figures 5.13 through 5.17. These were determined using the S2-L2

Table 5.4 - Natural Frequencies and Damping Values for the First Nine Modes of Vibration of the Parsons Building

N-S TRANSLATION				E-W TRANSLATION			
Mode	Frequency Hz	Period Second	Damping % Critical	Mode	Frequency Hz	Period Second	Damping % Critical
1	0.523	1.91	2.5	1	0.566	1.77	4.1
2	1.36	0.74	4.8	2	1.57	0.64	6.4
3	2.13	0.47	4.1	3	2.57	0.39	4.4

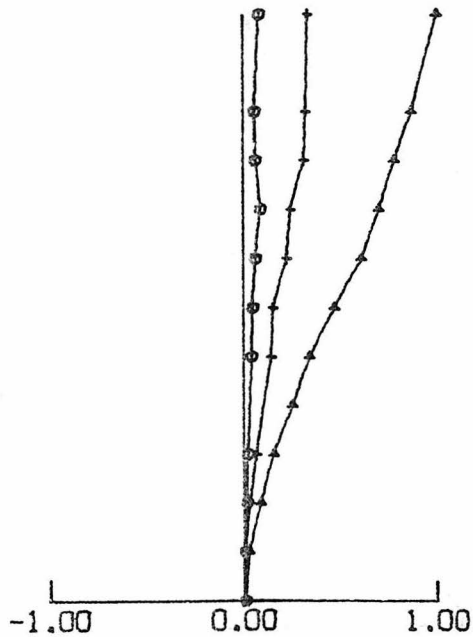
TORSION			
Mode	Frequency Hz	Period Second	Damping % Critical
1	0.612	1.63	4.0
2	1.38	0.72	4.8
3	2.02	0.50	-



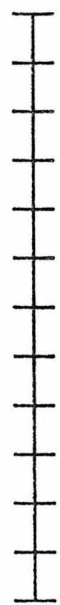
MODE 1  
0.523 HZ.



	X	Y	R0
12	1.00	0.10	-0.045
11	0.89	0.12	-0.069
10	0.77	0.078	-0.033
9	0.70	0.081	-0.021
8	0.58	0.068	-0.043
7	0.45	0.055	-0.029
6	0.33	0.055	-0.026
5	0.22	—	—
4	0.15	0.013	0.003
3	0.07	0.008	0.001
2	0.028	0.004	0.001
1	0.001	0.0002	0.0001

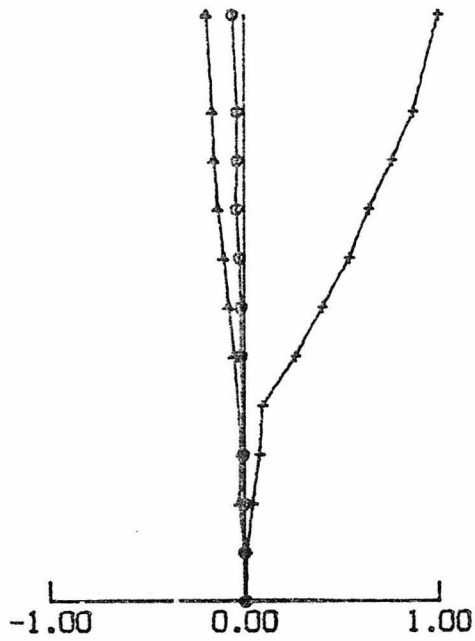


MODE 2  
0.566 HZ.



	X	Y	R0
12	0.076	1.00	0.33
11	0.054	0.87	0.32
10	0.057	0.78	0.31
9	0.085	0.70	0.24
8	0.057	0.61	0.22
7	0.042	0.47	0.15
6	0.036	0.34	0.14
5	—	0.25	—
4	0.017	0.15	0.065
3	0.011	0.081	0.027
2	0.002	0.025	0.003
1	0.0002	0.0026	0.0005

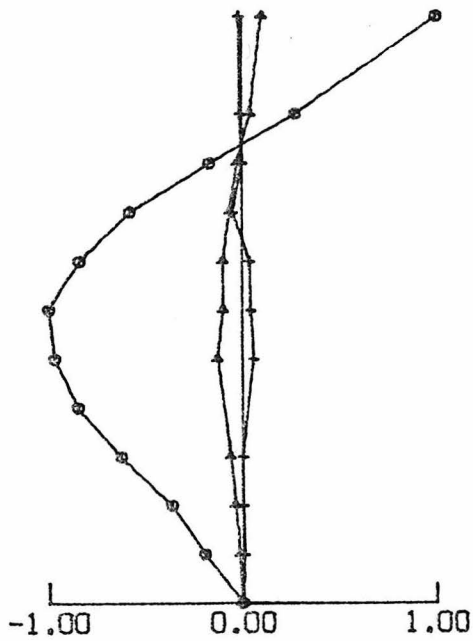
Figure 5.13 Natural frequencies and mode shapes of the Parsons building.



MODE 3  
0.612 HZ.



	X	Y	R0
12	—	—	—
11	-0.043	-0.17	0.87
10	-0.044	-0.16	0.76
9	-0.047	-0.14	0.64
8	-0.031	-0.11	0.54
7	-0.024	-0.089	0.40
6	-0.024	-0.055	0.26
5	—	—	0.088
4	-0.010	-0.024	0.072
3	-0.006	-0.030	0.040
2	-0.007	-0.006	0.009
1	-0.0002	-0.0006	0.0008

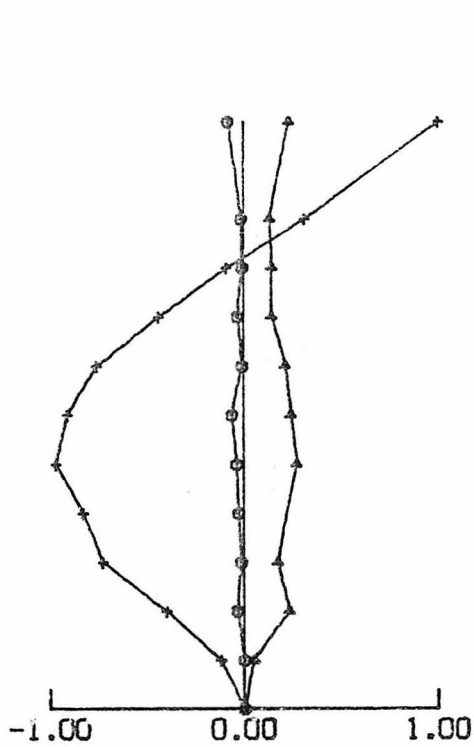


MODE 4  
1.36 HZ.



	X	Y	R0
12	—	—	—
11	0.27	0.036	-0.013
10	-0.17	-0.029	-0.002
9	-0.58	-0.069	-0.053
8	-0.84	-0.10	0.034
7	-1.00	-0.10	0.036
6	-0.97	-0.13	0.054
5	-0.85	—	—
4	-0.63	-0.067	-0.004
3	-0.37	-0.042	-0.002
2	-0.20	-0.020	0.002
1	-0.009	-0.013	-0.0003

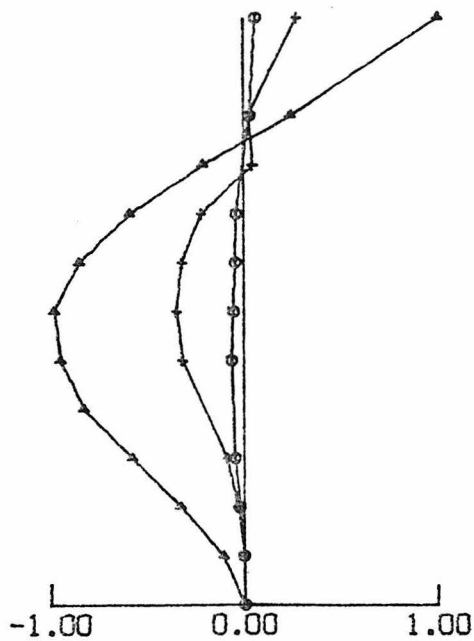
Figure 5.14 Natural frequencies and mode shapes of the Parsons building.



MODE 5

1.38 HZ.

	X	Y	R0
89			
R	-0.087	0.23	1.00
12	————	————	————
11	-0.019	0.13	0.31
10	-0.013	0.14	-0.092
9	-0.038	0.14	-0.44
8	-0.014	0.21	-0.76
7	-0.066	0.24	-0.91
6	-0.041	0.27	-0.97
5	-0.032	————	-0.83
4	-0.015	0.17	-0.73
3	-0.038	0.23	-0.40
2	-0.001	0.049	-0.12
1	-0.001	0.004	-0.004

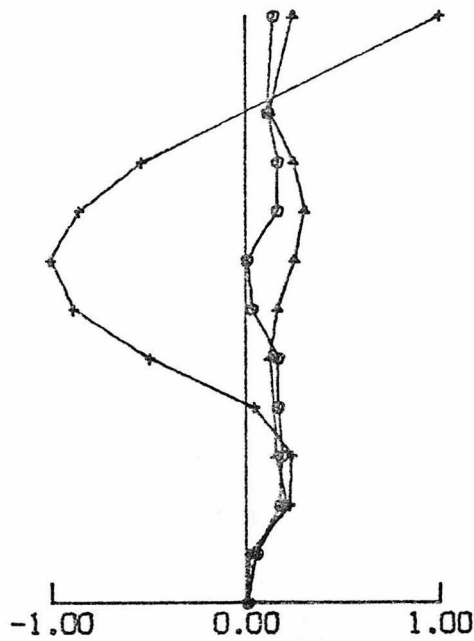


MODE 6

1.57 HZ.

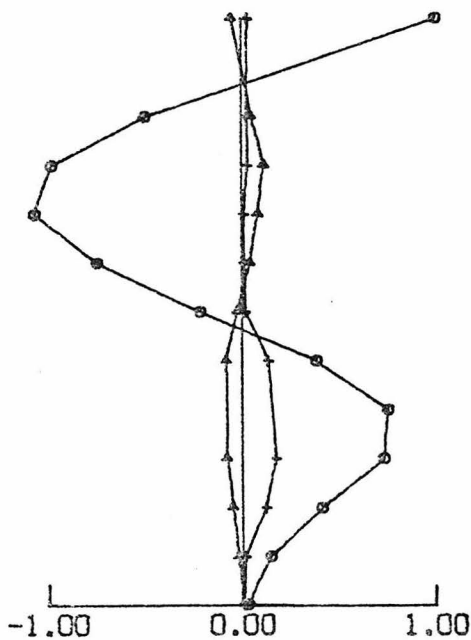
	X	Y	R0
89			
R	0.057	1.00	0.27
12	————	————	————
11	0.026	0.24	0.021
10		-0.21	0.041
9	-0.043	-0.59	-0.22
8	-0.048	-0.85	-0.32
7	-0.057	-0.98	-0.35
6	-0.069	-0.95	-0.32
5	————	-0.83	————
4	-0.052	-0.58	-0.093
3	-0.028	-0.33	-0.039
2	-0.006	-0.11	-0.004
1	-0.0006	-0.006	-0.002

Figure 5.15 Natural frequencies and mode shapes of the Parsons building.



MODE 7  
2.02 HZ.

R	X	Y	R0
12	0.14	0.24	1.00
11	0.11	0.12	
10	0.16	0.24	-0.54
9	0.16	0.30	-0.86
8	0.001	0.25	-1.01
7	0.027	0.16	-0.89
6	0.16	0.12	-0.50
5	0.16	—	0.04
4	0.18	0.15	0.23
3	0.17	0.20	0.22
2	0.048	0.042	0.014
1	0.003	0.001	0.004



MODE 8  
2.13 HZ.

R	X	Y	R0
12	1.00	-0.056	0.029
11	-0.50	0.042	0.024
10	-0.98	0.11	0.027
9	-1.07	0.077	0.007
8	-0.75	0.040	0.006
7	-0.22	-0.026	0.011
6	0.38	-0.089	0.13
5	0.75	—	—
4	0.73	-0.082	0.17
3	0.41	-0.053	0.12
2	0.14	-0.027	0.015
1	0.021	-0.001	0.001

Figure 5.16 Natural frequencies and mode shapes of the Parsons building.

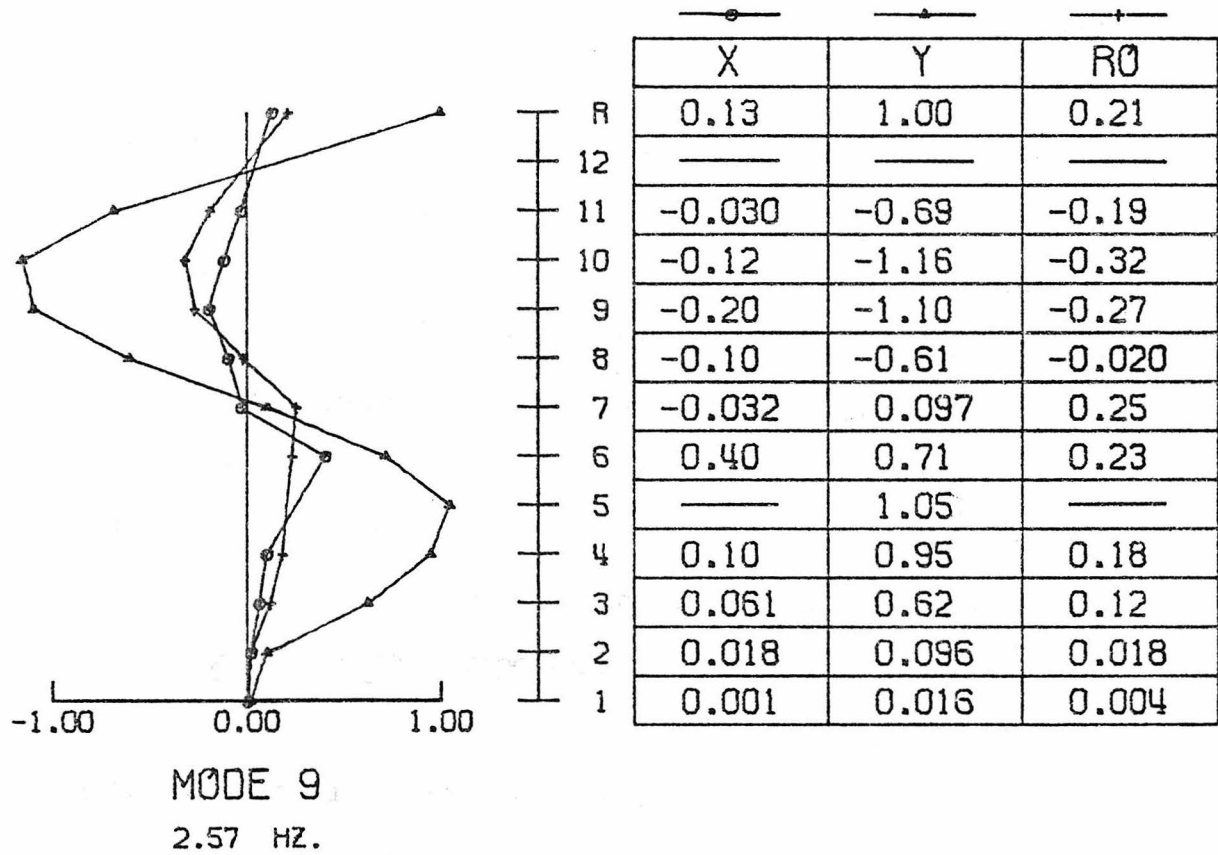


Figure 5.17 Natural frequencies and mode shapes of the Parsons building.

weight combination in the two shakers. The sign convention was chosen to be consistent with the one used for the finite element model of the structure which will be discussed in Chapter VI. Positive  $x$  corresponds to north for the building, while positive  $y$  is in the west direction. Counterclockwise rotation is positive. The center of the coordinate system was chosen as the geometric center of the tower floor plan. Consequently, positive  $x$  and  $y$  movement corresponds to N and W motion, respectively, of the centroid of the floor. It was felt that when plotting the mode shape the value used for  $R$  should be the same for all floors. The radius of gyration is not the same for each floor so this was not used. The value chosen for  $R$  is the distance from the centroid of the tower floor plan to the nearest exterior column of the building which is  $59' - 1\frac{3}{8}"$ . Consequently, using the  $\underline{x}$ ,  $\underline{y}$  and  $\underline{R}\theta$  components of a particular mode, one can determine the motion of the exterior columns which would be the most highly stressed during an earthquake.

A few points are noteworthy for these figures. The mainly N-S modes (modes 1, 4, and 7) have relatively small components in the  $y$  and  $R\theta$  direction. This should be expected since the building is nearly symmetric about the N-S centerline. Another interesting detail is the apparent discontinuity at the fifth floor level for the  $\underline{R}\theta$  component of mode 3 which is the first torsional mode. This is the level at which the tower rises above the lower portion of the building. One might wonder whether or not the finite element model would predict this detail. A final point to note is that the E-W modes and

torsional modes are relatively highly coupled in the sense that they show relatively large secondary components of motion. This is due to the asymmetry of both stiffness and mass distribution in the E-W direction. The significance of this is that primarily torsional modes are more easily excited from pure E-W motion of the base of the building than if the building were symmetrical in the E-W direction.

#### 5.4 Three-Dimensional Motion of Three Floors and the Surrounding Ground

The results of the tests of Millikan Library which were presented in Chapter III revealed that, even though in-plane deformations of floor slabs are insignificant, the out-of-plane deformations that the slab experiences can often reveal interesting characteristics of the overall behavior of the structural system being investigated. If three components of motion are measured for each of several points on a floor slab of a building during forced excitation, a plot of the resulting displacement vectors gives an interesting view of the three-dimensional nature of the deformations of the slab. These measurements also seem to verify the accuracy of the assumption of negligible in-plane motion that is so useful in analysis for design.

Three-dimensional motions were measured for three floors of the Parsons building as well as the surrounding ground. These measurements were made using the same seismometer package and procedure that was used for the Millikan Library tests. The three components of motion were measured at approximately 16 points on the tenth floor for seven modes of vibration (three N-S, two E-W and two

torsional), at approximately 25 points on the fourth floor for six modes of vibration (three N-S, two E-W and one torsional) and at approximately 29 points on the first floor for six modes of vibration (three N-S and three E-W).

The results of these measurements are plotted in Figure 5.18 through 5.29 in the same format used for the Millikan test results. The circles represent the displaced position of the measured points. These are connected by the heaviest lines in the figures. Note that some of the points connected by heavy lines were not measured so there is no circle representing their displaced position. Their locations were inferred from the movement of the measured points. The scale of length 1.00 located at the upper left corner of each figure represents the major component of roof motion for that particular mode. For instance, 1.00 for a figure representing N-S excitation is the normalized displacement of the north translational component of the centroid of the roof for that mode; but it represents the  $R\theta$  component of motion for a torsional mode. This scheme was not used for the first floor figures, however, since the motion there was only one hundredth to one thousandth of the roof motion, the scale for these figures is in terms of absolute displacement and a different scale was selected for each of the first floor plots to increase their clarity.

The purpose of this set of figures is two-fold. They give a pictorial representation of the  $x$ ,  $y$ , and  $R\theta$  motions of the various floors, and they give a visual indication of the amount and significance

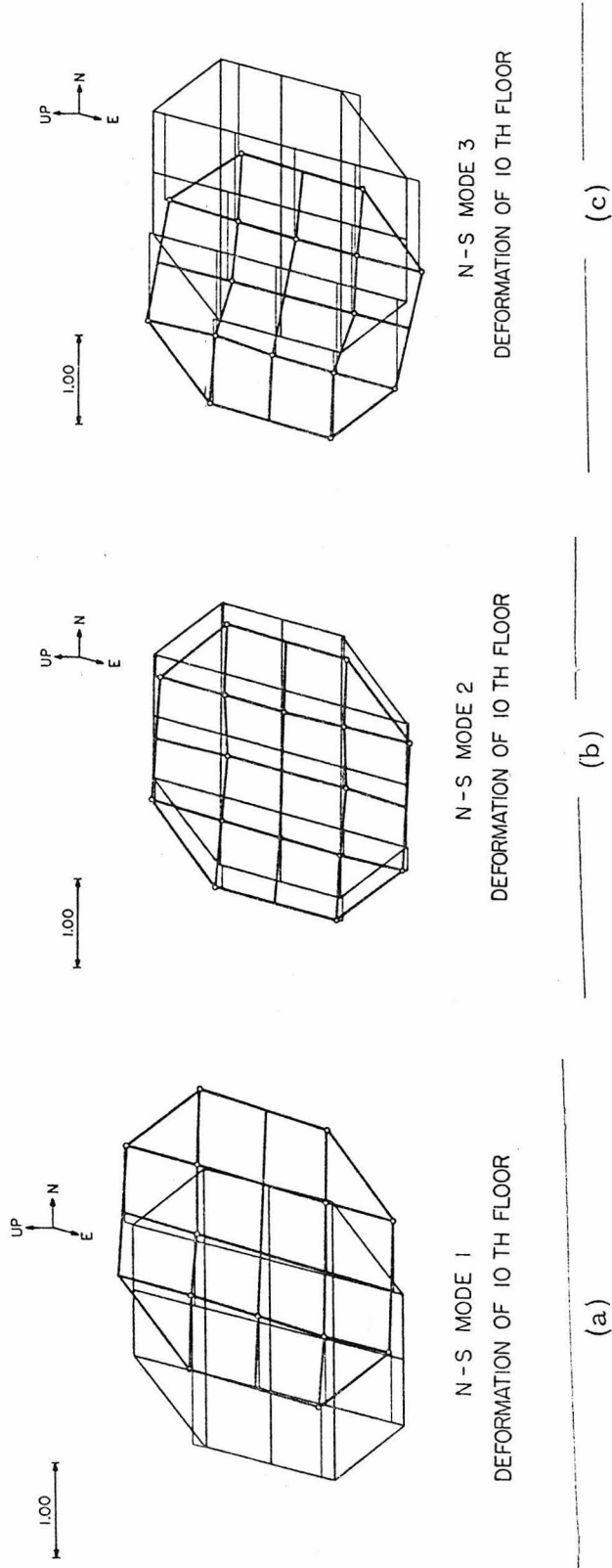
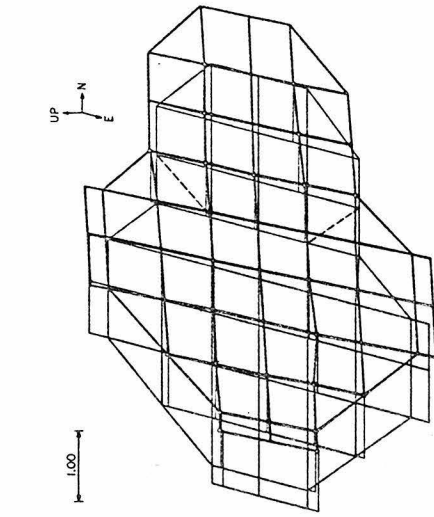
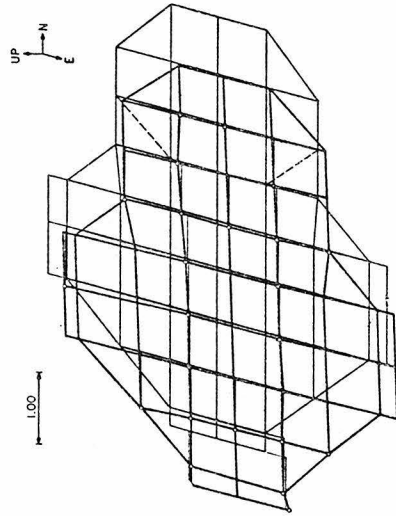


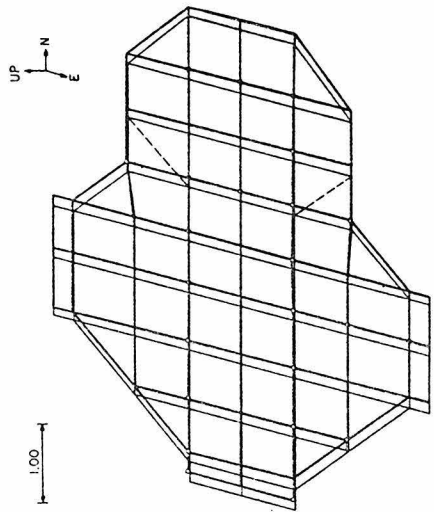
Figure 5.18



N-S MODE 3. DEFORMATION OF 4 TH FLOOR



N-S MODE 2. DEFORMATION OF 4 TH FLOOR



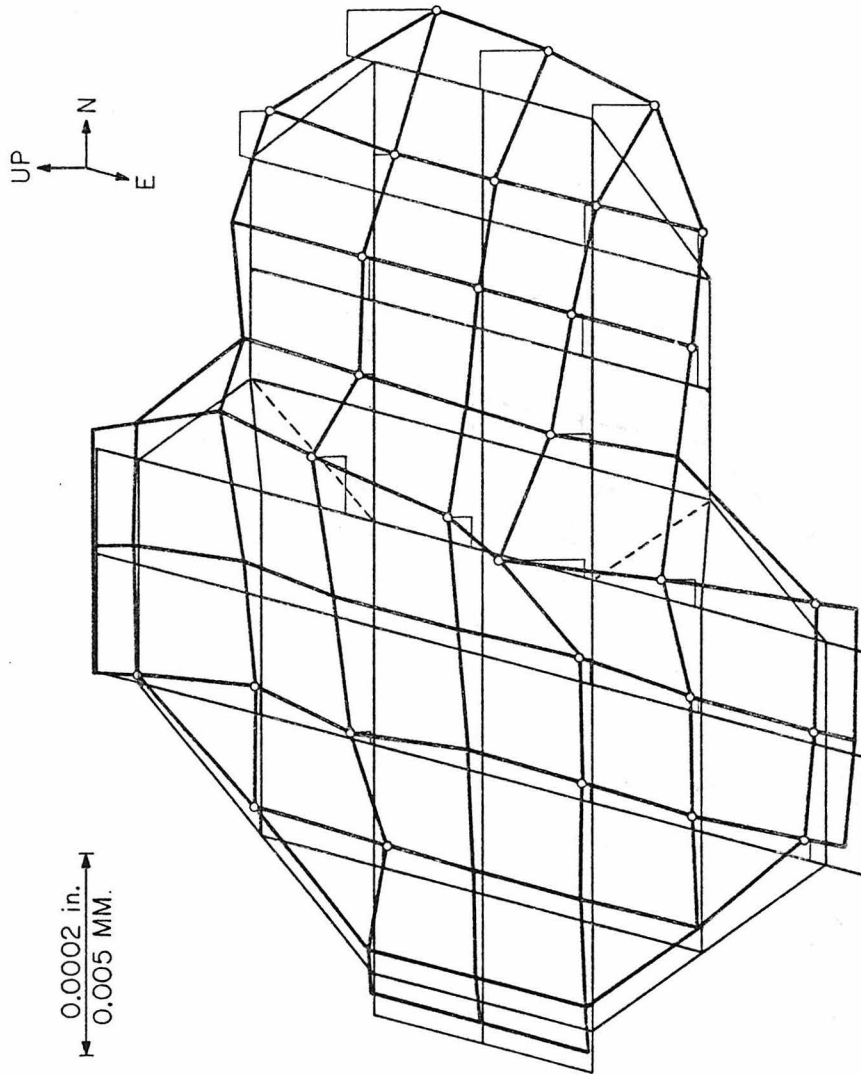
N-S MODE 1. DEFORMATION OF 4 TH FLOOR

(a)

(b)

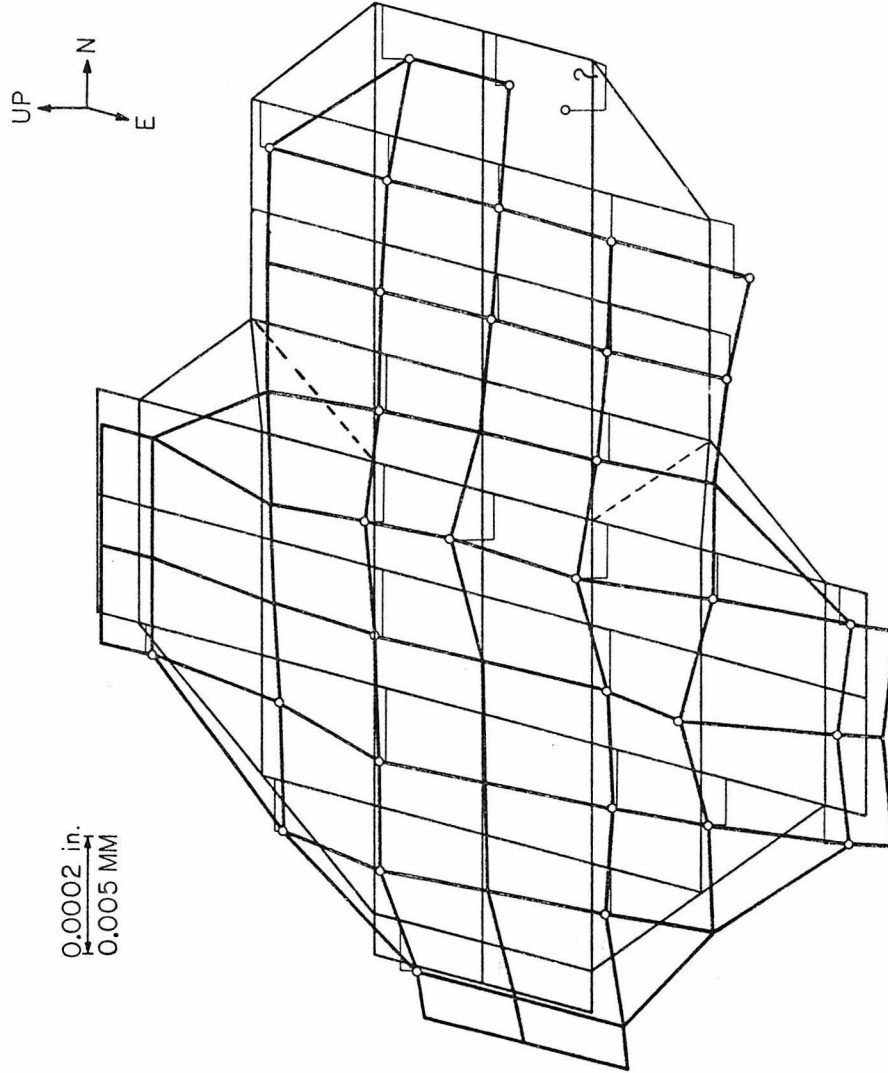
(c)

Figure 5.19



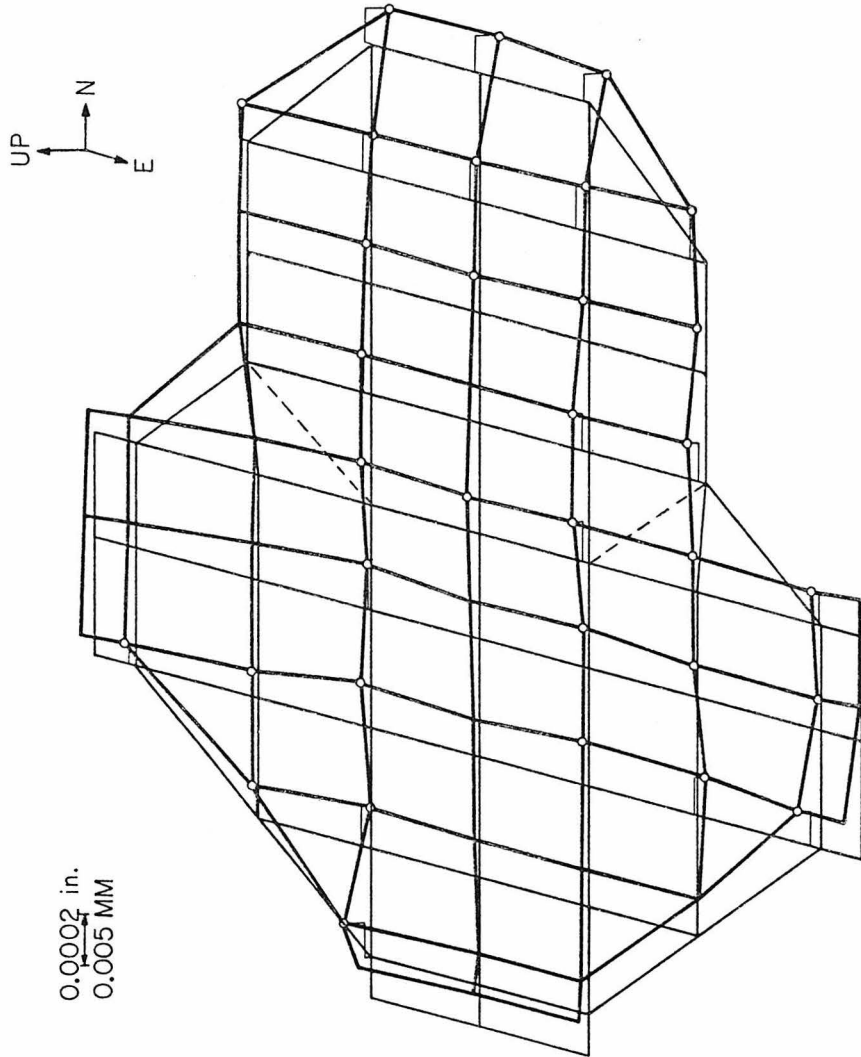
N-S MODE I. DEFORMATION OF 1 ST FLOOR

Figure 5.20



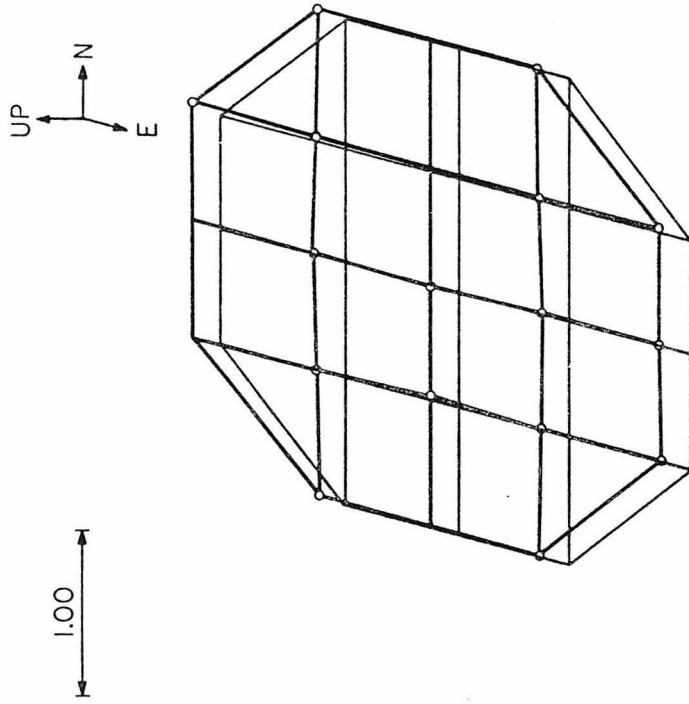
N-S MODE 2. DEFORMATION OF 1 ST FLOOR

Figure 5.21

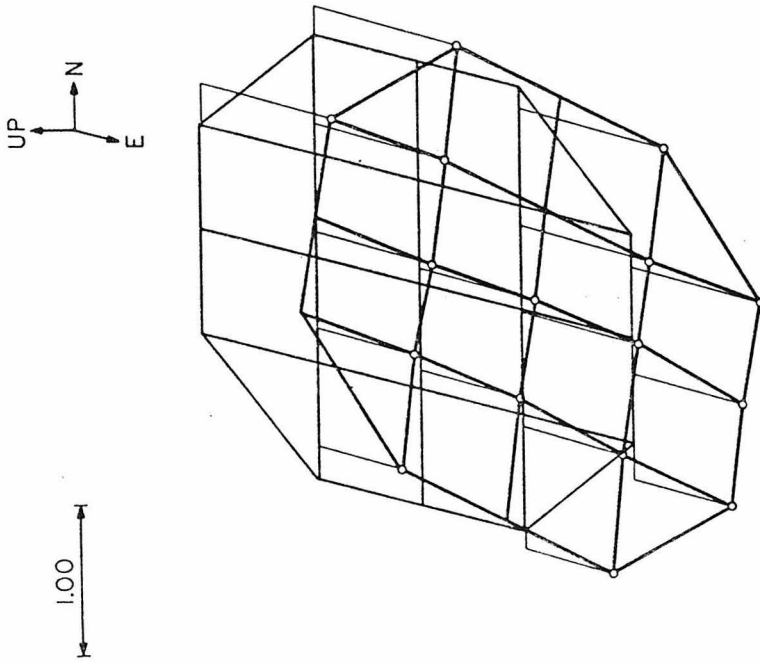


N-S MODE 3. DEFORMATION OF 1 ST FLOOR

Figure 5.22

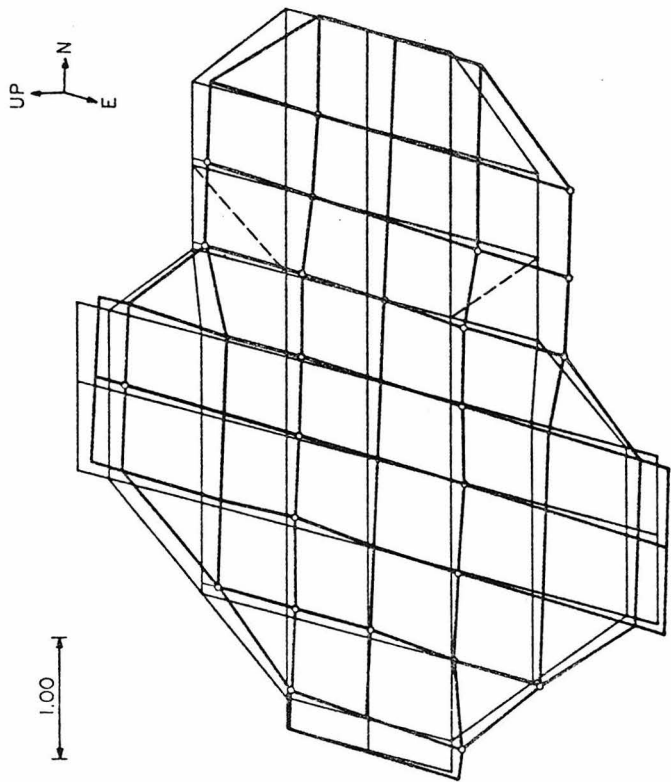


E - W MODE 2  
DEFORMATION OF 10 TH FLOOR



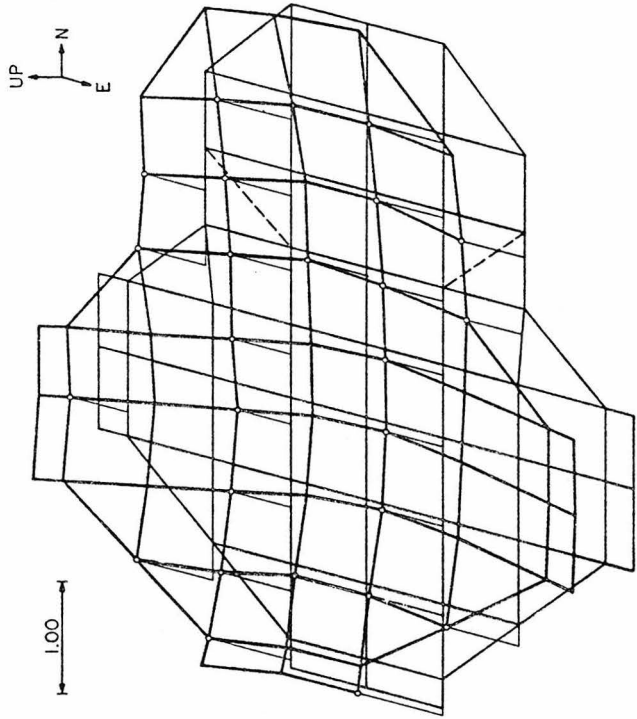
E - W MODE 1  
DEFORMATION OF 10 TH FLOOR

Figure 5.23



E-W MODE 1. DEFORMATION OF 4 TH FLOOR

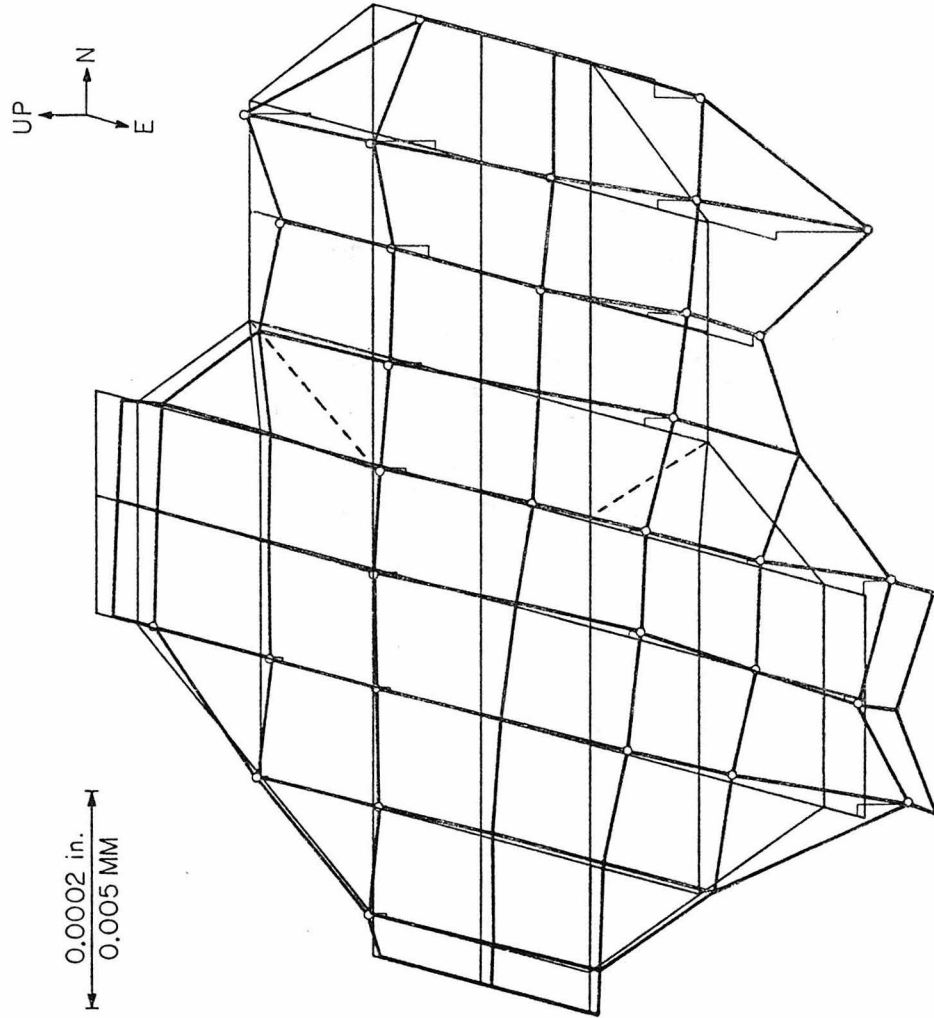
(a)



E-W MODE 2. DEFORMATION OF 4 TH FLOOR

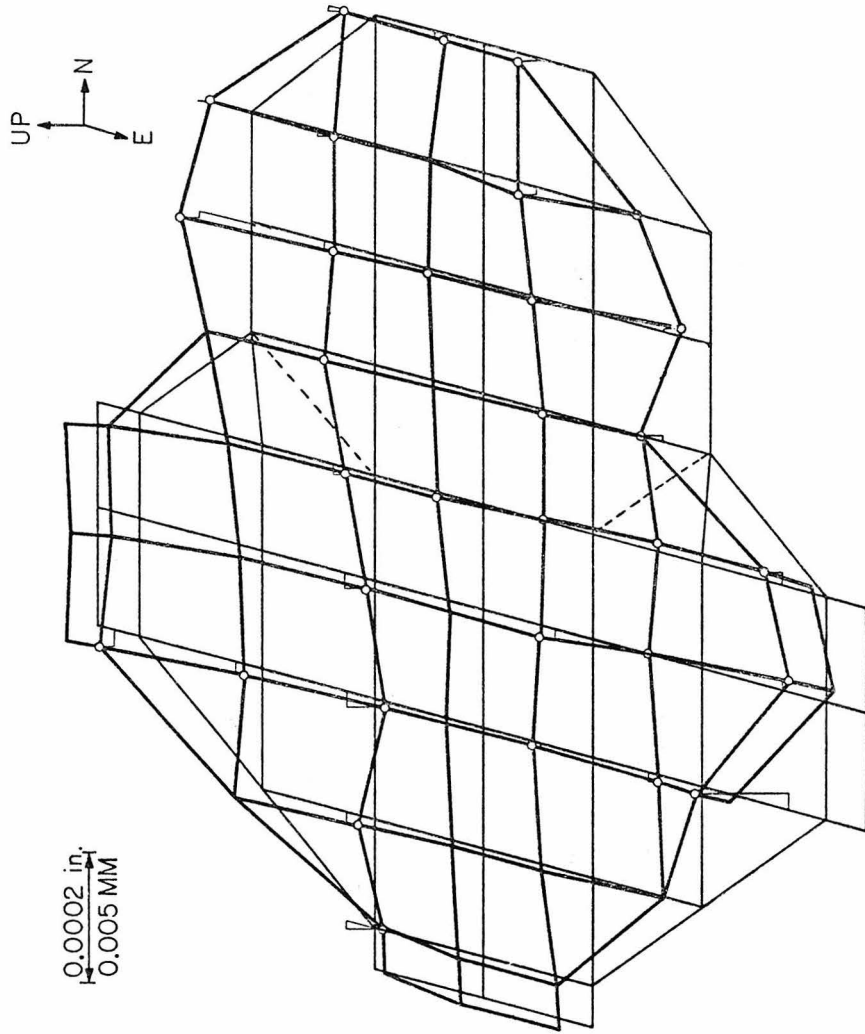
(b)

Figure 5.24



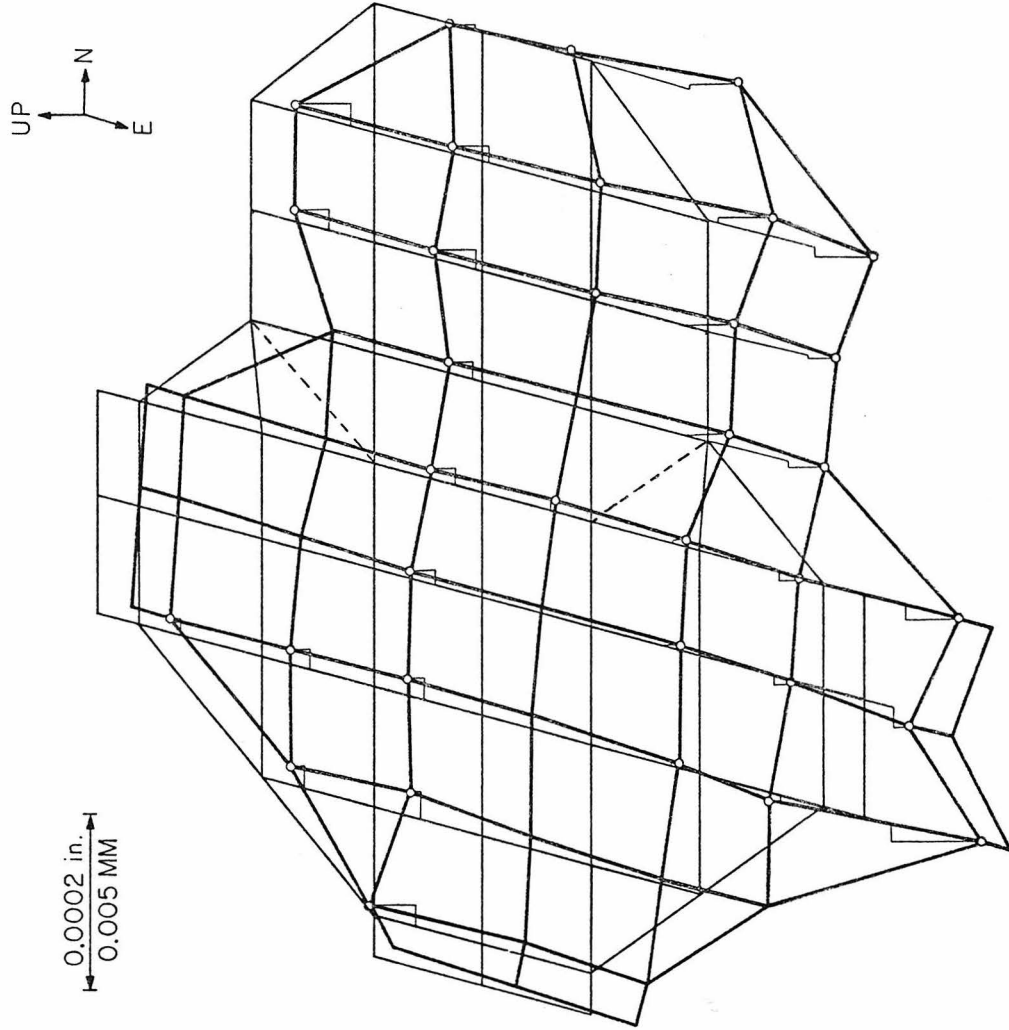
E-W MODE I. DEFORMATION OF 1 ST FLOOR

Figure 5.25



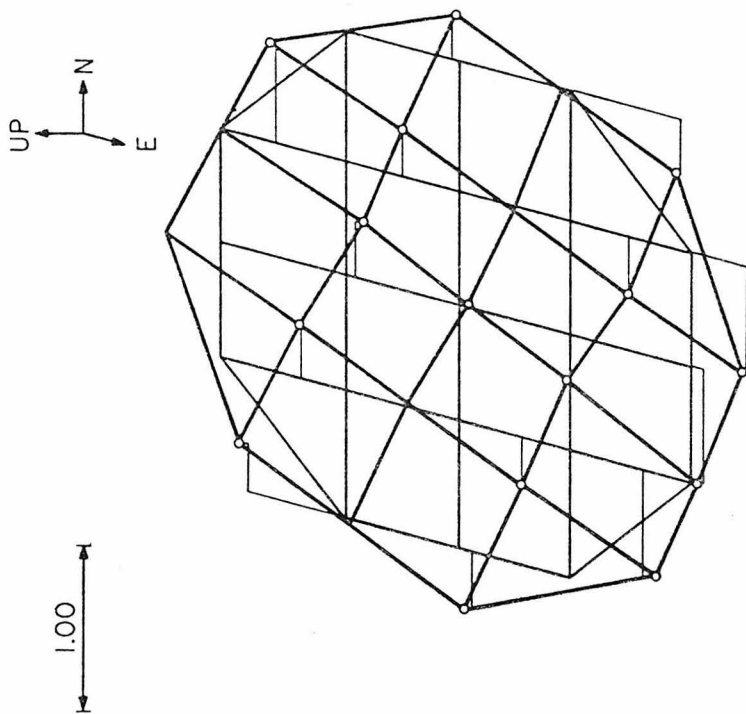
E-W MODE 2. DEFORMATION OF 1 ST FLOOR

Figure 5.26



E-W MODE 3. DEFORMATION OF 1 ST FLOOR

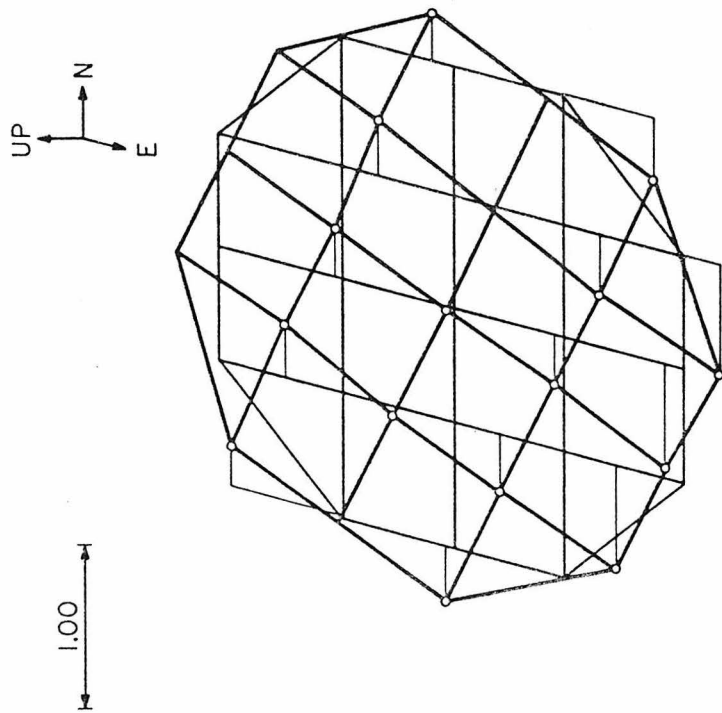
Figure 5.27



TORSION MODE 1

DEFORMATION OF 10 TH FLOOR

(a)



TORSION MODE 2  
DEFORMATION OF 10 TH FLOOR

(b)

Figure 5.28

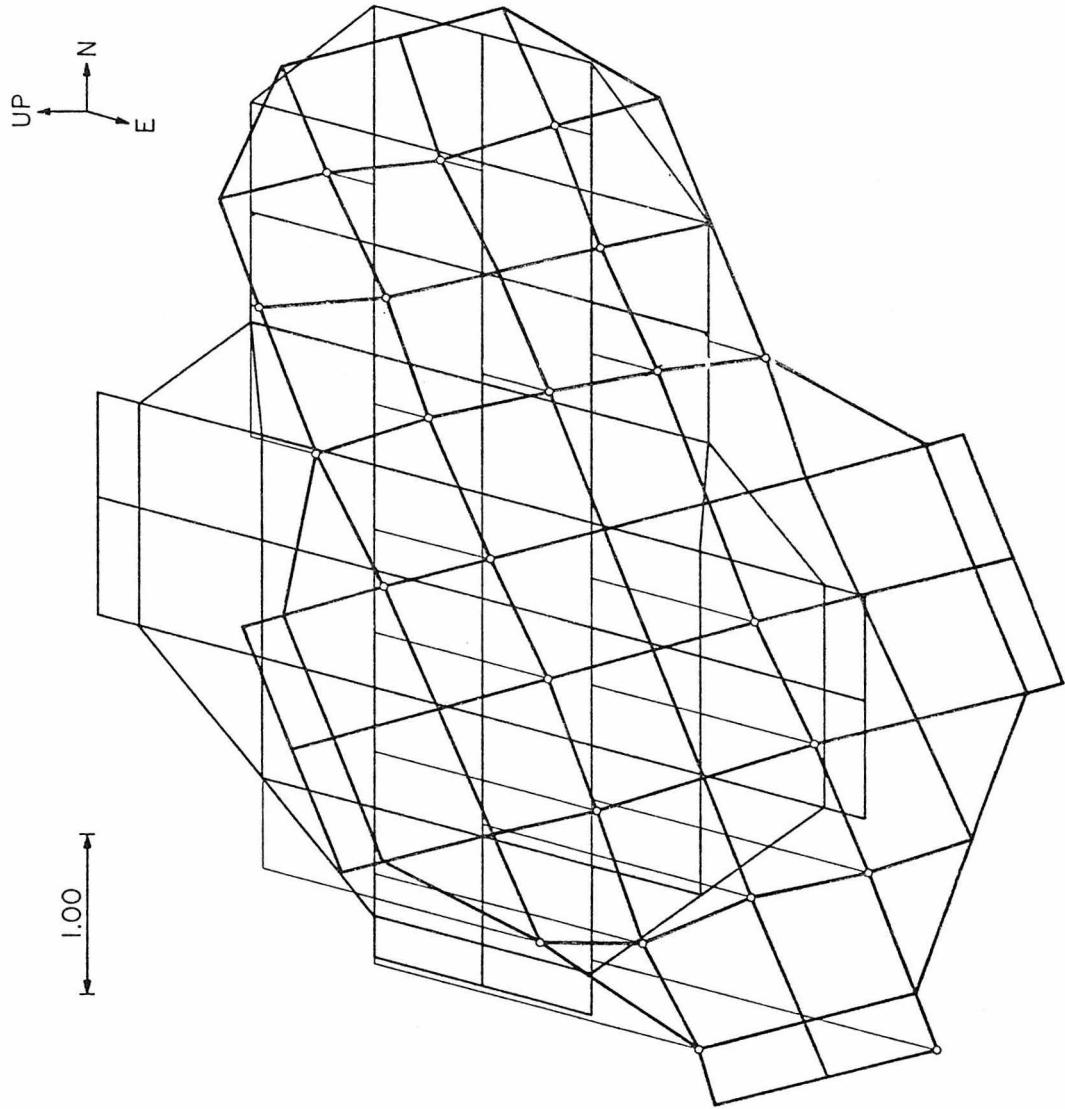


Figure 5.29 TORSION MODE 2. DEFORMATION OF 4TH FLOOR

of vertical motions.

The three-dimensional motions for the first three N-S modes of vibration for floors ten, four and one are shown in Figures 5.18, 5.19 and 5.20 through 5.22, respectively. The interpretation of these figures for the tenth and fourth floors is rather straightforward. The major component of motion for these floors is N-S translation as was discussed in the preceding section. The largest rotational motions occurred for the third mode for each floor. The vertical motion was relatively small in all cases for these two floors. The largest relative vertical motion for the tenth floor and the fourth floor occurred in the second mode at points E4 and E6 (see Figure 5.3 for location designations). These were approximately 6 percent as large as the roof translation for the tenth floor and 5 percent for the fourth floor.

The relative motion on the first floor was quite small for all three N-S modes. The largest first floor motions were vertical for the first N-S mode and occurred at points A4 and E6. These are on the northernmost and southernmost column lines of the tower section. These were about twice as large as the average translational motions of the first floor. Since these vertical motions are only 0.3 percent of the roof motion they are not directly important to the overall dynamic behavior of the building. The maximum vertical motion for the first floor for the second and third N-S modes occurred on the same E-W column lines as for the first mode, but were smaller in magnitude. The maximum vertical motion for the second N-S mode was 20 percent of the average translational motion of the base or

0.1 percent of the roof motion. For the third N-S mode the largest vertical motion of the first floor was 65 percent as large as the average floor translation and 0.6 percent of the N-S roof translation.

The only really unusual result of the first floor measurements occurred for vibration in the second N-S mode and is shown in Figure 5.21. The motion of the easternmost column of the E-W column line at the north edge of the tower (point A6 of Figure 5.3) appears to move up as the adjacent points move down. This is not believed to be representative of the true behavior of the slab at this point. A separation joint runs along the north edge of the first floor of the tower to provide isolation from an underground structure which extends to the north of the building. Due to architectural features of the building in this vicinity it was not possible to locate the column exactly. Consequently, the seismometer package may have been placed on the northern side of the separation joint outside of the tower or possibly even directly on it. If this was the case, a complicated interaction of the two structures across this joint may account for this anomaly.

The deformations of the tenth, fourth and first floors for vibration in the E-W modes are shown in Figures 5.23 through 5.27. The rotational component of these motions is clearly present as was discussed in the previous section. This effect is most noticeable for the tenth floor for the first E-W mode; but there seems to be only a small amount of rotation of the tenth floor for the second E-W mode. The vertical motions are in general less than one percent of the translational component and are therefore insignificant.

A surprising result is seen in Figure 5.24. For vibration in the second E-W mode, it appears that there is a rather large in-plane deformation of the floor slab. Nielsen<sup>49</sup> observed a similar phenomenon when testing Building 180 of the Jet Propulsion Laboratory. He identified it as a vibrational mode of the floor slab vibrating as a free-free beam. The geometry of the floor slab he studied was quite different, however, since the length-to-width ratio for Building 180 is about 5.5. For the fourth floor of the Parsons building it is variable and ranges between one and two. Also, the pattern of deformation seen in the figure is clearly a two-dimensional phenomenon. These two aspects of the problem preclude any simple modeling of the slab as a simple beam. A more complex analysis of the slab system would be required to assess the significance of the observed phenomenon. Since this type of behavior was not observed for any of the other floors and since the deformation is small compared to the overall translation of the slab, its effect on the overall dynamic behavior of the building is believed to be small.

Care should be taken in interpreting Figures 5.25 through 5.27 which show the first floor deformations for the first three E-W vibrational modes. The graphical presentation of these figures is difficult to interpret due to the small angle between the vertical axis and the E-W axis. The deformations seen in the first floor of all three E-W modes are about as one would expect. There is an overall translation and rotation of the first floor slab as well as a substantial amount of deformation in the slab itself. The largest vertical motions occurred on the exterior

columns of the E-W moment resisting frame of the tower portion during vibration in the first E-W mode. The largest vertical motions were about 130 percent of the maximum translational component for this case. For the second and third modes the maximum vertical motion occurred at point G8. The vertical motion there was about 2.5 times larger than the E-W horizontal component at this point for the second mode, and it was about 1.3 times greater in the third mode.

The motion of the tenth floor, shown in Figure 5.28, is almost a pure rotation for the first two torsional modes. There are small E-W and N-S translational components but the vertical motion was almost undetectable. This is also true for the fourth floor vibrating in the second torsional mode as is seen in Figure 5.29. This figure gives a good visual representation of the potential hazard of torsional motions in buildings. Since the center of rotation of the floor is located in the tower section, the lateral motion due to this rotation is amplified towards the south end of the building. Consequently, if this mode is excited, the columns at the south end of the structure will experience considerably higher stresses than if only purely translational motion was present. Any analysis of the dynamic response of the building should account for this effect.

Measurements of the three-dimensional deformations of the ground surrounding the Parsons building were made for shaking in the first three N-S modes and the second and third E-W modes. Due to the small amount of motion associated with the lower modes, measurements were only taken on an E-W line that extends through the center

of the tower for the first and second N-S and E-W modes. These results are shown in Figure 5.30 and Figure 5.31 for the first and second N-S modes. Results for the second E-W mode are shown in Figure 5.33. Measurements were taken at about 50 points for shaking in the third N-S mode and third E-W mode and the results are plotted in Figure 5.32 and Figure 5.34, respectively.

One feature of the result of these measurements was that the points next to, but outside of, the building moved only about half as much as adjacent points inside the building. Apparently this is due to the effect of the separation joints surrounding the first floor slab.

A surprising phenomenon appears in Figure 5.32 which shows the ground deformations for vibration of the building in its third N-S mode. The figure indicates almost all of the points on the ground surrounding the structure move upward as the roof of the structure moves to the north. This is not consistent with the downward movement of the points on the first floor inside the building which are north of the E-W centerline of the tower. This is probably caused by interaction between the tower and the satellite structures. The points outside and to the north of the tower are located on a parking lot directly under the satellite structures. Since the third N-S mode of the main building has an antinode between its fourth and fifth floors, a relatively large amount of energy is input to the satellite structure through the separation joints between the buildings. As the tower motion forces the satellite structures northward, the southernmost

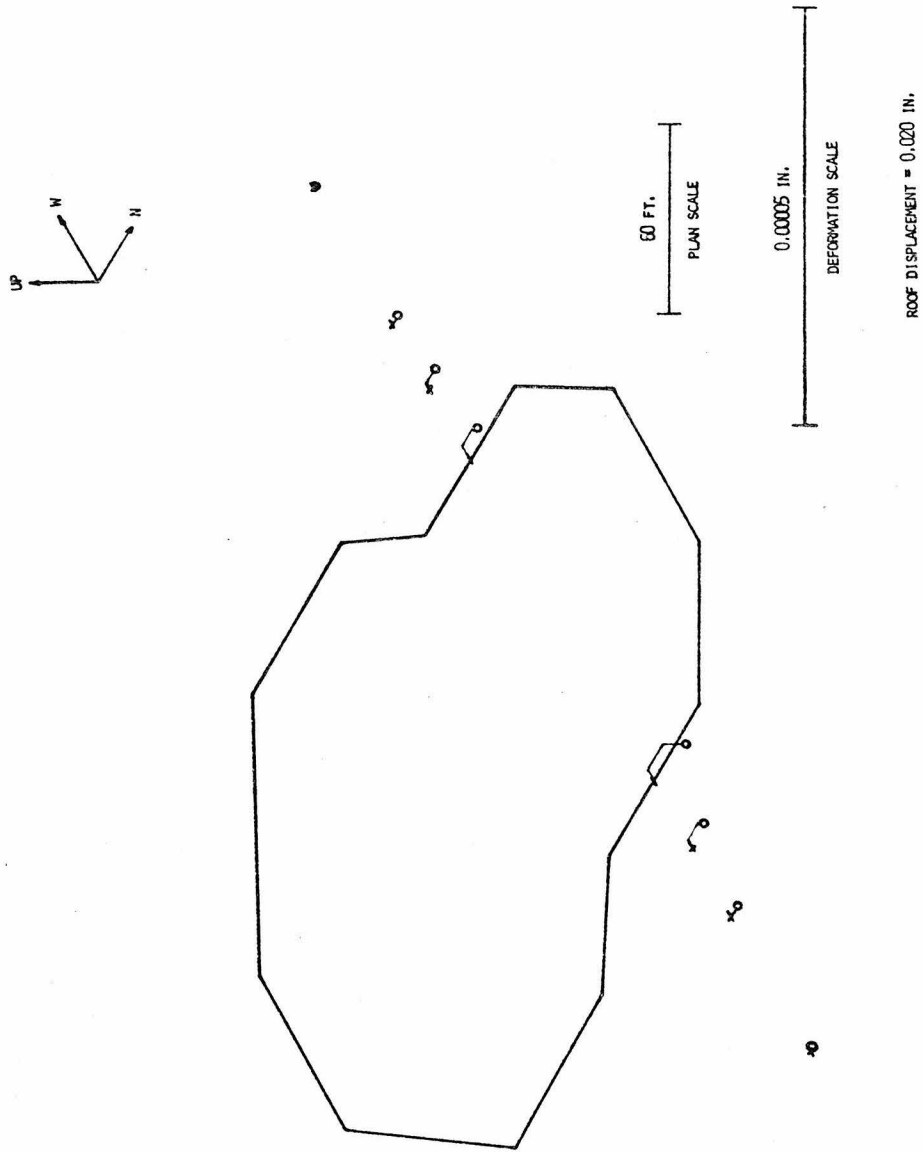


Figure 5.30 Deformation of the ground around the Parsons building for excitation in the first N-S mode.

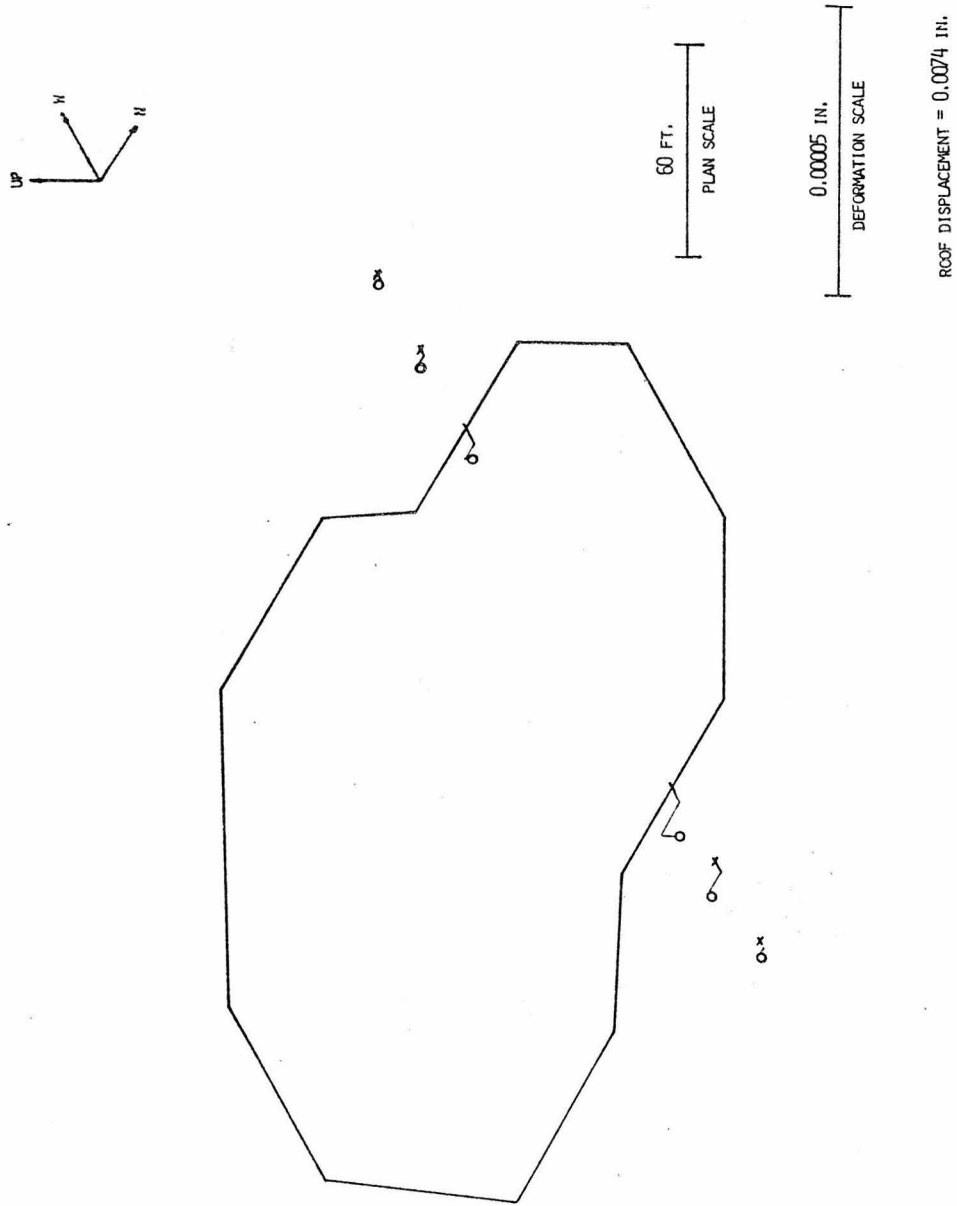


Figure 5.31 Deformation of the ground around the Parsons building for excitation in the second N-S mode.

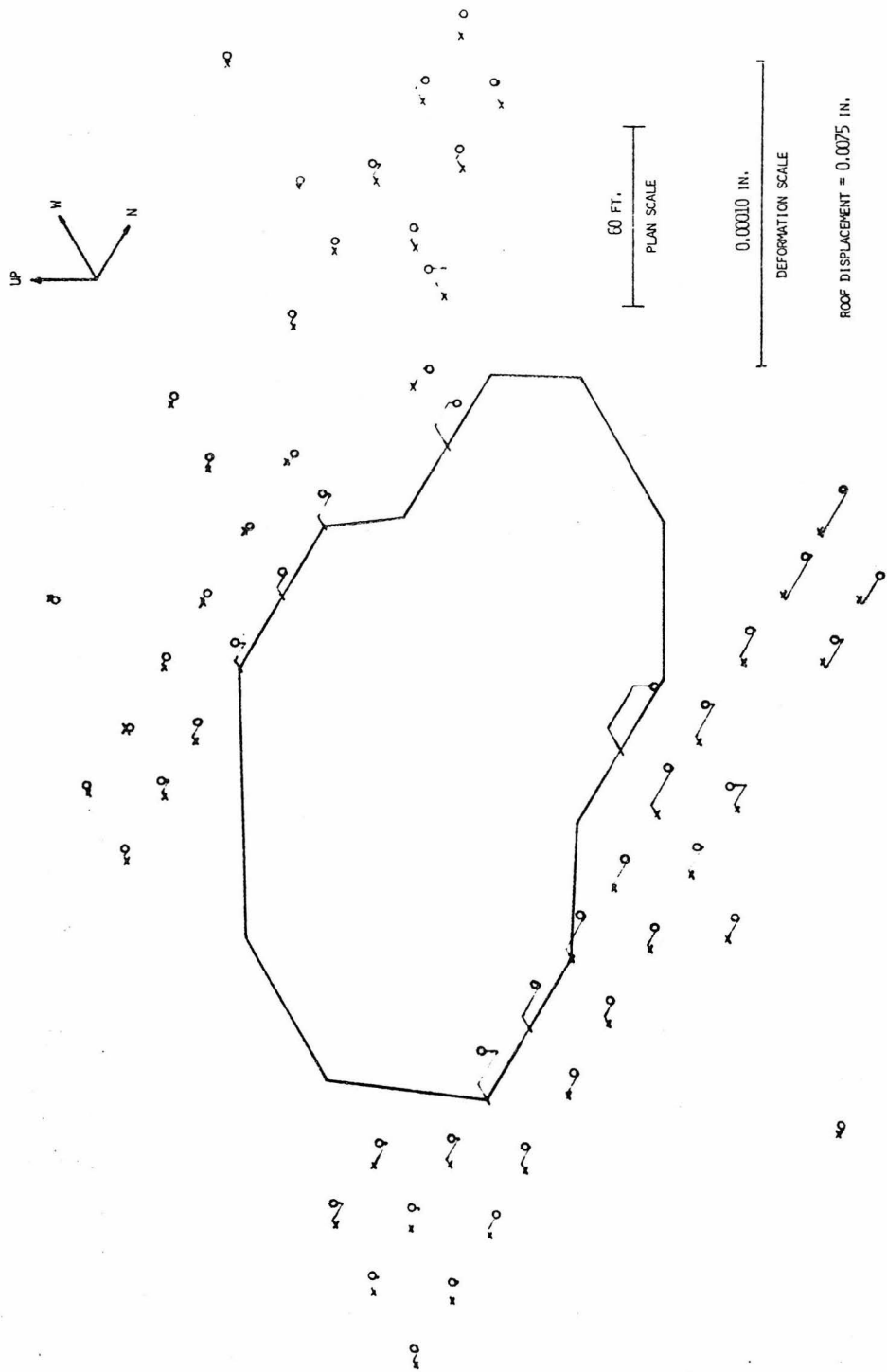


Figure 5.32 Deformation of the ground around the Parsons building for excitation in the third N-S mode.

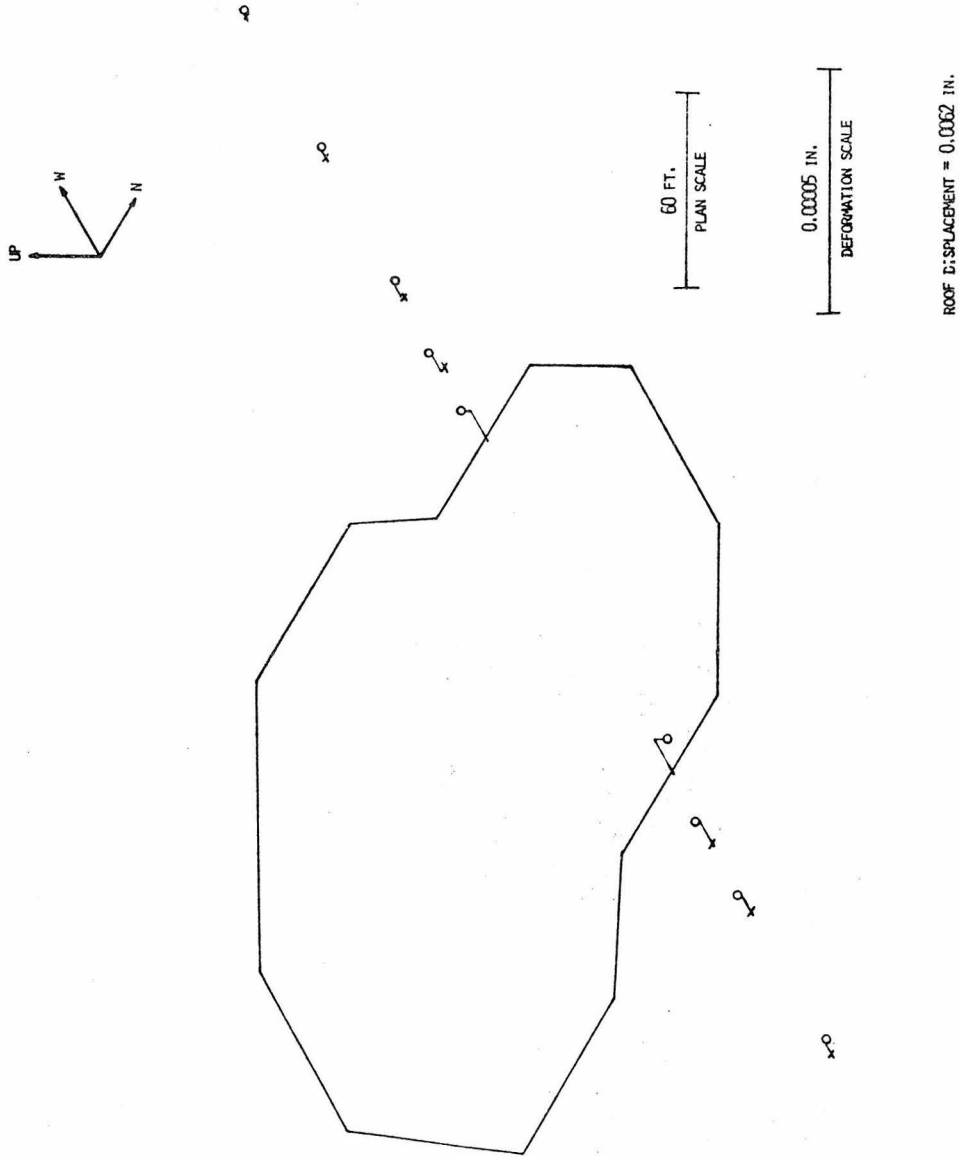


Figure 5.33 Deformation of the ground around the Parsons building for excitation in the second E-W mode.

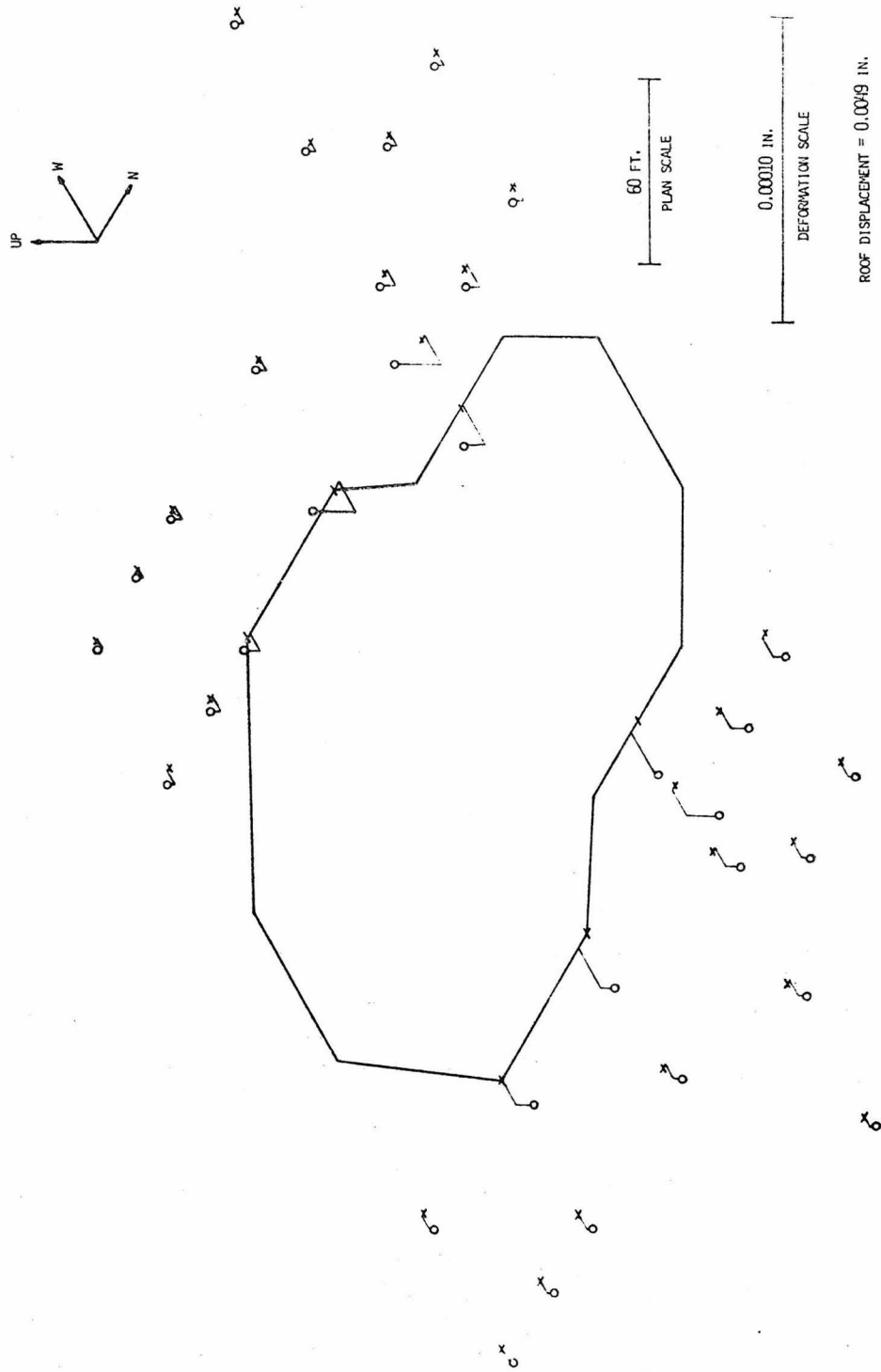


Figure 5.34 Deformation of the ground around the Parsons building for excitation in the third E-W mode.

columns of the satellite structures would be in relative tension (neglecting gravity loads) which could "lift" the ground in this area.

The small amount of energy being transmitted to the ground for shaking at these low levels of excitation makes accurate measurement of the resulting motions quite difficult. Also, the signal conditioner had unusually large dc transients for the low-attenuation settings required for measuring these small motions. This further complicated the experiment. In spite of these difficulties, the figures indicate that, under favorable conditions, meaningful measurements of ground deformations may be obtained during forced vibration tests. This data is required to verify analytical models of soil-structure interaction.

With the exception of the apparent deformation of the fourth floor slab in the second E-W mode, the figures in this section revealed few surprises. They verified the fact that, for this building, three degrees of freedom per floor would be adequate to model the dynamic behavior of the structure for response to wind or earthquake. Also, since the foundation motion was on the order of 0.1 percent of the roof motion, a fixed base model would be appropriate for this building.

Since these types of detailed measurements require a large amount of time to perform and analyze, they should be restricted to structures with complex lateral load resisting systems, such as the Millikan Library building, where an understanding of the interaction of the various systems is desirable. When all of the lateral load

resistance is provided by simple frames, such as the Parsons building, the needed information may be obtained with much more ease. For these structures, the three-dimensional measurements could be restricted to the grade level where information concerning soil-structure interaction would be obtained.

### 5.5 Measurement of Strain in the Moment Resisting Frame

A unique aspect of the Parsons tests was that dynamic strains were measured for one of the columns of the moment resisting frame during forced vibration. It is believed that this was the first successful attempt at making this type of measurement on a full-scale structure. This has not been done before because of the very small amount of strain in the members associated with the low levels of excitation during forced vibration tests. The importance of this type of measurement was mentioned in the introduction to this thesis and will be discussed in more detail in Chapter VI.

The column chosen for these measurements was the box-section column located between the fourth and fifth floors of the tower at point D4 of Figure 5.3. This column was chosen because it is an integral part of the lateral load resisting system since it participated in both the N-S and the E-W directions. Access to the column was gained by removing two tiles from the suspended ceiling of the technical library on the fourth floor. Since the building was fully occupied at the time of the tests, it was not feasible to remove architectural walls to improve accessibility to the columns. This limited accessibility caused some minor difficulties in obtaining the desired measurements.

It was initially hoped that strain could be measured on all four faces of the column so that contributions due to bending and axial deformation could be separated. This was not possible since only the east, west and north faces of the column were accessible from this vantage point. Also, due to restricted space in the vicinity where the measurements were taken the LVDT had to be mounted closer to where the girders intersect the column than was desirable. This could result in complicated stress patterns in the column where the measurements were taken.

The measurements were made using two Schaevitz model 050 HR LVDT (Linear Variable Differential Transformer) with a Brush carrier preamplifier and 220 strip recorder. The LVDT was chosen as the transducer for these measurements because of its high resolution and because of its high output. The signal was low-pass filtered between the carrier and the recorder using two Krohn-Hite analog filters with a cutoff frequency of 5 Hz and a roll-off of 24 db/octave. The entire system was calibrated in the field before and after the actual measurements. Special aluminum clips were designed for mounting an LVDT to the column. These were attached to the centerline of the column with epoxy. The locations of the mountings of the LVDT with respect to the structural frame are shown in Figure 5.36. Typical traces from the Brush recorder are shown in Figure 5.37.

The actual quantity measured by the LVDT was the relative displacement between the two points of attachment of the clips holding the LVDT. The measured displacement divided by the 9.5 inch gage

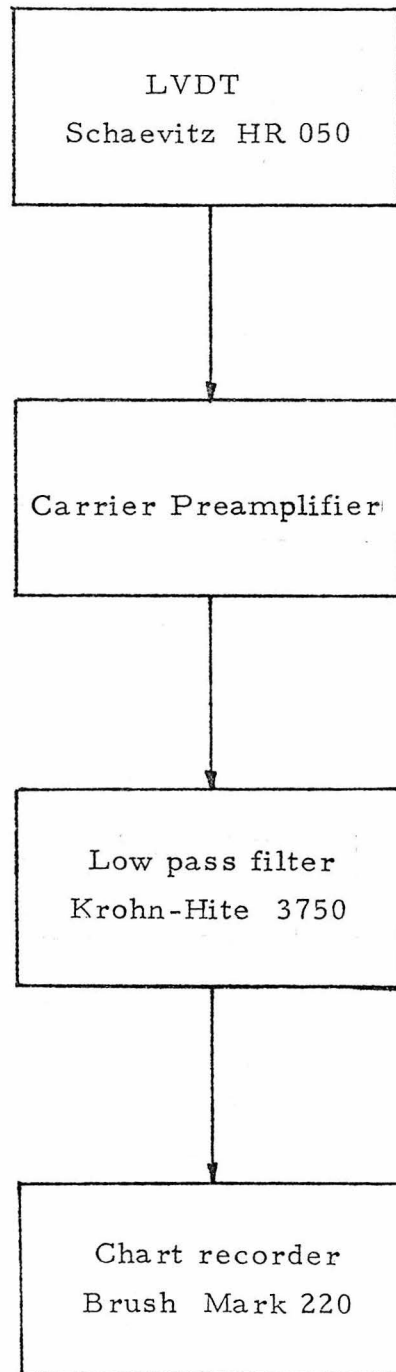


Figure 5.35 Diagram of instrumentation used for measuring strain.



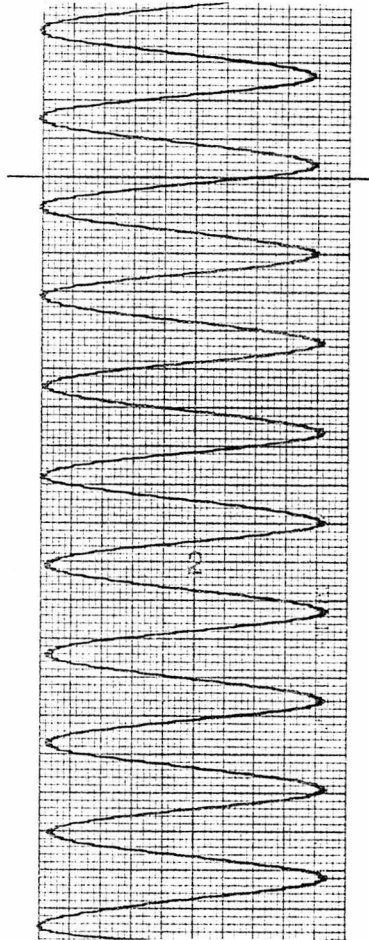


Figure 5.37 Sample traces taken while measuring strain in a column during forced excitation of the Parsons building.

length yields an average strain over this region. These strains were measured for the S4-L4 force level for shaking in the first three N-S modes, the first two E-W modes and the first two torsional modes. Where simultaneous measurements were taken on opposite faces of the columns, the axial component of the stress could be obtained by adding the two values algebraically and dividing by two; and the bending component could be obtained by subtracting the two components and dividing by two. Results of the measurements are listed in Table 5.5. These indicate that the stresses associated with these low levels of excitation are quite small. The values range from about 3 psi for the first torsional mode to 50 psi for the third N-S mode. In Chapter VI, these values will be compared to values predicted by a finite element model of the Parsons building for the same loading conditions.

The real significance of these measurements may not lie in the actual numerical results, since they were only taken from one column of the structure; but, more likely, the importance of these tests lies in the demonstration of their feasibility. In future full-scale tests, perhaps on a building under construction where only the structural frame is present, these types of measurements could be invaluable in the identification of accurate stiffness parameters associated with a finite element model of the structure being tested. Without a direct measurement of strain in the structural members of a frame, there is no guarantee that a finite element model derived solely on the basis of measured frequencies and mode shapes will accurately predict the stress-displacement relationship of the real structure.

Table 5.5 - Column Strains and Corresponding Roof Displacements Measured During Forced Vibration Tests.

Mode	Roof Disp. (in.)	Bending Strain (in./in.) $\times 10^{-6}$	Axial Strain (in./in.) $\times 10^{-6}$	Total Strain (in./in.) $\times 10^{-6}$
N-S 1	0.032	—†	—†	0.8
N-S 2	0.014	—†	—†	1.7
N-S 3	0.014	—†	—†	1.2
E-W 1	0.022	0.7	0.1	0.8
E-W 2	0.012	1.2	0.03 ?	1.2
Torsion 1 ( $\bar{R}\theta$ )	0.014	0.1	0.02 ?	0.1
Torsion 2 ( $\bar{R}\theta$ )	0.006	0.5	0.1	0.6

† Only the total strain could be measured for this mode.

### 5.6 Investigation of Apparent Nonlinearities in the Dynamic Response of the Parsons Building

In past investigations, researchers have discovered that buildings behave in a nonlinear fashion when excited by different force levels during forced vibration tests.<sup>32,49</sup> This nonlinear behavior was demonstrated by the decreases in the natural frequencies of the modes of vibration of a structure as the exciting force was increased. This type of behavior is typical of a softening dynamic system. Also, it has been noted that the fundamental periods of vibration of multi-story buildings may lengthen by as much as 20 percent to 50 percent during an earthquake without any apparent structural damage being sustained by the building.<sup>15,35,65,69</sup>

In an attempt to isolate potential causes of this nonlinear behavior, a series of frequency sweeps at different force levels was performed. The Parsons building was well suited for this type of study since several modes of vibration were within the operating range of the vibration generating system. This allowed study of the relationship between the observed nonlinear behavior and various modal quantities.

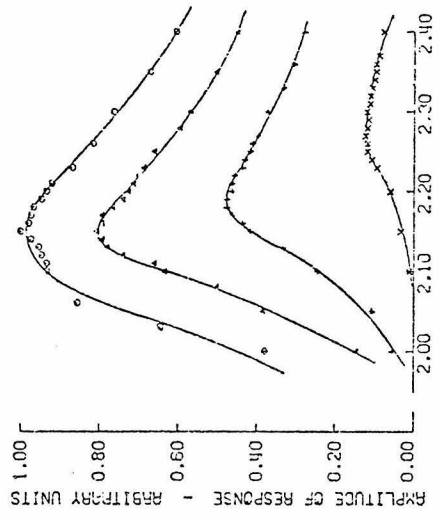
The tests were completed in two parts. The first stage of the tests involved performing the frequency sweeps and the second stage involved shaking the structure at the predetermined apparent resonant frequency for each force level and measuring the mode shape at this frequency. For the frequency sweeps, one Ranger was located at the geometric center of the roof and pointed in the direction of the excita-

tion for the N-S and E-W sweeps. For the torsional sweeps, four transducers were used. One transducer was located at each of the north, east, south and west edges of the roof slab. For the determination of the mode shapes, four measurements were taken for each floor (with the exception of floors 5 and 12) so that the  $x$ ,  $y$  and  $R\theta$  component of the mode could be determined. Five force levels were used to excite each of the first six modes of vibration of the building and four were used for modes 7, 8 and 9. The dynamic force had the following ranges at resonance for each mode:

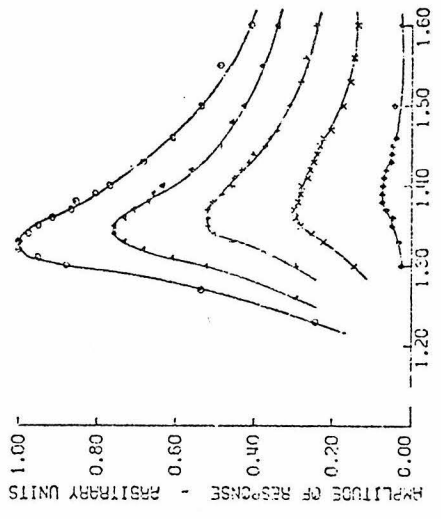
N-S	1	35.8 lbs - 418.6 lbs
N-S	2	239.4 lbs - 2846.0 lbs
N-S	3	637.4 lbs - 5674.0 lbs
E-W	1	45.6 lbs - 511.8 lbs
E-W	2	281.8 lbs - 3966 lbs
E-W	3	1035 lbs - 8446 lbs
Tors	1	2,440 ft-lbs - 34,700 ft-lbs
Tors	2	12,400 ft-lbs - 177,000 ft-lbs
Tors	3	24,300 ft-lbs - 370,000 ft-lbs

The results of the frequency sweeps are shown in Figure 5.38 for the first three N-S modes, in Figure 5.39 for the first three E-W modes and in Figure 5.40 for the first three torsional modes. The figures for N-S and E-W sweeps represent the total response of the center of the roof versus frequency. Two curves are shown for each torsional frequency sweep. These represent the absolute value of the

- S3-L3
- ▲ S2-L2
- △ S1-L1
- × S0-L0



- S3-L3
- ▲ S2-L2
- △ S1-L1
- × S0-L0



- S3-L3
- ▲ S2-L2
- △ S1-L1
- × S0-L0

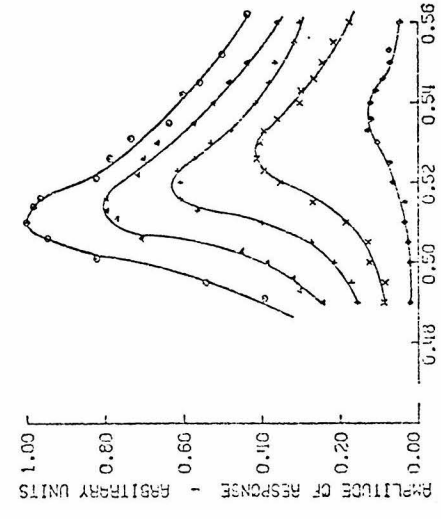


Figure 5.38 Frequency sweeps in the N-S direction for five different levels of excitation.  
(a) - Mode 1 (b) - Mode 2 (c) Mode 3.

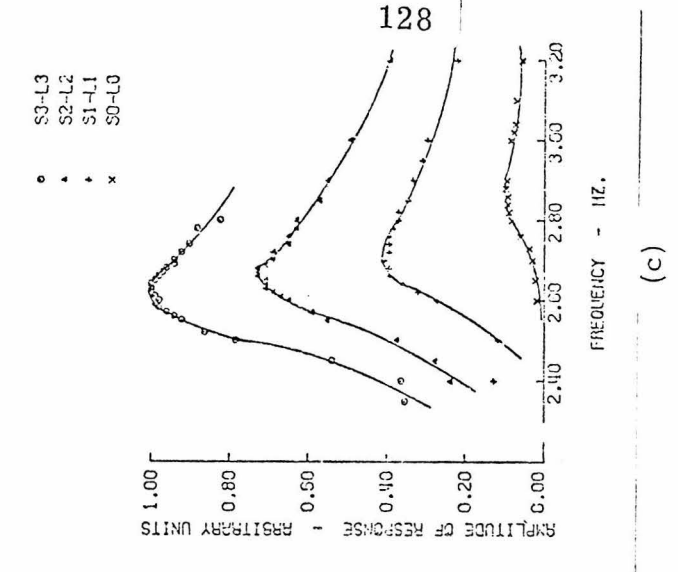
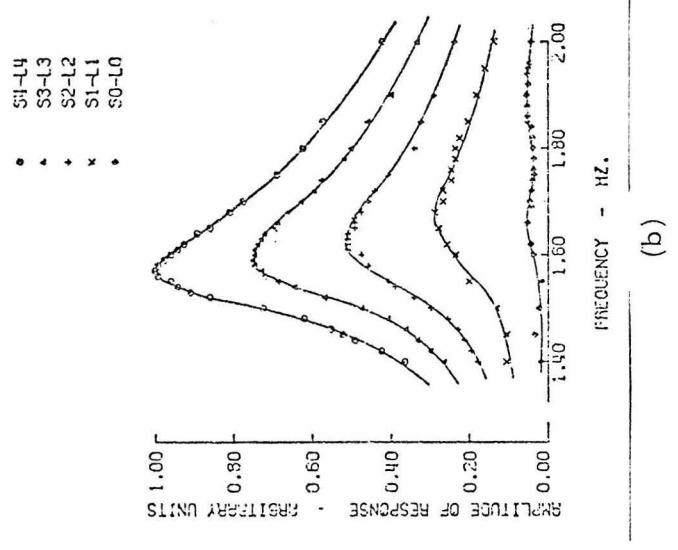
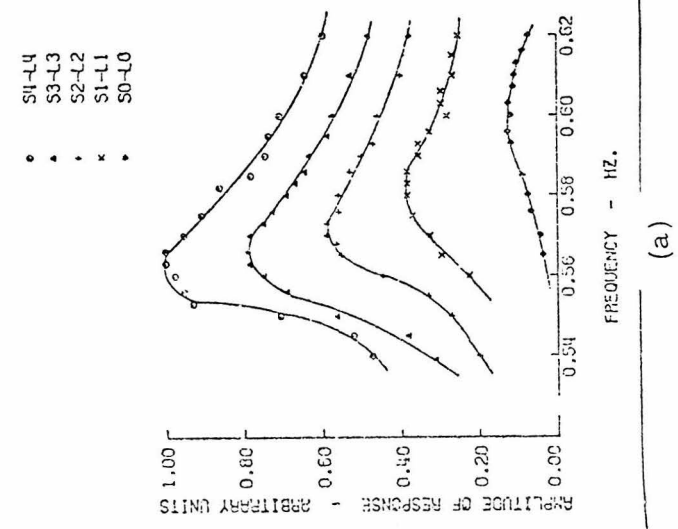
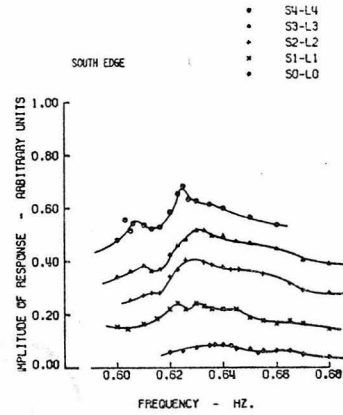
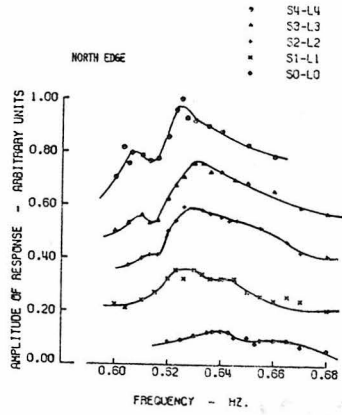
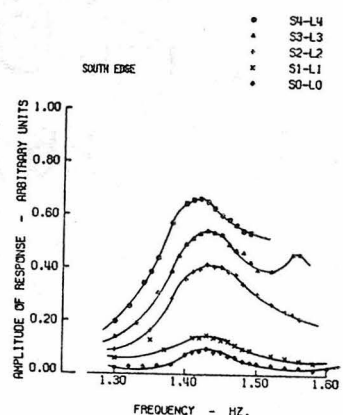
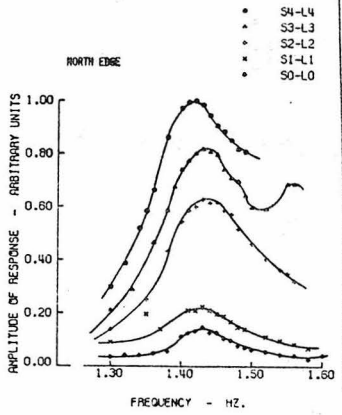


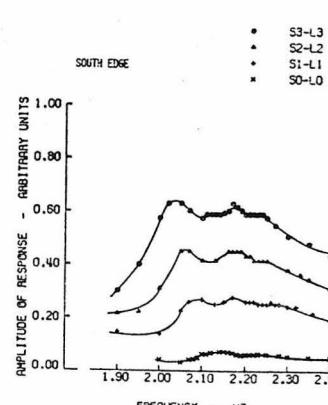
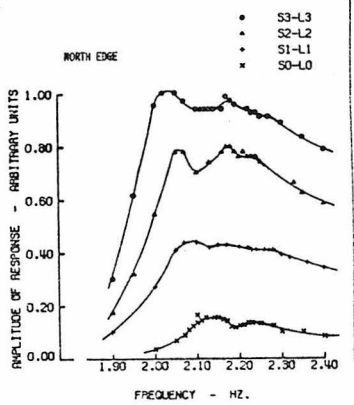
Figure 5.39 Frequency sweeps in the E-W direction for five different levels of excitation.  
 (a) - Mode 1 (b) - Mode 2 (c) - Mode 3



(a) Mode 1



(b) Mode 2



(c) Mode 3

Figure 5.40 Frequency sweeps for torsional motion for five different levels of excitation.

total response for the north and south edges of the slab. The decrease in the apparent natural frequencies of vibration with increasing amplitudes of response are quite apparent for all of the N-S and E-W modes. The torsional frequency sweeps are not so clear however. The presence of modal interference is seen in all three of the torsional frequency sweeps. Since modal interference can cause a shift in the apparent frequency of vibration of a particular mode,<sup>24</sup> little useful information may be gained concerning the nonlinear behavior of the torsional modes. It is possible that more useful results might have been gained by placing the instruments at an antinode lower in the building and by measuring the 90° out-of-phase part of the total response.

The frequencies at resonance for the first three N-S modes and the first three E-W modes are listed in Table 5.6. The percentage changes in natural frequencies presented in this table were computed by dividing the total change by the value for the S2-L2 force level. These changes are similar to, but somewhat larger than, those demonstrated by other buildings at similar force levels.<sup>32,49</sup> A possible explanation for this might be in the fact that the Parsons building is a softer structure for its height than the average steel-framed building. Consequently the relative story motions and the total displacements were larger in absolute value than for these other buildings.

The mode shapes were very stable. Any differences for the mode shapes were within the expected errors in their measurement

Table 5.6 - Apparent Natural Frequencies of Vibration for Five Levels of Response

Loading Combination	S0-L0	S1-L1	S2-L2	S3-L3	S4-L4	% Change
MODE						
N-S 1	0.536	0.527	0.520	0.514	0.510	5.0
N-S 2	1.39	1.38	1.36	1.35	1.33	4.4
N-S 3	2.26	2.19	2.15	2.15		5.1
E-W 1	0.604	0.582	0.572	0.566	0.564	7.0
E-W 2		1.67	1.63	1.59	1.57	6.1
E-W 3	2.88	2.71	2.66	2.62		9.8

and therefore could not be attributed to nonlinear sources. This result was also true for the foundation response which was considered as a possible candidate for nonlinear action.

Various modal quantities were considered as possible indices of measure of the nonlinear behavior of the building. The first of these was interstory drift. This is defined as the absolute value of the difference in maximum displacement between two floors divided by the story height. This would be a logical choice if the building were behaving as a nonlinear softening spring since it is a function of the strain energy stored in a particular mode. In order to compare the responses in the various modes a normalized frequency squared was plotted versus the summation of the interstory drifts for the first two N-S and the first two E-W modes. The resonant frequencies were normalized by dividing them by the resonant frequency obtained at the S2-L2 level of excitation of a particular mode. This was done to facilitate the visual comparison of the results for all the modes. If interstory drift contributed to the nonlinearity of the response one would expect the first mode responses in either direction to show similar trends as well as the second mode responses since the mode shapes are similar in appearance. One would not necessarily expect the first mode in a particular direction to behave similarly to the second mode, however, since the spatial distribution of the nonlinearity would be different for each. The trends demonstrated in Figure 5.41 (a) mildly support this theory. The results of the first E-W and first N-S modes are clearly similar, and these differ some-

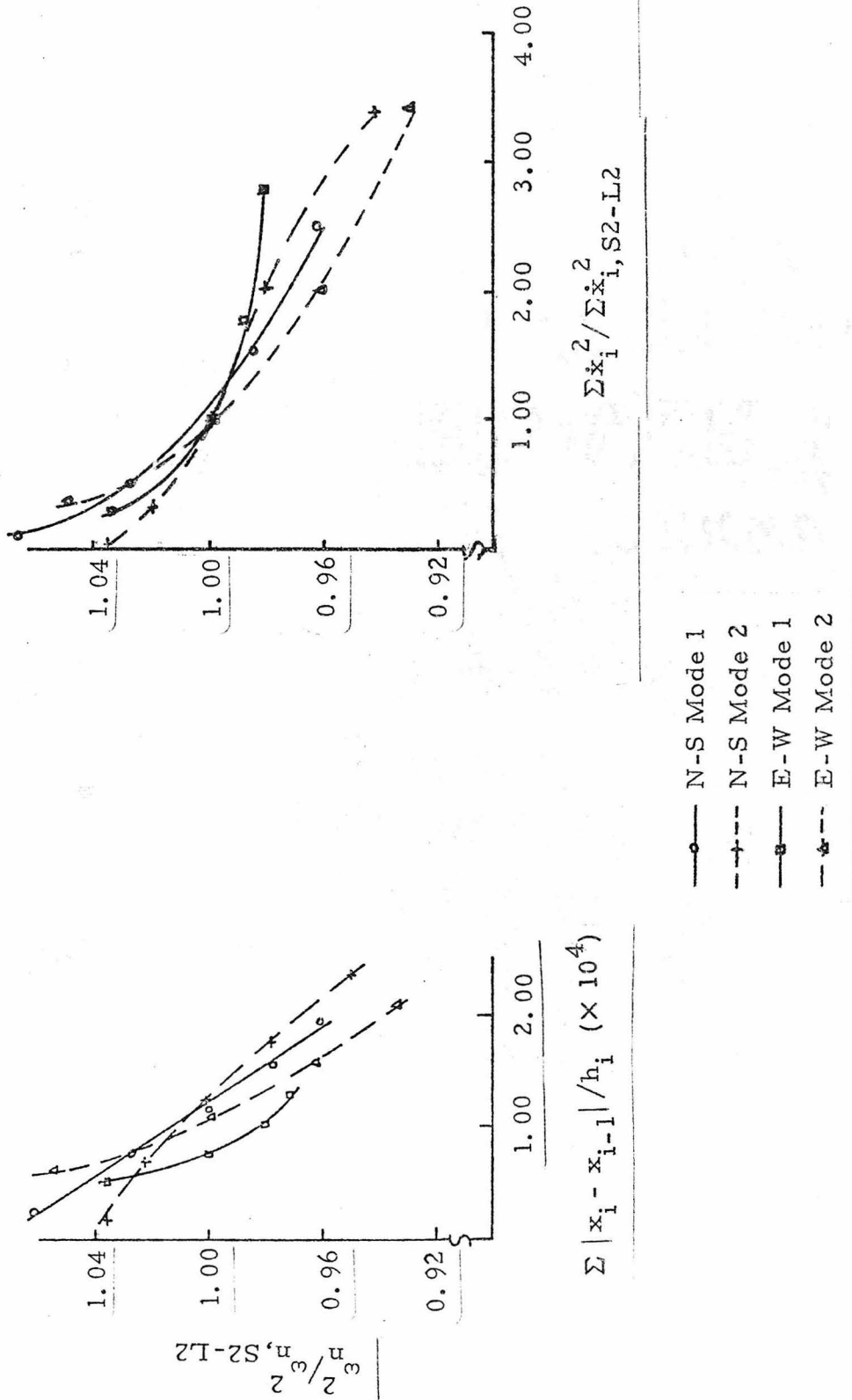


Figure 5.41 Plot of modal indices versus normalized frequencies demonstrating nonlinear characteristics of the response of the Parsons building.

what from the trends demonstrated by the second E-W mode but are similar to those of the second mode in the N-S direction.

A second quantity that was considered as a possible index was the summation of the square of the floor velocities for each mode. This would be related to the total kinetic energy of vibration of an individual mode. If the nonlinearities were associated with this quantity one might expect to see similar trends for all of the modes since the character of this behavior would probably not depend on the spatial distribution of the velocities. It would more likely depend on the total kinetic energy. Results of this comparison are shown in Figure 5.41 (b). The trends for all four modes are clearly similar. This argument supports the suggestion that the nonlinearities might be correlated with the maximum kinetic or potential energy of vibration.

Final comparisons were made for total base shear and for the overturning moment for vibration in the four modes. Base shear may also be thought of as a modal force. These quantities would be expected to be of significance if the nonlinearities occurred in the foundation compliance of the structure. These results are plotted in Figure 5.42 (a) and Figure 5.42 (b). These show the least agreement of any of the comparisons which should be expected since the foundation action was demonstrated to be linear.

The results of this section suggest that the nonlinear character of the response of the Parsons building may be related to the magnitude of the interstory drifts or to the total kinetic energy of vibration of the

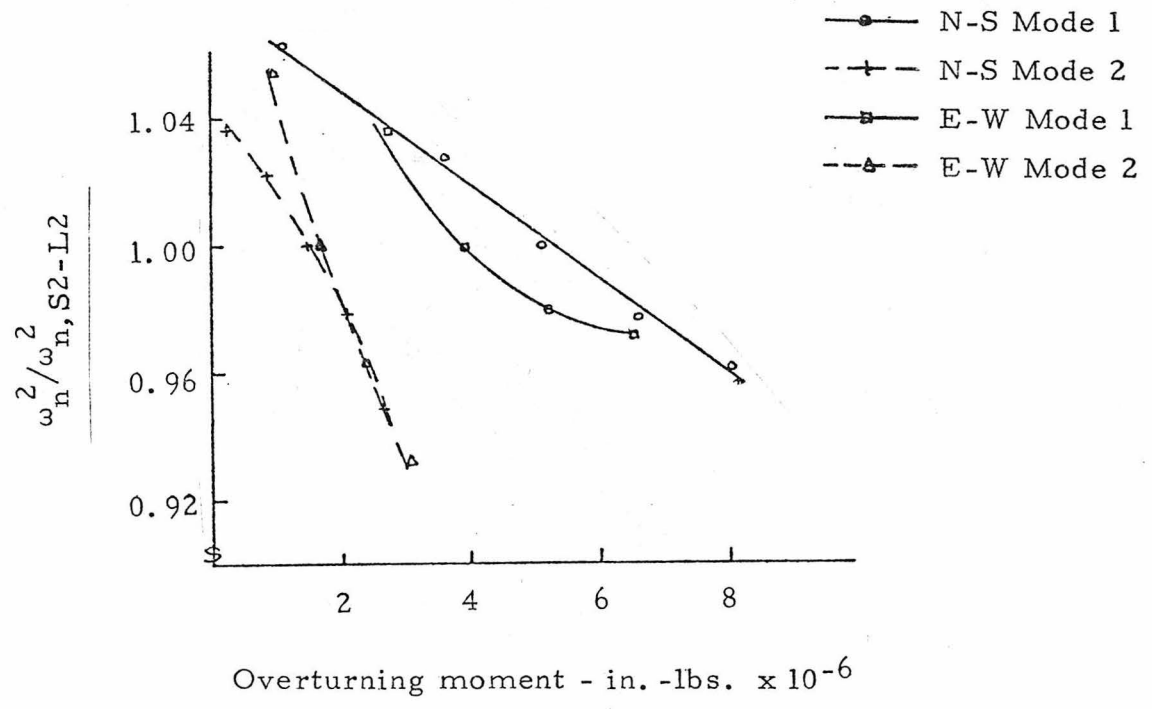
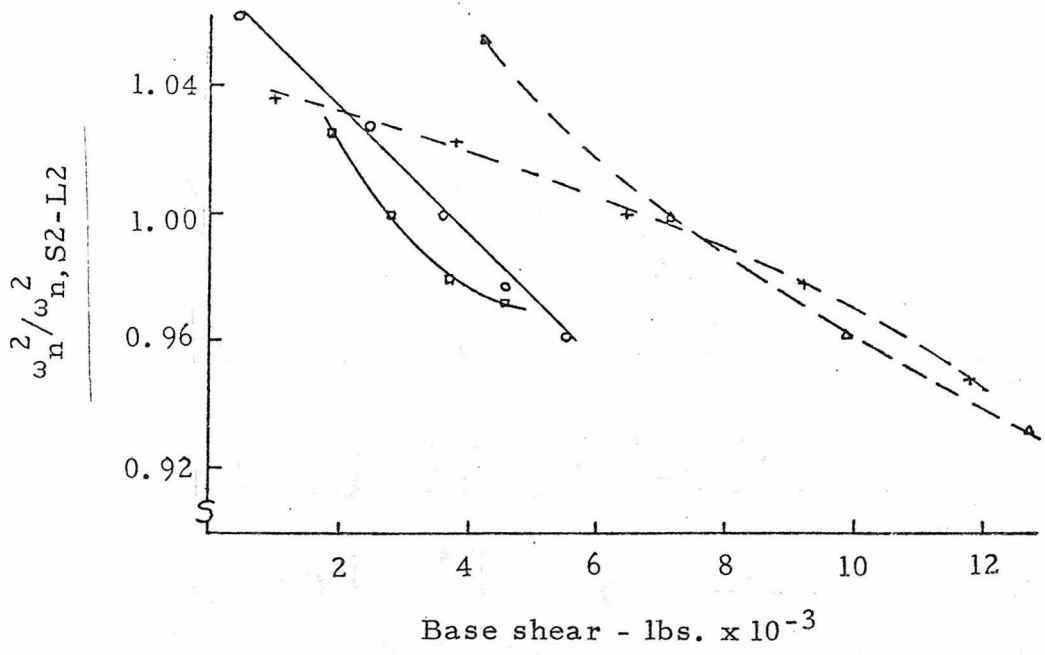


Figure 5.42 Plot of modal indices versus normalized frequencies demonstrating nonlinear characteristics of the response of the Parsons building.

building. The first of these relations is the most obvious and has been mentioned by many investigators (e.g., hysteresis in the interfloor stiffness relations). The second relation, however, is somewhat more subtle and would require further investigations into the possible physical mechanisms for this behavior before more positive statements could be made.

#### 5.7 A Study of the Response of the Parsons Building to Ambient Excitation

The final stage of the testing program for the Parsons building involved the measurements of the response of the structure to ambient excitation. The ambient forces which excite the structure are the result of wind currents and microseismic waves of various origins. The naturally occurring forces used in ambient testing are an attractive feature when compared to forced vibration tests since the installation of a vibration generating system usually requires a great deal of work.

The ambient tests were performed with two goals in mind. First, these tests were to provide additional information regarding the accuracy of natural frequencies and mode shapes determined through this type of testing. Previous comparisons of this type have produced favorable results but with some limitations. These limitations include inaccurate estimates of modal amplitudes of certain floors due to modal interference, difficulties in distinguishing between closely spaced modes, the inability to distinguish between those peaks in the spectrum which are due to structural vibrations and those which are due to mechanical and electrical noise, and overestimates of damping param-

eters due to modal interference and due to the effects of smoothing the spectrum. Also, many of the ambient tests reported in the literature were performed on structures which were at least twice the height of the Parsons building. Since the wind generates larger forces on these buildings, the resulting floor responses are larger and therefore produce relatively larger and more distinguishable peaks in the resulting Fourier spectra of the recorded responses. In other words, the peaks in the Fourier spectrum due to structural response are higher compared to the noise level than for a structure the size of the Parsons building. For a building 20 stories or higher it would not be uncommon to be able to determine 12-18 modes of vibration from ambient tests. For the Parsons building and other buildings this size or smaller, it can be difficult to distinguish even the second or third mode of vibration in any given direction.

A second reason for making these measurements was that the results from these final ambient tests could be compared to those of the preliminary ambient tests to determine if the building period had changed measurably as a result of the forced vibration tests. After an earthquake it is not uncommon for the fundamental period of a building as determined by ambient tests to be longer by a few percent than it was before the event. A similar "loosening up" phenomenon has not been observed during forced vibration tests of other buildings. However, few buildings have experienced the number of tests that the Parsons building has sustained.

It was briefly mentioned above that damping is overestimated

from ambient tests when compared to values determined during forced vibration tests. Several factors contribute to these overestimates. One factor is the presence of adjacent peaks in the spectrum either due to closely spaced modes of vibration or due to noise. Another contributor to these overestimates is the time window that one chooses for sampling the data. All windows diminish the spectral peak and broaden the bandwidth at the half power point, both of which increase the damping estimate. Also, nonstationarity of the response of the building can broaden the bandwidth. All of these factors preclude accurate estimates of damping from ambient tests. This should not necessarily be considered a drawback of ambient tests (at least for multistory buildings), however, since accurate estimates of damping at these low levels of excitation tell us little about the levels of damping that one may expect during an earthquake. Consequently, they are of limited interest. In light of this discussion, no attempt was made to estimate the modal damping from these ambient tests.

The first part of the procedure involved two calibration tests, one in the N-S direction and one in the E-W direction. For these measurements Rangers were placed at adjacent points near the center of the roof. The response of the roof was then recorded simultaneously by all of the transducers. The data from these tests were later analyzed so that the relative magnitudes of the output for each transducer for all frequencies of interest could be determined. This step was necessary since mode shapes were to be determined; it could have been skipped if only natural frequencies had been desired. Next, the

instruments were placed at the center of each floor of the building and oriented in the N-S direction. The responses of the floors were then recorded simultaneously for five minutes. The transducers were then oriented in the E-W direction and the process was repeated. Next, two Rangers were placed on each floor, one each on the east and west edge of the slab. The responses of the floors in the N-S direction were then recorded. Two Rangers were used on each floor so that the signals could be algebraically subtracted to enhance the torsional motions and diminish the effects of the N-S modes. During all of these tests the signals were passed through a low-pass analog filter with a cut-off frequency of 12.5 Hz and a roll-off of 18 db/octave. In the laboratory, the resulting signals were digitized at a rate of 30 samples per second which resulted in a Nyquist frequency of 15 Hz. A Fast Fourier Transform (FFT) was then computed for 4096 points (136.5 seconds of data) of each record resulting in 2048 spectral ordinates and phase angles.<sup>11</sup> The spectra were next passed through a digital Hann window to reduce the effects of side lobes and then smoothed using five point averaging to increase the accuracy of the spectral estimates. Figure 5.43 shows the unsmoothed Fourier spectra of the response of the roof in both the N-S and the E-W directions. These spectra were then smoothed and replotted in Figure 5.44.

The smoothing of the spectra facilitates the selection of the natural frequencies of vibration of the building being tested. Normally, the statistical accuracy of estimates of structural parameters increases with the length of record used in their determination. The response of

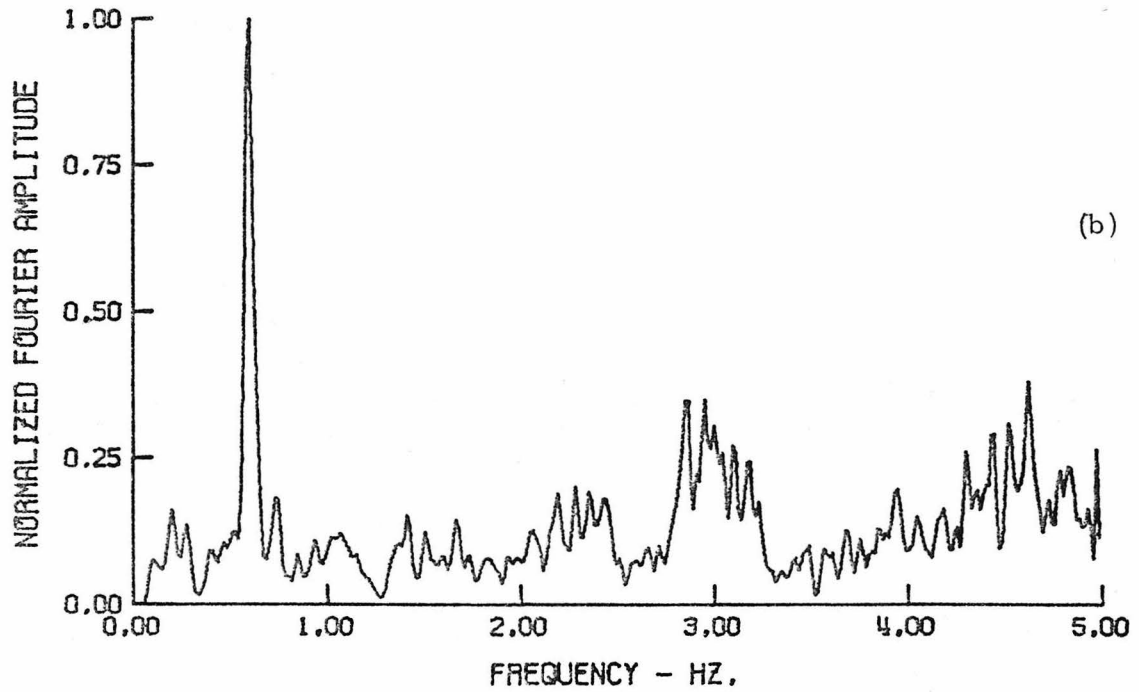
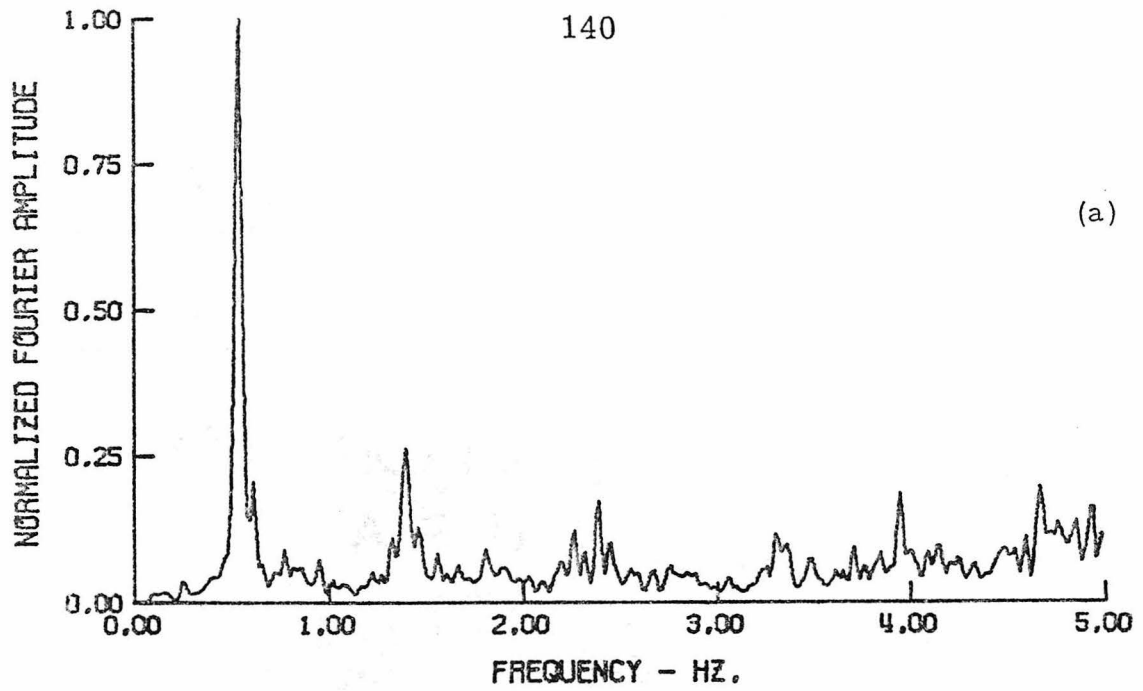


Figure 5.43 Unsmoothed Fourier amplitude spectra of roof response; (a) N-S direction, (b) E-W direction.

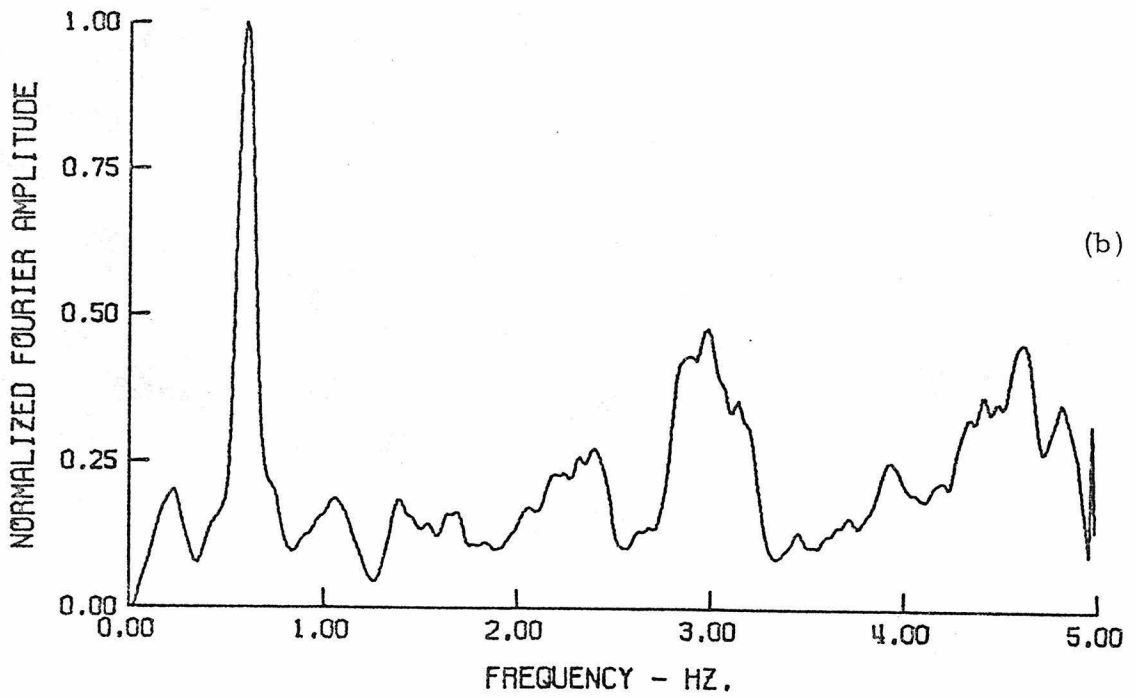
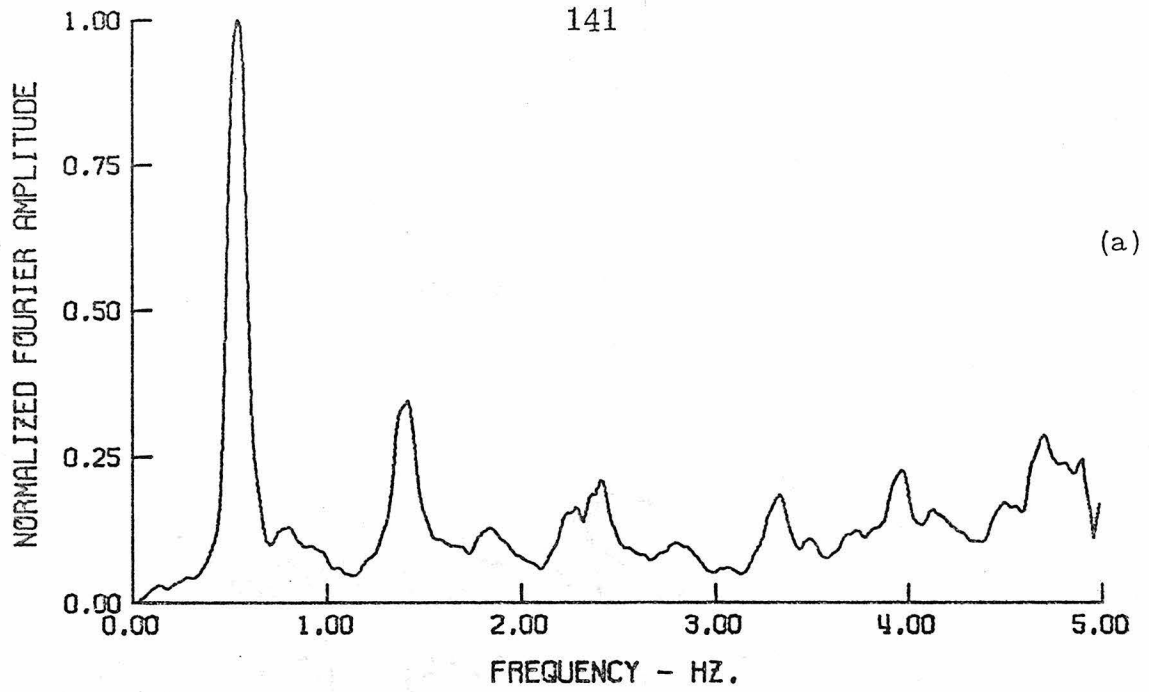


Figure 5.44 Smoothed Fourier amplitude spectra of roof response; (a) N-S direction; (b) E-W direction.

a multistory building to ambient forces, however, is noticeably non-stationary. This is clearly evident if one views the Fourier amplitude spectrum of building response on a continuous real time spectrum analyzer such as the Spectral Dynamics Corporation model SD 360 digital signal processor. While monitoring the spectrum for several minutes, it is not uncommon to see the peak representing the first mode response of the building rise at a given frequency, fall to a barely noticeable level and rise again at a slightly, but measureably, different frequency. The significance of this on the FFT of the entire length of record is that one broad peak may result which would, more or less, average the frequency content of the response; or two or three closely spaced peaks may appear, depending on the length of time that the building responded at each frequency, and depending on the frequency resolution of the FFT. Thus, by smoothing the spectrum a more meaningful representation of the frequency content of the response of a building is obtained.

The results shown in Figure 5.44 are good indications of a difficulty that can arise when analyzing ambient data taken on a building for which the vibrational characteristics are unknown. Only the fundamental modes in each direction and possibly the second mode in the N-S direction were excited enough for proper identification. One reason for this was that on the night these tests were made there was very little wind. The responses measured on this particular night were averaged 5-10 times smaller than on the night that the preliminary ambient tests were performed. Fortunately, the responses measured

for some of the lower floors contained relatively larger higher mode contributions than the roof. This greatly helped the selection of the appropriate natural frequency for each mode.

The mode shapes were determined in a manner quite similar to that used for the forced vibration tests. A reference instrument was placed at the center of the roof and its response was recorded simultaneously with that of all the other floors. The amplitude of the Fourier spectrum of the response of a given floor of the building is proportional to the amplitude of the mode shape at this location for each of the natural frequencies. The amplitude of the smoothed spectrum for each floor at a particular natural frequency was divided by the amplitude of the roof spectrum at that frequency to give a mode shape normalized to 1.00 at the top. The phase of the response was compared to that of the reference instrument to determine the sign of the modal amplitude.

The results of the mode shapes and frequencies determined by the ambient tests for N-S excitation are compared in Figure 5.45 to similar results obtained by forced excitation. The agreement between the mode shapes is surprisingly good considering the low level of response in the higher modes. The only relatively large differences occur near the nodes of the higher modes. This is due to modal interference.<sup>64</sup>

The natural frequencies are somewhat higher for the ambient tests. This is consistent with the nonlinear behavior of the building associated with increasing levels of response.

The first two natural frequencies were identical to those measured during the preliminary ambient tests and the third mode values differed

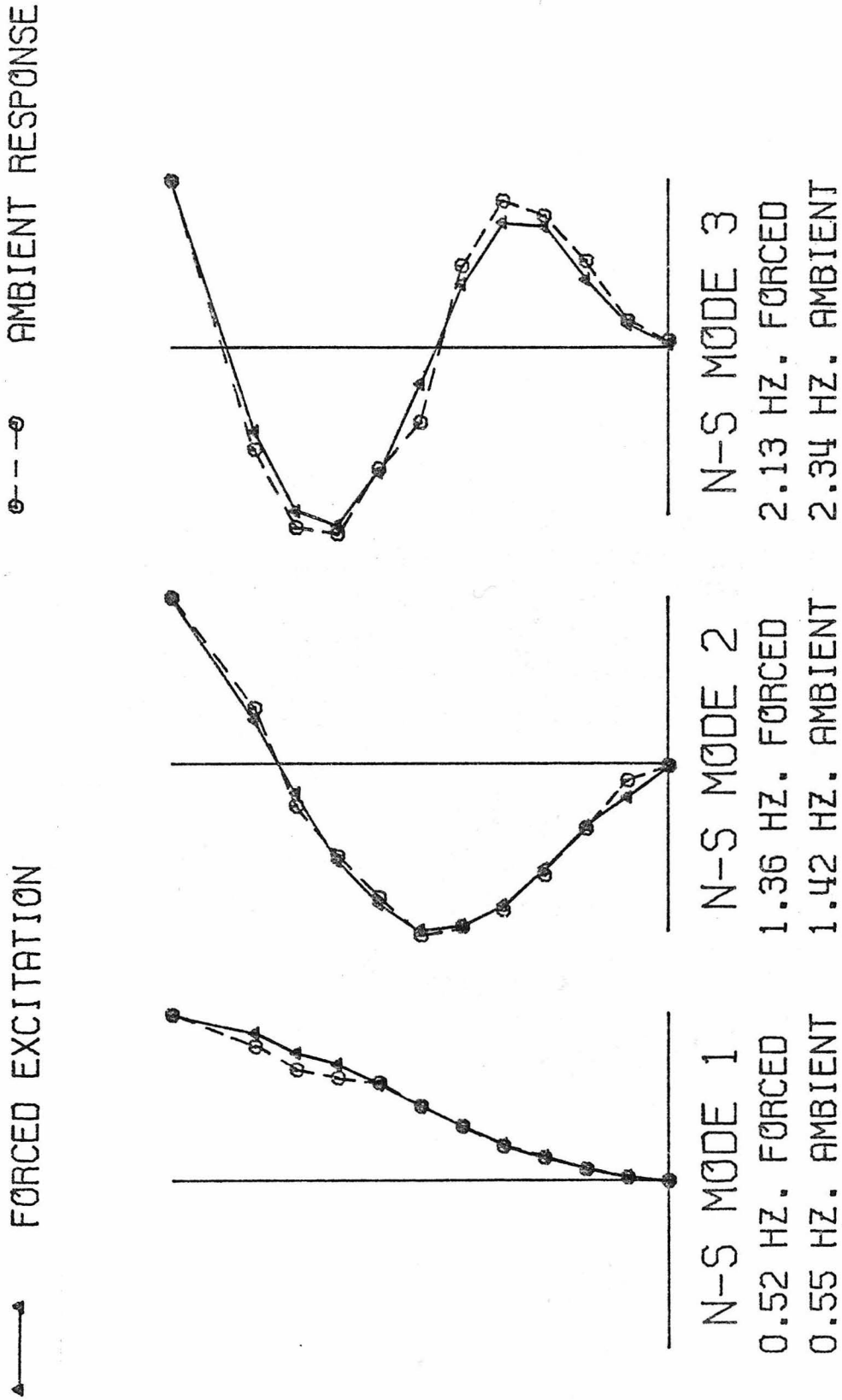


Figure 5.45 A comparison of natural frequencies and mode shapes from ambient and forced tests of the N-S direction.

by 1 percent. This indicates that the building has not changed as a result of the forced vibration tests. It is possible that the building had experienced a slight loosening up prior to the tests as a result of strong winds or aftershocks of the San Fernando earthquake.

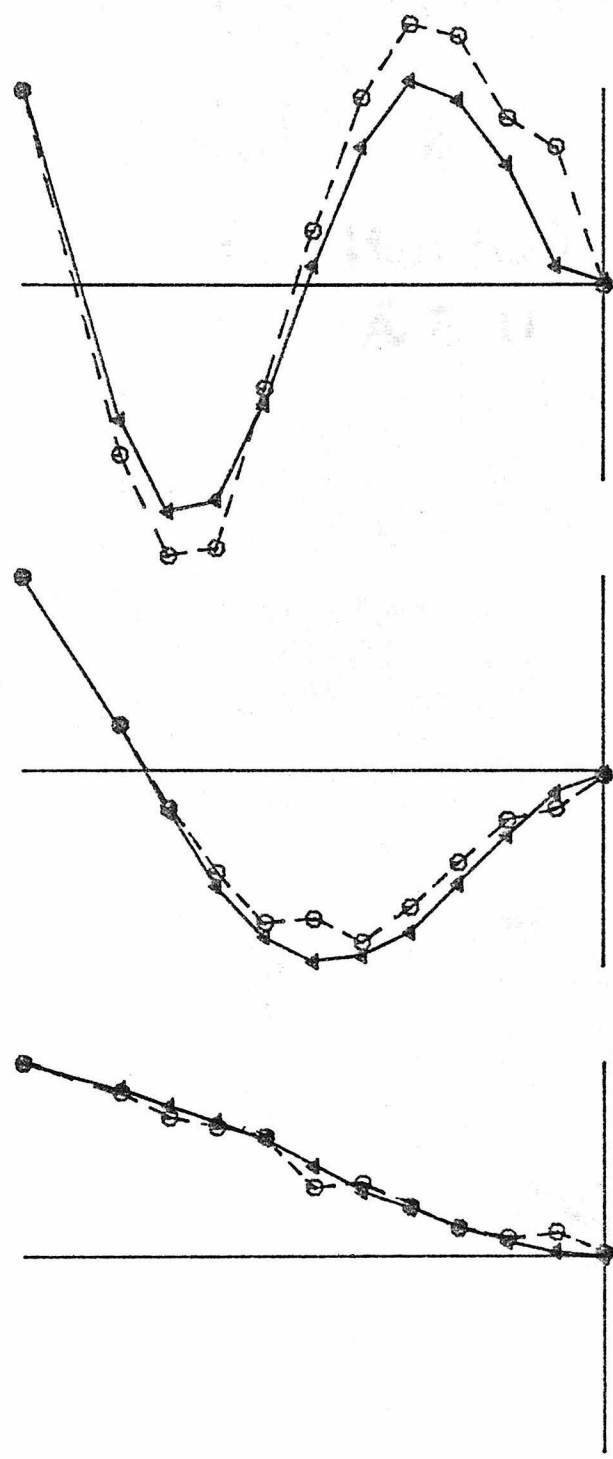
Results of the natural frequencies and mode shapes determined for E-W ambient responses are shown in Figure 5.46 where they are compared to corresponding quantities determined during the forced vibration tests. The agreement is thought acceptable but they do not compare as favorably as the N-S results. The first mode shape is reasonably good; the second mode shape is adequately identified for most floors; and the third mode shape is very poorly estimated. The first two natural frequencies are in the expected range based on the preliminary ambient tests and on the forced vibration tests. The third natural frequency, however, seems too high. From analysis of the forced vibration tests it is concluded that these ambient measurements probably do not represent the third E-W mode. It is more likely they are the result of mechanical noise at about 3 Hz. Again, these poor results for the third E-W mode seem to be the result of the small levels of excitation available on that particular night.

Vibration in the torsional modes was so slight that the natural frequencies could not be determined. This was the case even though the response of opposite edges of the floor slabs were subtracted to enhance the torsional response. This also seems to be the result of the low levels of excitation since reasonably good estimates of the torsional frequencies were obtained during the preliminary ambient tests.

FORCED EXCITATION

AMBIENT RESPONSE

←→



E-W MODE 1      E-W MODE 2      E-W MODE 3  
 0.57 HZ. FORCED      1.57 HZ. FORCED      2.57 HZ. FORCED  
 0.60 HZ. AMBIENT      1.70 HZ. AMBIENT      2.98 HZ. AMBIENT

Figure 5.46 A comparison of natural frequencies and mode shapes from ambient and forced tests of the E-W direction.

In spite of the poor conditions under which these tests were conducted, the results of the ambient tests indicate that reasonably accurate estimates of natural frequencies and the principal components of the translational mode shapes may be determined by ambient testing. The torsional modes are more difficult to identify, however, and may require more favorable conditions for their measurement.

The limited time available for these tests precluded more extensive studies. Whether or not ambient tests may be used to determine the  $x$ ,  $y$ , and  $R\theta$  components of each mode or to investigate the three-dimensional nature of the floor deformations remains to be determined.

### 5.8 Conclusions

During the discussion of the various aspects of the tests of the Parsons building, several points concerning the behavior of the building were made. Also, several suggestions were made concerning forced vibration testing. A brief review and discussion of these should be helpful to those planning similar tests.

During preliminary frequency sweeps to determine roughly the natural frequencies of vibration of the structure, several extraneous peaks were observed that were the result of modal coupling and modal interference. These were properly identified by observing the relationship between the amplitudes and phases of the responses of several instruments that were measuring responses simultaneously at various points on the roof. It is suggested that future investigators follow a similar practice of placing three to five transducers at selected points

on the roof during preliminary frequency sweeps to aid in interpreting the dynamic characteristics of the structure during the early stages of the investigation.

A method for determining the natural frequencies, mode shapes and damping coefficients was presented which required the measurement of the component of the total response of a floor that was  $90^\circ$  out-of-phase with the exciting force. This method is very helpful in interpreting data when modal interference is present. An extension of earlier studies of this method revealed that, although the resonance curve should not be expected to be symmetric about the resonant frequency, the bandwidth is quite stable. Thus reliable estimates of damping may be expected when the nonsymmetry is present, and the amount of asymmetry expected can be identified.

The natural frequencies, mode shapes and damping coefficients were determined for the first nine modes of vibration of the Parsons building. The relatively low natural frequencies for the lowest modes in each direction indicate that the Parsons building is somewhat more flexible than the average twelve-story steel-frame building. Also, the damping values were somewhat higher than are normally encountered during tests at these low levels of excitation. This was possibly related to the relatively higher interstory drifts associated with the greater flexibility of the Parsons building. The mode shapes associated with N-S excitation had only small E-W and rotational components. This was due to the near symmetrical distribution of stiffness and mass for vibration in the N-S direction. The E-W and torsional mode shapes

were often coupled, however, since the centers of mass and rigidity did not coincide in the E-W direction. The result of this is that torsional motions are more easily excited from unilateral excitation than would be the case for a perfectly symmetrical building.

Three-dimensional motions measured for two floors of the building revealed only small out-of-plane deformations of the floor slabs. With the exception of the fourth floor during vibration in the second E-W mode, no significant in-plane deformations of the floor slabs were detected although measurable deformation did occur. This justifies characterizing the dynamic response of each floor by one rotation and by two translational components of motion. Three-dimensional measurements taken at grade level in the building and on the ground surrounding the structure verified that these types of tests may be used for experimental verification of analytical soil-structure interaction models.

An important aspect of these tests was that measurements of strain were made on one of the columns of the moment resisting frame during forced excitation of the building. This is an important extension of forced vibration tests since the method may be used by future investigators to provide essential information for detailed system identification studies. Results of these tests will be compared in Chapter VI to corresponding values predicted by a finite element model of the structure.

The building demonstrated the nonlinear characteristics of a softening dynamic system. This was indicated by the lengthening of

the periods of vibration by as much as 9 percent with increasing levels of response. The translational and rotational components of the mode shapes were quite stable, however. Also, the foundation compliance was shown to be linear over this range of testing, so the observed non-linearity is confined to the structure. Several modal indices were used to investigate the sources of the nonlinearities. The observed non-linear behavior appeared to correlate best with the interstory drift and with the total kinetic energy of vibration.

In the final stages of the tests, mode shapes and frequencies for the N-S and E-W modes of vibration were determined by ambient tests. The results compared quite favorably to those determined by forced vibration tests in all cases except the third E-W mode. This again shows that ambient tests, when conducted under favorable conditions, provide a relatively easy means of determining the first few natural frequencies and mode shapes of most multistory buildings. It is not possible to gain the amount of detailed information available through forced vibration tests, however, since the investigator cannot control or determine the magnitude, the duration, or the frequency content of the exciting forces.

## CHAPTER VI

Dynamic Characteristics of the Parsons Building  
Predicted by a Finite Element Model

A finite element model of the Parsons building was developed and used to compute the first nine natural frequencies and mode shapes. The values were then compared to those measured during forced vibration tests. In the analysis, sinusoidal excitation was applied to the model with the same magnitude and location as for the full-scale tests. This enabled a direct comparison of computed roof displacements and member strains with those measured during the forced vibration tests.

6.1 Description of the Model

The purpose of this phase of the testing program was to assess the ability of a finite element model of a multistory building to predict the overall dynamic characteristics of the structure and to predict the maximum responses and member strains for a given excitation. For these results to be meaningful for engineering design, it was necessary to employ the same assumptions commonly used in engineering practice. One exception to this, however, is that translational and rotational motions were considered simultaneously. Typically, for a structure the size of the Parsons building the design engineer would model planar motion in the two principal translational directions with separate finite element models and would approximate the effects of torsion by a more simplified analysis.

The finite element model derived for the Parsons building was based on the structural design calculations and structural drawings for the building which were supplied by the Parsons company. Only a few additional assumptions were necessary. The total floor weights used were those used in the structural design. They were distributed to the nodal points according to tributary area for the uniform loads and by the location of various machinery and architectural walls. The total weights for several of the floors were determined independently by this investigator and were within 5 percent of the original estimates. The total weights for each floor are as follows: roof,  $1.45 \times 10^6$  lbs.; floors 12-6,  $9.00 \times 10^5$  lbs.; floor 5,  $2.075 \times 10^6$  lbs.; floors 4 and 3,  $1.65 \times 10^6$  lbs.; and floor 2,  $1.75 \times 10^6$  lbs. Thus, the total weight of the building is approximately  $1.5 \times 10^7$  pounds.

In general, only the moment resisting frames are considered in the earthquake design analysis of a structure. With a few exceptions, this practice was followed for this model as well. In order to predict accurately the torsional motions, it is necessary to model the spatial distribution of the mass of the various floors. To accomplish this for the Parsons building, additional columns were included in the model at the periphery of the four-story portion of the structure at points E2, F2, G2, E8, F8 and G8 (see Figure 5.3). These columns were connected to the moment resisting frame and to each other by truss elements (one-dimensional elastic bars). Since the slab was not of composite design, it is believed to provide only small bending rigidity to the frame. The slab will offer significant in-plane rigidity at each floor level, however. This was also modeled using truss elements.

Care must be taken not to use extremely "stiff" elements for this purpose since numerical inaccuracies can arise. The axial area used for these elements for this model was 200 sq. in., which is approximately the axial area of the largest beam element of the frame. This use of truss elements is generally not done in engineering practice because the various frames of a structure are usually considered independently. In this practice horizontal elements of the frame provide in-plane rigidity. These elements are necessary, however, if the "rigid-body" type rotations that the floors demonstrate during the dynamic tests are to be simulated in the model. Otherwise, the finite element model could predict modes in which the different frames of the structure move independently at the various floor levels in a way which would not be possible for the real structure. A plan view of the model is shown in Figure 6.1. The heavy lines represent the moment resisting beam elements and the lighter lines represent the truss elements. The circles represent the nodal points and column locations of the model. A section along the N-S centerline of the structure is shown in Figure 6.2.

There appears to be no clear concensus regarding the appropriate method to model the joint behavior of a moment resisting frame. Normally, the designer would use either the clear span or the centerline dimensions of the columns in the model, depending on the relative stiffnesses of the girders and the columns. These are sometimes referred to as "rigid joint" and "flexible joint" models respectively, although these names are not strictly accurate. Since the girder depths were on the order of 1.8 times larger than the column widths, the basic model used in this study

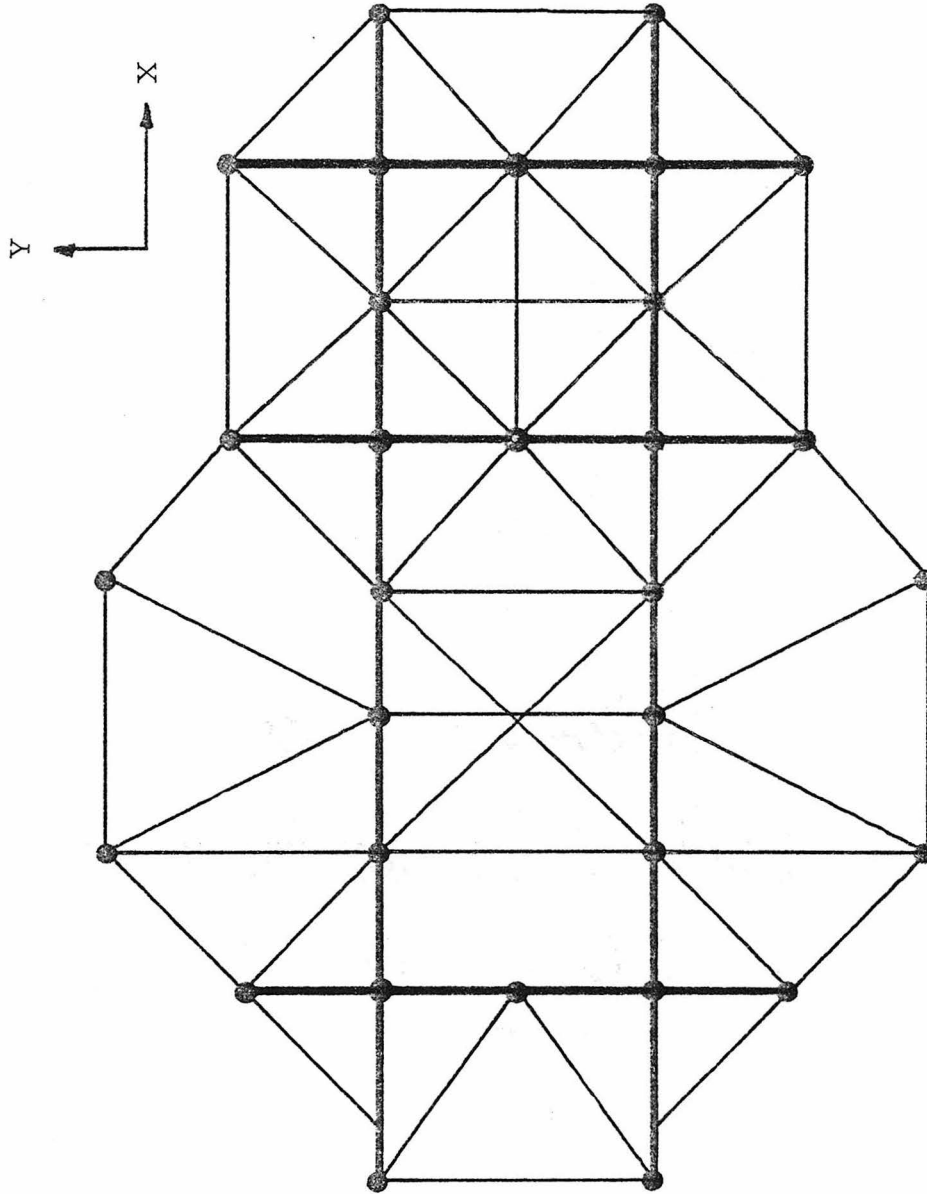


Figure 6.1 Plan view of a finite element model of the Ralph M. Parsons World Headquarters Building. Heavy lines indicate beam elements and light lines represent truss elements. Circles locate columns and nodal points.

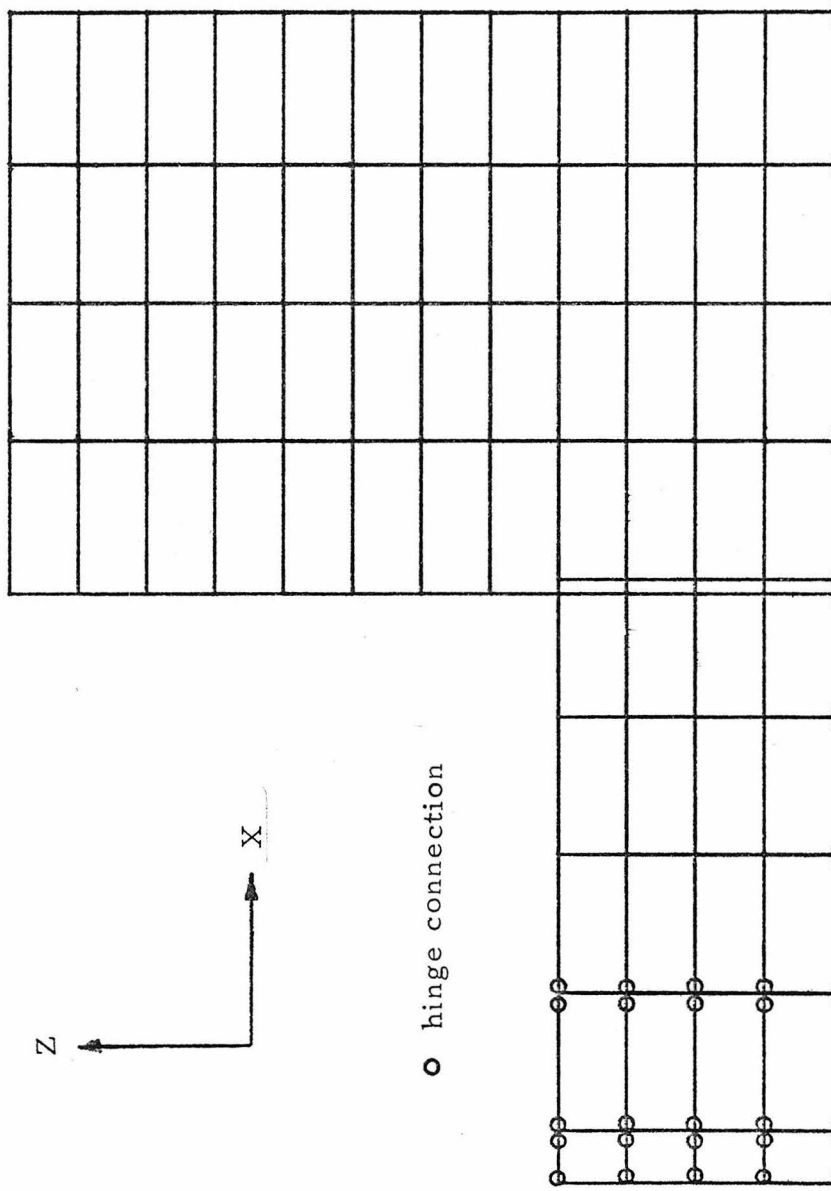


Figure 6.2 Elevation view of the model of the Parsons building.

assumed clear span dimensions for the column lengths and centerline dimensions for the girder lengths. It was also assumed that the model was fixed at the base. This assumption should be good for this building since measured first-floor motions were generally less than one percent of the roof motions.

As mentioned previously, the purpose of this portion of the research was to derive a finite element model of the Parsons building by employing as closely as possible the same design procedures and assumptions that might be used in a design office. Consequently, no adjustments were made to the model to reconcile differences in measured and predicted responses. The model input data could be artificially modified in such a way that most measured and predicted characteristics would be nearly identical (e.g., by adjusting the modulus,  $E$ ). This has been done in some investigations where the intent was to study specifically the effects of various nonstructural elements on the dynamic characteristics of a particular structure.

A question may be raised as to variability that would be expected in the predicted dynamic characteristics of the building as a result of the modeling assumptions that were made. It is likely to be true that if five engineers completed finite element models of the Parsons building, five different values for the fundamental period of the building would result. The estimates of the total mass of the structure might vary from 5-10 percent. This would cause roughly a 3-5 percent change in the natural frequencies of the model. It is unlikely that one would attempt to model the bending effect of the slab or the added stiffness of the nonmoment resisting frames as their

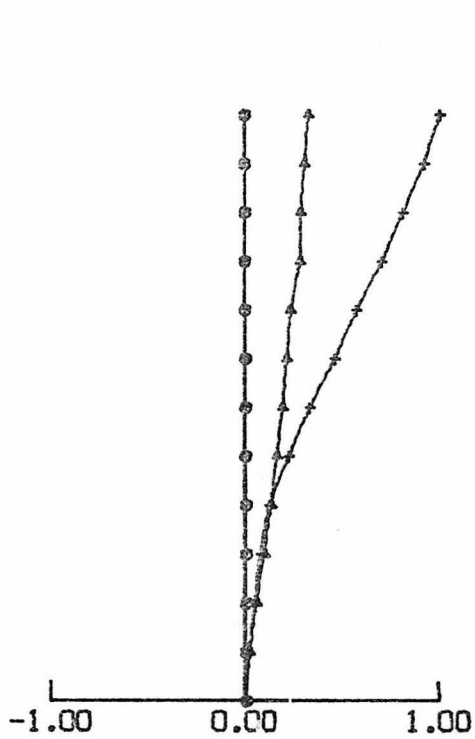
effects on the stiffness of the structure are probably small and are certainly difficult to ascertain. The design assumptions that would contribute substantially to differences between models developed by different engineers are those concerning the behavior of the joints. The predictions of the fundamental period of vibration of the Parsons building, based on clear span or centerline dimensions for column lengths differ by about 25 percent. Specific comparisons between these two models will be given later in this chapter. Based on this discussion, it is expected that the variability of periods calculated for design might be about 20-30%.

The finite element model was developed using a modified version of SAP IV, a general purpose program developed at the University of California at Berkeley. The model had 290 nodes which included 33 at the first floor level which were assumed fixed, 33 nodes each at floors 2-5 and 16 nodes each at floors 6-roof. Five degrees of freedom were considered at each node for a total of 1300 equations. Axial shortening of the columns was neglected after the analysis of a simplified model of one N-S moment resisting frame indicated that the inclusion of this lengthened the fundamental period by less than one percent. The computation of nine eigenvalues and eigenvectors required 19.3 minutes of computing time on an IBM 370 computer. Using a bandwidth minimization subroutine reduced the computing time to approximately 14.8 minutes, a savings of roughly 23 percent.

## 6.2 Computed Natural Frequencies and Mode Shapes for the Model of the Parsons Building

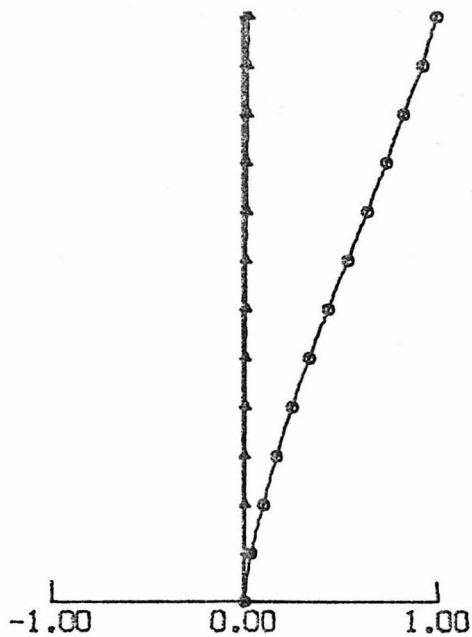
The computed natural frequencies and the  $\underline{x}$ ,  $\underline{y}$ , and  $\underline{R\theta}$  components of the mode shapes of the first nine modes of vibration of the model of the Parsons building are shown in Figures 6.3 through 6.7; they are numbered according to increasing frequency. These figures should be compared to Figures 5.12 through 5.16, which show the corresponding measured quantities. In viewing these figures, one should be careful to make the proper comparisons since the mode numbers of the measured and computed modes of vibration do not necessarily correspond. For instance, the first measured mode shape is mainly N-S in nature but the first computed mode shape is mainly torsional. The major component of the measured and computed mode shapes for the first three modes in the N-S, E-W and torsional directions are shown in Figures 6.8 through 6.10.

Certain similarities and differences between the measured and computed mode shapes and frequencies are indicated by the figures and should be discussed. The first three measured and computed mode shapes for which the major component of motion is N-S are all quite similar. These are the measured Mode 1, Mode 4 and Mode 8 and the computed Mode 2, Mode 5 and Mode 8. For these modes the E-W and rotational components of motion are relatively small in both cases with the smallest values associated with the model. This is because the model is nearly symmetric about the N-S centerline. The real structure, however, has asymmetries in both mass and stiffness which were not accounted for in the model. The first three



MODE 1  
0.343 HZ.

	X	Y	R0
159			
R	-0.015	0.32	1.00
12	-0.015	0.30	0.92
11	-0.013	0.28	0.81
10	-0.011	0.28	0.70
9	-0.010	0.23	0.57
8	-0.008	0.21	0.46
7	-0.006	0.19	0.33
6	-0.005	0.16	0.22
5	-0.004	0.13	0.12
4	-0.002	0.092	0.075
3	-0.001	0.053	0.043
2	-0.001	0.020	0.015
1	0.00	0.00	0.00



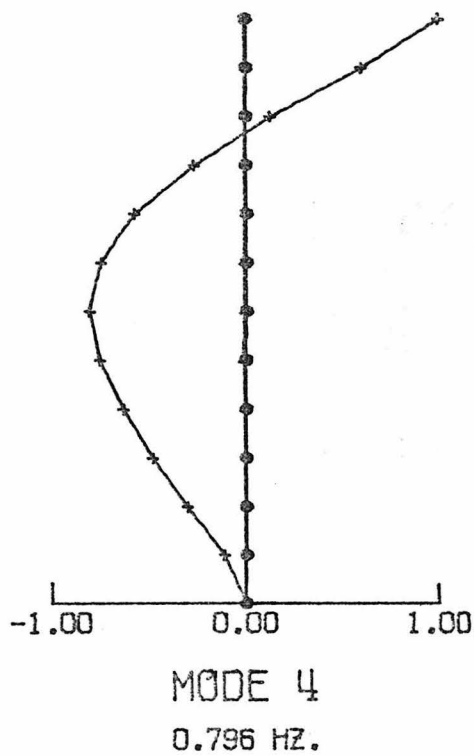
MODE 2  
0.404 HZ.

	X	Y	R0
159			
R	1.00	0.027	0.007
12	0.93	0.025	0.008
11	0.83	0.023	0.008
10	0.74	0.020	0.008
9	0.64	0.018	0.006
8	0.54	0.015	0.006
7	0.44	0.012	0.005
6	0.34	0.010	0.005
5	0.25	0.007	0.003
4	0.17	0.005	0.002
3	0.10	0.003	0.001
2	0.035	0.00	0.001
1	0.00	0.00	0.00

Figure 6.3 Computed mode shapes and frequencies of the Parsons building.

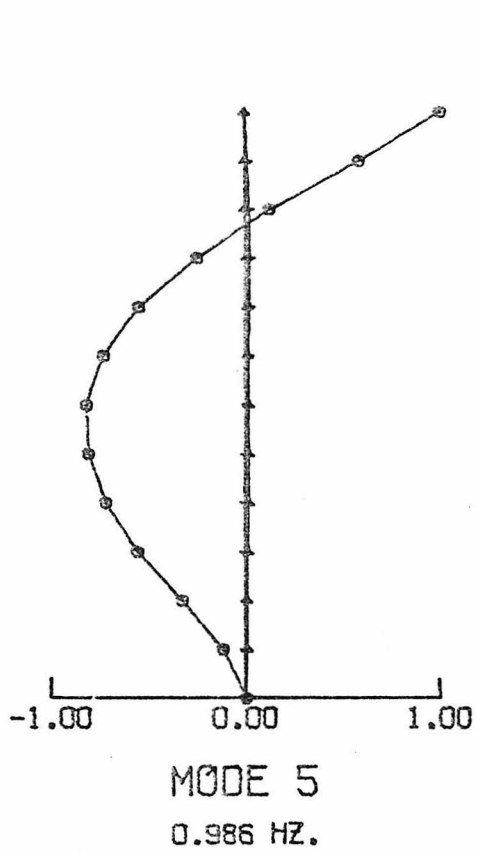


	X	Y	R0
160	-0.003	1.00	-0.27
12	-0.024	0.93	-0.24
11	-0.022	0.84	-0.15
10	-0.020	0.74	-0.16
9	-0.017	0.64	-0.11
8	-0.014	0.54	-0.072
7	-0.012	0.44	-0.030
6	-0.009	0.34	0.008
5	-0.010	0.24	0.031
4	-0.005	0.16	0.026
3	-0.003	0.095	0.020
2	-0.001	0.035	0.005
1	0.00	0.00	0.00

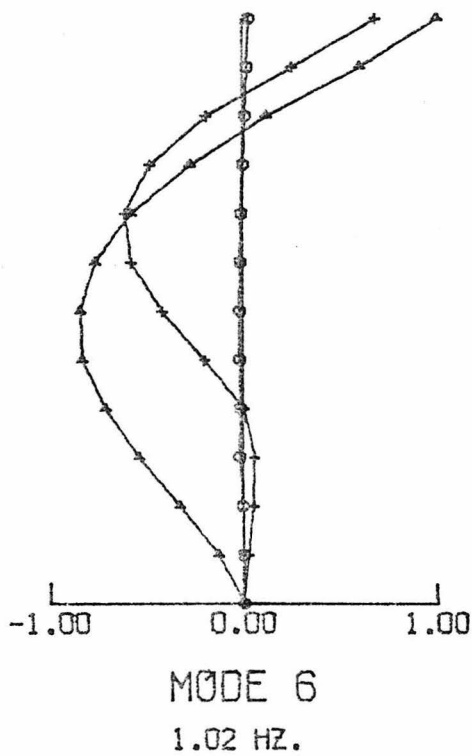


	X	Y	R0
160	-0.001	0.008	1.00
12	0.003	0.006	0.60
11	0.004	0.003	0.13
10	0.005	0.001	-0.26
9	0.006	0.001	-0.57
8	0.006	-0.003	-0.74
7	0.006	-0.004	-0.80
6	0.005	-0.005	-0.75
5	0.004	-0.004	-0.63
4	0.003	0.001	-0.48
3	0.001	0.003	-0.30
2	0.001	0.002	-0.11
1	0.00	0.00	0.00

Figure 6.4 Computed mode shapes and frequencies of the Parsons building.

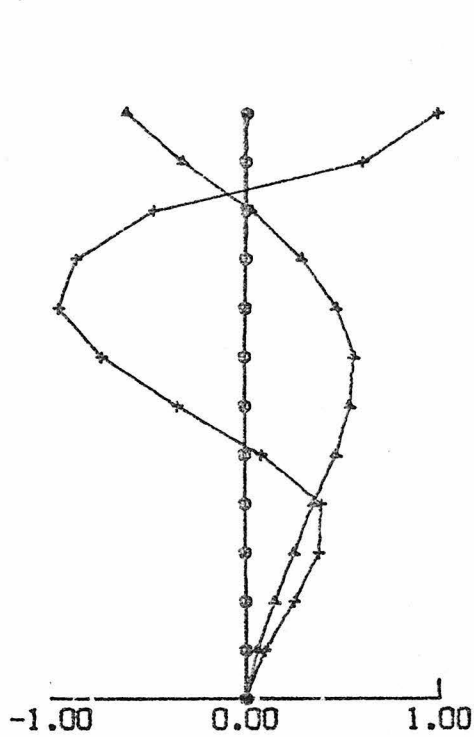


	X	Y	R0
161	1.00	-0.014	-0.011
R	1.00	-0.014	-0.011
12	0.58	-0.009	0.003
11	0.12	-0.005	0.014
10	-0.25	0.003	0.018
9	-0.55	0.007	0.017
8	-0.73	0.010	0.014
7	-0.82	0.012	0.007
6	-0.81	0.012	-0.001
5	-0.72	0.011	-0.006
4	-0.56	0.008	-0.006
3	-0.33	0.005	-0.004
2	-0.12	0.002	-0.002
1	0.00	0.00	0.00



	X	Y	R0
161	0.027	1.00	0.68
R	0.027	1.00	0.68
12	0.018	0.60	0.25
11	0.006	0.12	-0.19
10	-0.004	-0.27	-0.48
9	-0.012	-0.58	-0.61
8	-0.018	-0.76	-0.58
7	-0.021	-0.84	-0.42
6	-0.021	-0.83	-0.20
5	-0.019	-0.71	-0.002
4	-0.022	-0.54	0.051
3	-0.009	-0.33	0.050
2	-0.003	-0.13	0.021
1	0.00	0.00	0.00

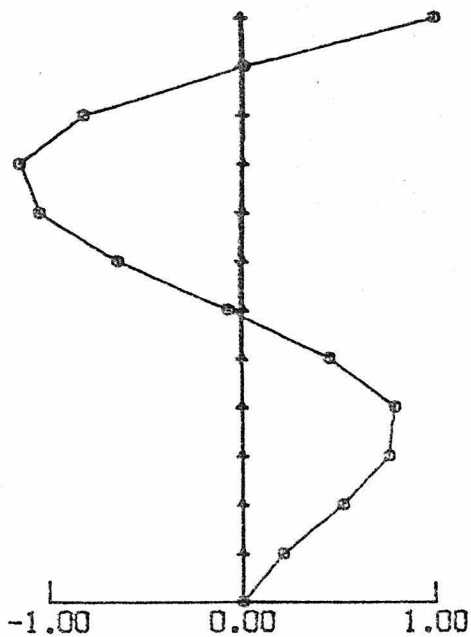
Figure 6.5 Computed mode shapes and frequencies of the Parsons building.



MODE 7  
1.13 HZ.

162

	X	Y	R0
R	0.011	-0.61	1.00
12	0.001	-0.32	0.61
11	0.006	0.027	-0.47
10	0.002	0.29	-0.87
9	-0.002	0.47	-0.96
8	-0.005	0.56	-0.74
7	-0.007	0.54	-0.35
6	-0.008	0.47	0.079
5	-0.007	0.35	0.39
4	-0.006	0.25	0.38
3	-0.004	0.15	0.25
2	-0.001	0.06	0.098
1	0.00	0.00	0.00



MODE 8  
1.59 HZ.

	X	Y	R0
R	1.00	-0.005	0.001
12	0.016	-0.001	0.014
11	-0.81	0.004	0.015
10	-1.14	0.006	0.007
9	-1.04	0.006	-0.007
8	-0.64	0.004	-0.014
7	-0.074	0.001	-0.014
6	0.45	-0.002	-0.008
5	0.79	-0.004	-0.001
4	0.76	-0.004	0.001
3	0.52	-0.002	0.001
2	0.21	-0.001	0.001
1	0.00	0.00	0.00

Figure 6.6 Computed mode shapes and frequencies of the Parsons building.

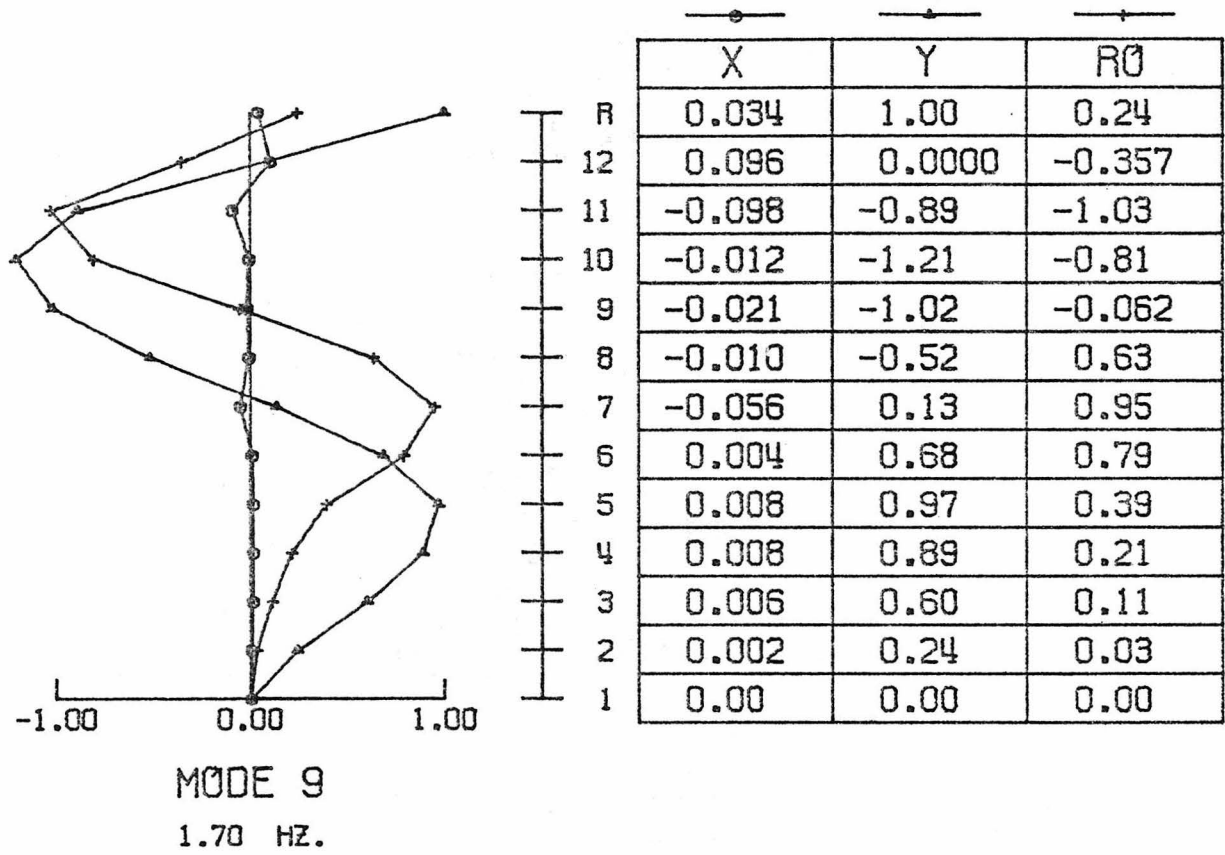


Figure 6.7 Computed mode shapes and frequencies of the Parsons building.

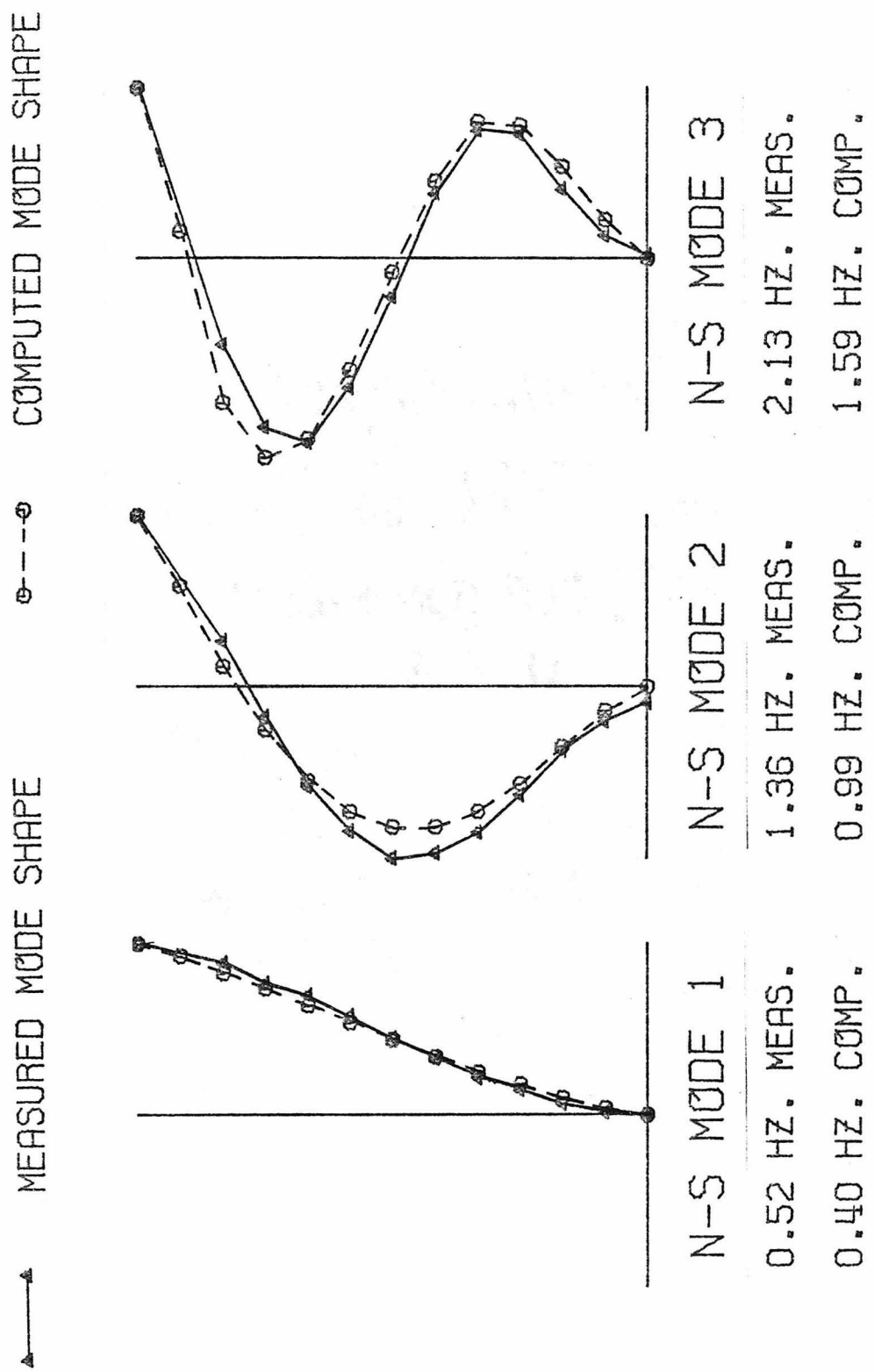


Figure 6.8 Comparison of measured and computed mode shapes for major components of N-S modes.

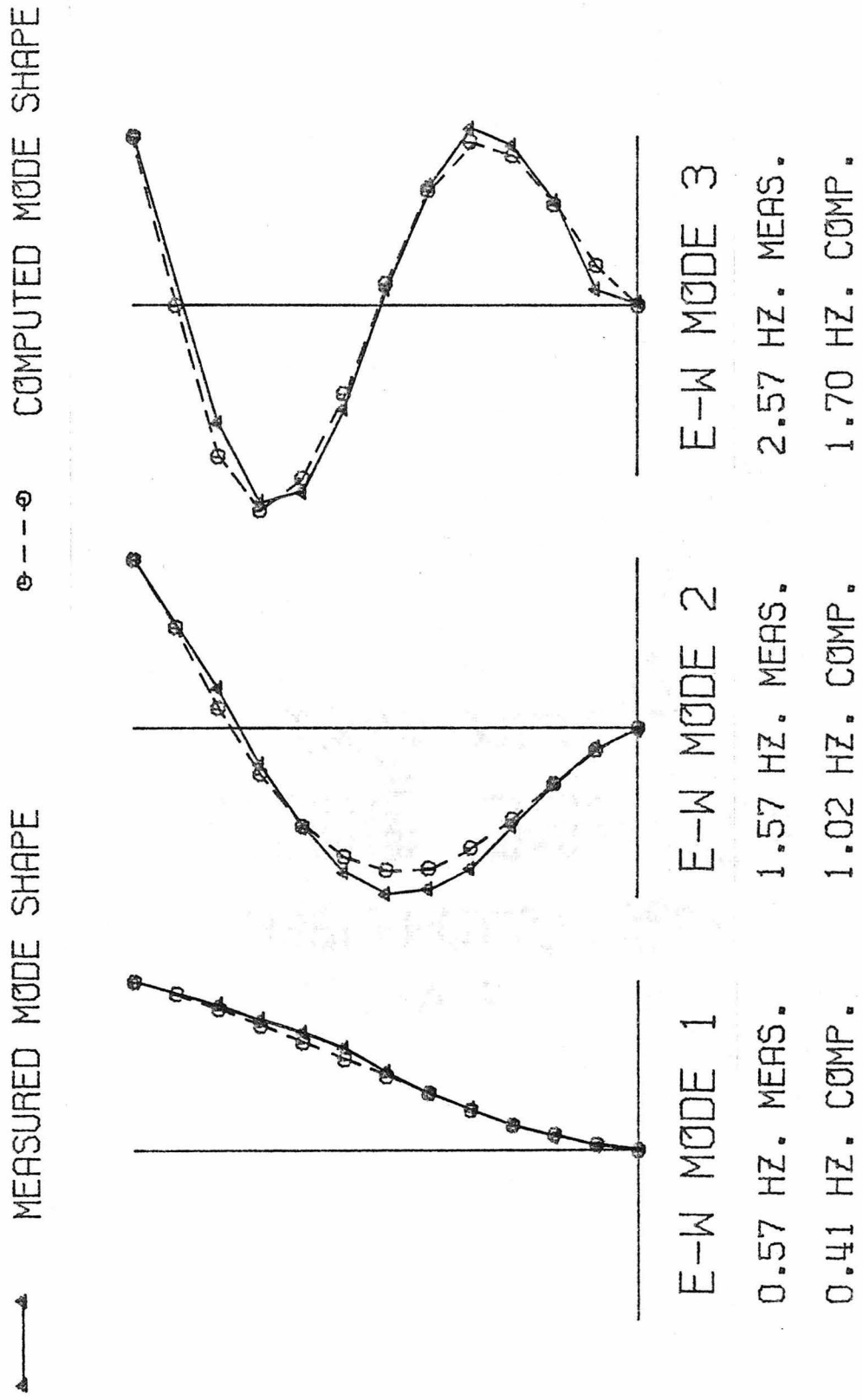


Figure 6.9 Comparison of measured and computed mode shapes for major components of E-W modes.

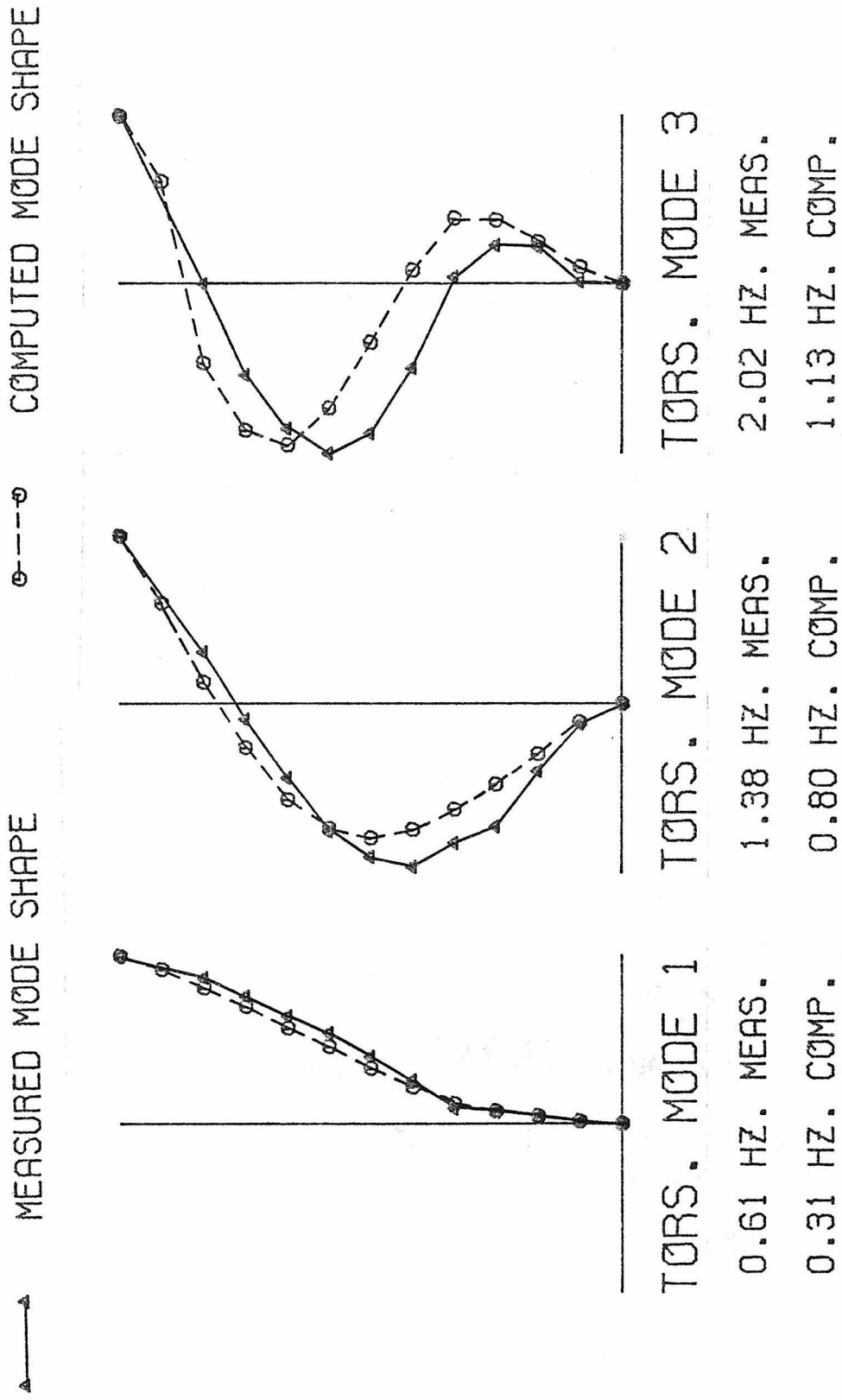


Figure 6.10 Comparison of measured and computed mode shapes for major components of torsional modes.

measured N-S natural frequencies are 20, 26 and 27 percent higher than those computed for the model. This is likely due to the added stiffness contributed by the nonstructural elements. These would include partition walls, emergency stairways, the vertical load carrying frame, mechanical and electrical ducts, etc.. Also, a major contributor of this added stiffness would be the precast concrete panels which are bolted to the periphery of the frame. It should be noted that the computed frequencies may be more representative of those exhibited by the building during an earthquake since it is not uncommon to see a decrease in the natural periods of buildings of over 30 percent<sup>15, 35, 65</sup> during the larger amplitude vibration that the structure experiences during these events.

The modes which are predominantly E-W in nature are Mode 3, Mode 6 and Mode 9 for the model and Mode 2, Mode 6 and Mode 9 for the real structure. The first E-W modes are reasonably similar for both cases. The rotational components for the model are generally larger than those measured for the building. Possible reasons for this phenomenon will be discussed later. In all cases the measured E-W natural frequencies were higher than those of the model. They differed by 28, 24, and 34 percent respectively for the first three E-W modes.

The first computed torsional mode shape (Mode 1) is quite similar to the first measured mode shape (Mode 3) with even the apparent discontinuity at the fifth floor being predicted. The effect is more pronounced for the real structure however. The second torsional mode is Mode 4 for the model and Mode 5 for the building.

A surprising fact about the computed mode shape is that there are relatively small E-W components. The E-W components of the third torsional mode are considerably different from those measured. In this case the model exhibits much larger E-W motions than the real structure. The torsional frequencies are not very well predicted either. The measured and predicted values differ by 49, 42 and 44 percent for the first three modes.

The major differences between the measured and predicted E-W and torsional mode shapes can be attributed to the lower rotational stiffness of the model. This causes the rotational components of the E-W modes of the model to be larger than for the actual structure. Also, since the rotational stiffness of the building is distributed differently throughout the structure than the model predicts, the actual and predicted locations of the center of rotation of the various floors will differ. This could give rise to the larger E-W components of the predicted torsional modes. The larger rotational stiffness of the real structure could possibly be attributed to the effect of the precast panels at the periphery of the frame. These would have a more pronounced effect on the torsional modes than upon the translational modes for two reasons. First, all of the walls would act to resist torsion whereas only those in line with the translational direction under consideration would be effective for that case. Secondly, elements that resist torsion increase in effectiveness as their distance from the center of rotation increases. This hypothesis is supported by the fact that the predictions of the torsional frequencies are nearly twice as low as those for the N-S and E-W modes.

Clearly, all of the differences between the measured and predicted values should not be attributed to these precast panels. Plaster wall partitions, electrical and mechanical ducts and emergency stairwells have also been shown in the past<sup>49</sup> to have a significant effect on the translational and rotational dynamic characteristics of a real structure. Another likely contributing factor would be the interaction of the satellite structures with the main structure. Although separation joints were provided, a certain amount of indirect coupling of the structures was evident in the tests. This would account for the generally larger disagreement between measured and predicted values for the higher frequencies. Since the motions in the lower floors are larger for these modes than for lower modes, the interaction would be more pronounced.

### 6.3 Comparison of Measured and Computed Responses

A necessary aspect of a finite element model of a structure is that it predict accurately the maximum displacements of the various floors of the building for a given excitation. This is essential if the model is to determine accurately the maximum stresses in the structural elements. To test the adequacy of this model in that respect, a sinusoidal force of equal magnitude to that used during the test was applied to the roof of the model. To match the test conditions, however, the frequency of the excitation was taken as the natural frequency of the model of the particular mode under consideration. The damping assumed was that measured for the corresponding mode of the real structure. The excitation was continued until steady state response

was achieved which was about 30 seconds for the first three modes and 20 seconds for the higher modes. The magnitude of the measured and computed steady-state displacements are shown in Table 6.1.

The computed roof displacements are larger than the measured values in all cases. This is consistent with the fact that the model is considerably more flexible than the real structure as indicated by the lower natural frequencies. A more complete understanding of this may be gained by observing Equation (5.1). This indicates that the displacement responses in a given mode should differ between the model and the structure in proportion to two factors. One factor depends on the mode shapes and the other factor varies as  $1/\omega^4_j$ . In this case the latter term would have the most pronounced effect.

An equally, if not more, important aspect of a finite element model is that it accurately predict the member stresses for a given configuration of floor displacements. Using the same simulated test as described for computing the roof displacements, the member bending strains were computed for the same fourth-floor column (column D4) for which strains were measured. Since the predicted displacements for the model were different from the measured values, a more meaningful comparison of the measured and predicted strains would be the member stress divided by the roof displacement. These measured and predicted quantities are listed in Table 6.2.

The column strains computed by the model will depend significantly upon the column length assumed. Therefore, the same computations were made for a model in which the column lengths were assumed to be the centerline dimensions of the girders instead of the

Table 6.1 - Comparison of Measured and Predicted Roof Displacements

Mode	F . sin( $\omega t$ ) Excitation	
	Measured Roof Displacement (in.)	Computed Roof Displacement (in.)
N-S 1	0.032	0.053
N-S 2	0.014	0.028
N-S 3	0.014	0.025
E-W 1	0.022	0.038
E-W 2	0.012	0.024

Table 6.2 - Comparison of Measured and Predicted  
(Column Bending Stress)/(Roof Displacement)

Mode	Measured $\sigma_c/\Delta_r$ (psi/in.)	Computed $\sigma_c/\Delta_r$ Short Column Model (psi/in.)	Computed $\sigma_c/\Delta_r$ Long Column Model (psi/in.)
N-S 1	719 <sup>†</sup>	1830	1130
N-S 2	3571 <sup>†</sup>	4614	3101
N-S 3	2642 <sup>†</sup>	1960	--
E-W 1	1000	1445	875
E-W 2	3083	4042	2914

<sup>†</sup>Total stresses. Bending stresses could not be determined for this mode.

clear span height. These results are also listed in Table 6.2 under the heading "long column model". One would expect that the computed values using the two models would provide upper and lower bounds on the actual stress in the column. This was indeed the case for all but the first N-S mode for which both models predicted higher values than the measured quantity.

There are several possibilities for this discrepancy for the first N-S mode. Since it was only possible to mount one LVDT on the north face of the column, one would be measuring the total strain which would be the combination of an axial component and a bending component. These would have different signs for the north face of the column for the first N-S mode. Consequently the stress due to bending alone would be higher than the measured value. Also, complicated stress patterns due to end effects caused by the closeness of the girders to the point of measurement would cause unpredictable effects on the measurements. However, this effect might also be expected for the higher modes in this direction as well. This is not clearly evident in the results. Furthermore, although no experimental errors could be found, the measured roof displacement seems somewhat large compared to that measured for the first E-W mode. Differences between the measured and computed mode shapes may also play a secondary role in this discrepancy. Limited time and access precluded retaking the measurements of strain for the first N-S mode to check for possible experimental error in the original measurement.

#### 6.4 Conclusions

The results presented in this chapter indicate that the natural frequencies and mode shapes calculated from the finite element model of the Parsons building for N-S and E-W modes of vibration were reasonably good estimates of those measured for the actual structure. The values for the N-S direction were somewhat better due to the near symmetric distribution of mass and stiffness in this direction. Rotational motions may not be modeled as well, however, due to their sensitivities to stiffening effects which occur at the periphery of the frame, which are not accounted for in the model. The predicted natural frequencies in the N-S and E-W directions were 20-30 percent lower than the measured frequencies. This was consistent with the fact that many stiffening elements in the real structure are not included in the model.

It was mentioned briefly in a previous section that it is not uncommon for the periods of vibration of multistory buildings of similar construction to the Parsons building to lengthen by 20 percent to 50 percent during a strong earthquake and yet sustain no apparent structural damage. The fundamental period of the Parsons building is relatively long to begin with, so it remains to be seen if the changes for this structure will be as large as this. If the lengthening in the periods of the structure are on the order of 20-30 percent for an earthquake that produces near yield conditions in the structural members of the building, the model would be expected to yield excellent estimates of the natural frequencies of vibration. Also, due to the overall loss

in stiffness implied by these changes in the natural frequencies, good estimates of the maximum floor displacements given the input acceleration should be expected.

The measured stresses in a column for a given roof displacement were generally bounded by those predicted by the rigid joint and flexible joint models and were within 25 percent of these values. The point of measurement of the stresses was located some distance from the girder-column joint where the maximum stresses occur. Consequently, the predicted stresses had to be reduced according to the distance away from the joint. Since this reduction was somewhat greater for the flexible joint model, the bounds on the maximum stress predicted by the rigid joint and flexible joint models were actually somewhat closer than those indicated in Table 6.2. This suggests that predictions of stresses for a given excitation based on the finite element model of the Parsons building should be within 25 percent of the actual stresses experienced by the real structure provided that the maximum floor displacements are also predicted accurately.

One must be careful of inferring generalizations from these results for this particular building. However, on the basis of this preliminary experiment, the "25%" figure would seem to be a reasonable number to assign to expectations of predicted stresses based on properly constructed finite element models of real multistory buildings.

## CHAPTER VII

Summary and Conclusions

The experimental procedure employed during the forced vibration tests of the Millikan Library involved the simultaneous measurement of the three components of motion for selected points on floor slabs of the structure. These measurements provided detailed information of a type that has not previously been available. By measuring out-of-plane deformations of floor slabs, the complex interaction between lateral and vertical load-carrying systems was revealed. This interaction between the different elements of a structural system may produce stresses in the structure which are significantly different from those predicted by planar models of the building.

An additional result of the Millikan Library tests was the discovery of an apparent change in the response of the foundation to a given excitation when compared to results of previous studies. The measurements indicated that the base of the library translated about twice as much and rotated approximately 25 times more than it did during these previous tests. This change in the deformational characteristics of the base was accompanied by a decrease in the natural frequency of vibration of about 11 percent. An Euler beam model of the building and a lumped-mass model (which included the effects of shear deformation in the structure) were constructed as aids to investigating this phenomenon. The conclusion based on this study was that the observed decrease in the natural frequency of vibration was

consistent with the measured changes in the mode shape. This change in the foundation response of the library was believed to have been the result of the San Fernando earthquake which occurred between the times that the two tests were performed.

Forced vibration tests of the Ralph M. Parsons Company World Headquarters building were conducted to determine the vibrational characteristics of this twelve-story steel framed structure. The natural frequencies, three-dimensional mode shapes and damping coefficients were measured for nine modes of vibration. These were determined by an extension of a previous method which utilized the component of response  $90^\circ$  out-of-phase with the exciting force. The mode shapes revealed that modes which were primarily E-W translational modes also contained significant rotational components. In addition, the torsional mode shapes contained relatively large E-W components of motion. These are examples of modal coupling. Another phenomenon that was observed was modal interference. Both modal coupling and modal interference can cause large torsional motions to results from purely unilateral base excitation of the structure. Consequently, these effects need to be accounted for in the analysis of a structure for earthquake resistant design. Since these "accidentally" induced torsional motions have only been identified to date during controlled tests of structures, it would be beneficial to place enough strong motion instruments in a multistory building to allow the detection of these effects should they occur in the building during its response to some future earthquake. The Parsons building

is ideally suited for such a study since the results of the tests suggest that some torsional components of motion should be present during its response to E-W excitation. Consequently, the author suggests that an instrumentation package be installed in the Parsons building which is extensive enough to determine the degree to which torsional motions are produced in the building during earthquake excitations.

Three-dimensional measurements taken on two floors of the building indicated that, unlike the Millikan Library, only small out-of-plane deformations occurred in the floor slabs of the Parsons building. They also indicated that, with possibly one exception, in-plane deformations of the slabs were small and insignificant. Thus, as expected, the analysis of this building based on two translational and one rotational degree of freedom per floor would be appropriate. Three-dimensional measurements taken in the basement and on the ground surrounding the structure reaffirmed that this type of testing may be used to provide data for the verification of analytical soil-structure interaction models; but the measurements did not indicate soil-structure interaction of a significant level for this building.

An important extension of forced vibration testing was the measurement of strain in one of the columns of a moment resisting frame of the Parsons building. This provides a method by which future investigators may obtain essential information for detailed system identification studies. This also provided information for the evaluation of a finite element model of the Parsons building.

The studies of the Parsons building also included the investigation of apparent nonlinearities in the response which are associated with increasing levels of excitation. This was indicated by a decrease in the natural frequency of vibration in a particular mode with an increased level of response. The mode shape remained quite stable, however; and the response of the foundation was determined to be linear over the range of testing. The study indicated that the nonlinearities seemed to be related to interstory drift and the total kinetic energy of vibration in a mode.

Two types of analyses were used in this investigation for the purpose of predicting the dynamic characteristics of the buildings that were studied. The method of analysis used to model the characteristics of the Millikan Library building stressed simple ideas in mechanics and required a minimum amount of computational effort. The approach used was a lumped-mass model which included the effects of shear deformation in the building and soil-structure interaction. The natural frequency of vibration of the model was 6% greater than that of the building during the San Fernando earthquake; and the mode shape of the model was nearly the same as that measured for the building. This is remarkable agreement considering the simplicity of the model and it is not thought to be typical. It does indicate, however, that useful, accurate dynamic analyses of structures may be accomplished in an engineering office without the penalty of excessive computer costs. For this building at least, this type of analysis can provide a more realistic estimate of the effects of earthquake loadings

on the structure than the use of a static analysis based on equivalent lateral loads; and about the same effort is required in both cases.

The analysis of the Parsons building employed a three-dimensional finite element model of the structure. A general purpose finite element code, SAP IV, was used in this investigation. The predicted mode shapes and frequencies of the predominantly N-S and E-W modes were predicted reasonably well. The frequencies were about 25-30 percent lower than the measured values. The torsional mode shapes and frequencies were not adequately predicted due to added stiffness at the periphery of the frame. Much of this stiffness is thought to be contributed by nonstructural precast concrete elements that would not usually be included in the analysis. A sinusoidal excitation identical in magnitude to that used during the tests was applied to the roof of the model. This analysis gave predictions of roof displacement that were 40-50 percent greater than those measured. This is due to the additional stiffness in the building provided by the nonstructural elements, by the vertical load carrying system and by other items not included in the model. When predictions of stress were normalized by the roof displacement, these values were about 25% greater than similar measured quantities. These predictions of normalized stress, obtained for this model, which assumed clear story heights as the column dimensions, and the results of a second model which used centerline dimensions as column heights, formed upper and lower bounds for the measured values; both of these predictions were within 25 percent of the measured values.

The simplified methods of analysis used for the Millikan Library and the finite element analysis employed in the study of the Parsons building are similar in the sense that they reduce to mathematical equations of the same form. Thus the results from either method based on similar assumptions should be comparable. Both of these analysis techniques provide valuable tools for studying the dynamic response of buildings. The choice of one over the other would depend on the type of building and the economics of the situation. The simplified analysis was included in this study to demonstrate that in some instances the dynamic characteristics of a structure may be modeled accurately by simple systems which are inexpensive to use and are easy to understand.

As an aid to future investigators, a few comments should be made about the instrumentation system used for these tests. The Ranger seismometers with their accompanying signal conditioners are excellent transducers for sensing motion at these low levels of excitation. Their high signal-to-noise ratio provides for accurate determination of the relative amplitudes and phases of motion between measured points. Their high output allows the accurate measurement of grade-level motions for soil-structure interaction studies. The VG-1 vibration generating system is also an improvement over the previous models. The greatest improvement involved the ease with which the two shakers could be operated synchronously. The measurement of strain during forced excitation was greatly facilitated by the use of the LVDT as the transducer. The high signal-to-noise ratio and the high output of this device provide clear and easily readable

signals even for displacements as small as  $10^{-6}$  in. The author would advise future investigators to employ more automation in the data collection system than was used in these tests. For example, signals could be recorded on magnetic tape, digitized, and then analyzed on a digital computer. This would relieve the drudgery of manually measuring over 7000 sine waves on strip chart recordings.

Two suggestions should be made regarding the direction of future programs for full-scale tests of structures. Valuable information could be gained by performing laboratory tests in conjunction with full-scale tests of a structure. Precise stiffness properties of the members and joints could be determined in the laboratory using static and dynamic loading conditions which would allow an accurate finite element model of the structure to be derived. Dynamic tests of the full-scale structure, preferably while it is under construction, could then be performed and accurate estimates of the effects of the non-structural elements of the building could be obtained. Another investigation that would be extremely beneficial would be the destructive test of a multistory building. This would provide much needed information about the energy absorbing capacity and the ductility provided by modern design methods. This information is not available at the present time. The combination of the two programs mentioned above would be ideal; and the information gained from this would be a highly significant contribution to the understanding of the dynamic behavior of full-scale structures.

## REFERENCES

1. American Concrete Institute, "Building Code Requirements for Reinforced Concrete (ACI 318-71), A. C. I., Detroit, Michigan, 1971.
2. Bendat, J. S. and A. G. Piersol, Measurement and Analysis of Random Data, New York: John Wiley & Sons, Inc., 1966.
3. Bernhard, R. K., "Artificial Vibration--A New Method of Dynamic Research," Civ. Eng., VII, April 1937, 286-287.
4. Bernhard, R. K., "Geophysical Study of Soil Dynamics," Trans. Amer. Inst. Mining & Metall. Eng., 138, 1940, 326-344.
5. Byerley, P., J. Hester, and J. K. Marshall, "The Natural Periods of Vibration of Some Tall Buildings in San Francisco," Bull. Seis. Soc. Amer., 21, 1931, 268-276.
6. Blume, J. A., "A Machine for Setting Structures and Ground into Forced Vibration," Bull. Seis. Soc. Amer., 25, 1934, 375-376.
7. Bouwkamp, J. G. and J. K. Blohm, "Dynamic Response of a Two-Story Steel Frame Structure," Bull. Seis. Soc. Am., 66, 1966, 1289-1303.
8. Bouwkamp, J. G. and D. Rea, "Dynamic Testing and the Formation of Mathematical Models," Earthquake Engineering, ed. by R. L. Wiegel, Englewood Cliffs, N. J.: Prentice-Hall, Inc., 1970.
9. Caughey, T. K., "Classical Normal Modes in Damped Linear Systems," J. Appl. Mech., 27, 1960, 269-271.
10. Coast and Geodetic Survey, Earthquake Investigations in California,

- 1934-1935, Carder, D. S., ed., Special Publication no. 201, U.S. Dept. of Commerce, Washington, D. C., 1936.
11. Cooley, J. W. and J. W. Tukey, "An Algorithm for the Machine Calculation of Complex Fourier Series," Math. of Comp, 19, 1965, 297-301.
  12. Desai, C. S. and J. F. Abel, Introduction to the Finite Element Method, New York: Van Nostrand Reinhold Co., 1972.
  13. Englekirk, R. E. and R. B. Matthiesen, "Forced Vibration of an Eight-Story Reinforced Concrete Building," Bull. Seis. Soc. Amer., 57, 1967, 421-436.
  14. Foutch, D. A., J. E. Luco, M. D. Trifunac and F. E. Udwadia, "Full Scale, Three Dimensional Tests of Structural Deformations During Forced Excitation of a Nine-Story Reinforced Concrete Building," Proc., U.S. National Conference on Earthquake Engineering, Ann Arbor, Michigan, June 1975, 206-215.
  15. Foutch, D. A., G. W. Housner, and P. C. Jennings, "Dynamic Responses of Six Multistory Buildings During the San Fernando Earthquake," EERL 75-02, California Institute of Technology, Pasadena, California, 1975.
  16. Foutch, D. A., "Recent Advances in Dynamic Testing of Full-Scale Structures," Proc., ASCE/EMD Specialty Conference on Dynamic Responses of Structures: Instrumentation, Testing Methods and System Identification, University of California, Los Angeles, March 1976, 160-168.
  17. Foutch, D. A. and G. W. Housner, "Observed Changes in the Natural Periods of Vibration of a Nine-Story Steel Frame Building,"

- Proc., Sixth World Conference on Earthquake Engineering, New Delhi, India, 1976.
18. Foutch, D. A. and P. C. Jennings, "Dynamic Tests of Full-Scale Structures," Proc., Sixth World Conference on Earthquake Engineering, New Delhi, India, 1976.
  19. Gates, W. E., "Design Lesson Learned from the Performance of Instrumented High-Rise Buildings in the San Fernando Earthquake," Proc., Fifth World Conference on Earthquake Engineering, Rome, 1974.
  20. Gersch, W., N. N. Nielsen, and H. Akaike, "Maximum Likelihood Estimation of Structural Parameters from Random Vibration Data," J. Sound Vibration, 31. No. 3, 1973, 295-308.
  21. Gersch, W. and D. A. Foutch, "Least Squares Estimates of Structural System Parameters Using Covariance Function Data," IEEE Trans. on Auto. Control, AC-19, No. 6, December, 1974, 898-903.
  22. Gobler, H. W., "Three-Dimensional Modeling and Dynamic Analysis of the San Diego Gas and Electric Company Building," M.Sc. Thesis, School of Engineering, University of California, Los Angeles, 1969.
  23. Hetenyi, M., Beams on Elastic Foundations, Ann Arbor, Mich.: University of Michigan Press, 1946. Revised 1974.
  24. Hoerner, J. B. and P. C. Jennings, "Modal Interference in Vibration Tests," J. of the Engr. Mech. Div., ASCE, 95, EM4, 1969, 827-839.

25. Hoerner, J. B. , "Modal Coupling and Earthquake Response of Tall Buildings," EERL 71-07, California Institute of Technology, Pasadena, California, 1971.
26. Housner, G. W. and T. Vreeland, The Analysis of Stress and Deformation, New York: The Macmillan Co. , 1966.
27. Hudson, D. E. , "Dynamic Tests of Full-Scale Structures," Earthquake Engineering, R. L. Wiegel, ed. , Englewood Cliffs, N.J.: Prentice-Hall, Inc. , 1970, 127-149.
28. Hudson, D. E. , "Synchronized Vibration Generators for Dynamic Tests of Full-Scale Structures," EERL, California Institute of Technology, Pasadena, California, 1962.
29. Hudson, D. E. , W. O. Keightley, and N. N. Nielsen, "A New Method for the Measurement of the Natural Periods of Buildings," Bull. Seis. Soc., Amer. , 54, 1964, 233-241.
30. Ibanez, I. , R. B. Matthiesen, C. B. Smith, and G. S. C. Wang, "San Onofre Nuclear Generating Station Vibration Tests," Nuclear Energy Lab and Earthquake Engineering and Structures Lab. , University of California, Los Angeles, 1970.
31. Jennings, P. C. , ed. , "Engineering Features of the San Fernando Earthquake," EERL 71-02, California Institute of Technology, Pasadena, California, 1971.
32. Jennings, P. C. and Kuroiwa, J. H. , "Vibration and Soil-Structure Interaction Tests of a Nine-Story Reinforced Concrete Building," Bull. Seis. Soc. Amer. , 58, No. 3, 1968, 891-916.

33. Jennings, P. C., R. B. Matthiesen and J. B. Hoerner, "Forced Vibration of a 22-Story Steel Frame Building," EERL 71-01, California Institute of Technology, Pasadena, California, 1971.
34. Jennings, P. C., R. B. Matthiesen and J. B. Hoerner, "Forced Vibration of a Tall Steel Frame Building," Int. J. Earthquake Eng. Struct. Dyn., 1, 1972, 107-132.
35. Jennings, P. C. and H. Iemura, "Hysteretic Response of a Nine-Story Reinforced Concrete Building," Int. J. Earthquake Eng. and Struct. Dyn. 3, No. 2, 1974, 183-202.
36. Jennings, P. C. and D. A. Foutch, "Recorded Response of Buildings During Strong Earthquake Motions," Proc. of the UN-ECE Seminar on Construction in Seismic Regions with Difficult Ground Conditions, Bucharest, Rumania, October, 1974.
37. Keightley, W. O., "A Dynamic Investigation of Bouquet Canyon Dam," EERL, California Institute of Technology, Pasadena, California, 1964.
38. Keightley, W. O., "Vibration Test of Structures," EERL, California Institute of Technology, Pasadena, California, 1963.
39. Kinometrics, Inc., "VG-1 Vibration Generating System, Instruction Manual," Kinometrics, Inc., San Gabriel, California, 1975.
40. Kholer, R., "The Resonance Method as an Aid in Seismological Investigations," Leitschr. Geophisics, 8, 1932, 461-467.  
From Blume, J.A., "The Building Vibrator," in reference 10.
41. Lord, J., "Post Earthquake Analysis of a 42-Story Tower," in reference 56.

42. Luco, J. E., and R. A. Westmann, "Dynamic Response of a Rigid Footing Bonded to an Elastic Half-Space," J. of App. Mech., ASME, 39, 1972, 527-534.
43. Luco, J. E., H. L. Wong and M. D. Trifunac, "A Note on the Dynamic Response of Rigid Imbedded Foundations," Int. J. Earthquake Eng. Struct. Dyn., 4, 1975, 119-127.
44. Kuroiwa, J. H., "Vibration Test of a Multistory Building," EERL, California Institute of Technology, Pasadena, California, 1967.
45. Manual of Steel Construction, American Institute of Steel Construction, Inc., New York, 7th ed., 1967.
46. Matthiesen, R. B. and C. B. Smith, "A Simulation of Earthquake Effects on the UCLA Reactor Using Structural Vibrations," UCLA-NEL-105, No. 66-56, Dept. of Engineering, University of California, Los Angeles, 1966.
47. Matthiesen, R. B. and C. B. Smith, "Forced Vibration Tests of the Carolinas-Virginia Tube Reactor (CVTR)," Nuclear Energy Lab. and Earthquake Engineering and Structures Lab., No. 69-8. University of California, Los Angeles, 1969.
48. Meyer, S. L., Data Analysis for Scientists and Engineers, New York: John Wiley & Sons, Inc., 1975.
49. Nielsen, N. N., "Dynamic Response of Multistory Buildings," EERL, California Institute of Technology, Pasadena, California, 1964.
50. Newmark, N. M. and E. Rosenblueth, Fundamentals of Earthquake Engineering, Englewood Cliffs, N.J.: Prentice-Hall, Inc., 1971.

51. Otnes, R. K. and L. Enochson, Digital Time Series Analysis, University Software Systems, New York: John Wiley & Sons, Inc., 1972.
52. Parmalee, R. A., D. S. Perelman and S. L. Lee, "Seismic Response of Multiple-Story Structure on Flexible Foundations," Bull. Seis. Soc. of Amer., 59, No. 3, 1969, 1061-1070.
53. Proceedings of the U.S. National Conference on Earthquake Engineering, EERL, Ann Arbor, Michigan, 1975.
54. Rea, D., J. G. Bouwkamp, and R. W. Clough, "The Dynamic Behavior of Steel Frame and Truss Buildings," Structures and Materials Research Report No. 66-24, University of California, Berkeley, 1966.
55. Rea, D., A. A. Shah, and J. G. Bouwkamp, "Dynamic Behavior of a High-Rise Diagonally Braced Steel Building," College of Engineering, No. EERC 71-5, University of California, Berkeley, 1971.
56. Report on the San Fernando Earthquake of February 9, 1971, EERI/NOAA, U.S. Government Printing Office, 1974.
57. Rouse, G. C. and J. G. Bouwkamp, "Vibration Studies of Monticello Dam," Research Report No. 9, Water Resources Technical Publication, U.S. Dept. of the Interior, Bureau of Reclamation, Washington, D. C., 1967.
58. Smith, C. B. and R. B. Matthiesen, "Forced Vibration Tests of the Experimental Gas-Cooled Reactor (EGCR)," Earthquake Engr. and Structures Lab. and Nuclear Energy Lab, University of California, Los Angeles, 1969.

59. Stephen, R. M., J. P. Hollings, and J. G. Bouwkamp, "Dynamic Behavior of a Multistory Pyramid-Shaped Building," EERC 73-17, University of California, Berkeley, 1974.
60. Teledyne-Geotech, "Ambient Vibration Survey of Building 180, Jet Propulsion Laboratory," report for the California Institute of Technology, Pasadena, California, 1971.
61. Teledyne-Geotech, "Post Earthquake Vibration Measurements of Millikan Library," prepared for the California Institute of Technology, Pasadena, California, 1971.
62. Timoshenko, S. P., D. H. Young, and W. Weaver, Vibration Problems in Engineering, 4th ed., New York: John Wiley & Sons, Inc., 1974.
63. Trifunac, M. D., "Ambient Vibration Test of a Thirty-Nine Story Steel Frame Building," EERL 70-02, California Institute of Technology, Pasadena, California, 1970.
64. Trifunac, M. D., "Comparison between Ambient and Forced Vibration Experiments," Int. J. Earthq. Engr. Struct. Dyn., 1, 1972, 133-150.
65. Trifunac, M. D. and F. E. Udwadia, "Time and Amplitude Dependent Response of Structures," Int. J. Earthquake Eng. and Struct. Dyn., 2, 1974, 359-378.
66. Veletsos, A. S. and J. W. Meek, "Dynamic Behavior of Building-Foundation Systems," Structural Research Report No. 20, Dept. of Civ. Eng., Rice University, Houston, Texas, 1973.

67. Ward, H. S. and R. Crawford, "Wind Induced Vibrations and Building Modes," Bull. Seis. Soc. Amer., 56, 1966, 793-813.
68. Wong, H. L., "Dynamic Soil Structure Interaction," EERL 75-01, California Institute of Technology, Pasadena, California, 1975.
69. Wood, H. J., "Earthquake Response Steel Frame Building," Int. J. Earthquake Eng. and Struct. Dyn., 4, 1976, 349-377.

APPENDIX A

Enlarged Figures Showing Floor Deformations  
Measured During Forced Vibration Tests of Millikan Library

# FLOOR DEFORMATION IN THE BASEMENT OF MILLIKAN LIBRARY

N-S EXCITATION

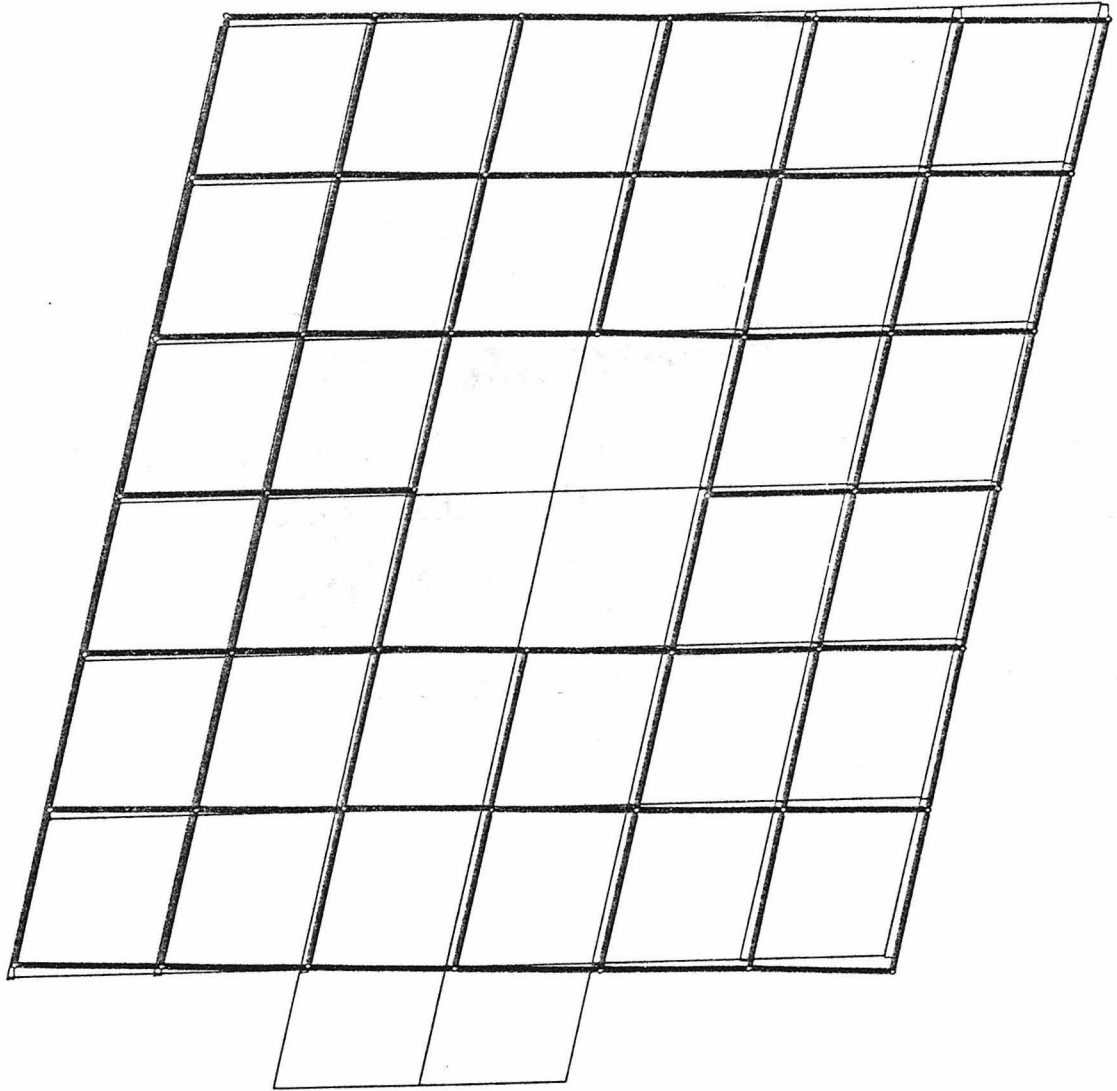
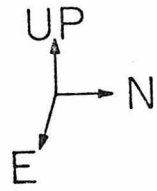


Figure A.1

DEFORMATION OF THE 2ND FLOOR  
OF MILLIKAN LIBRARY

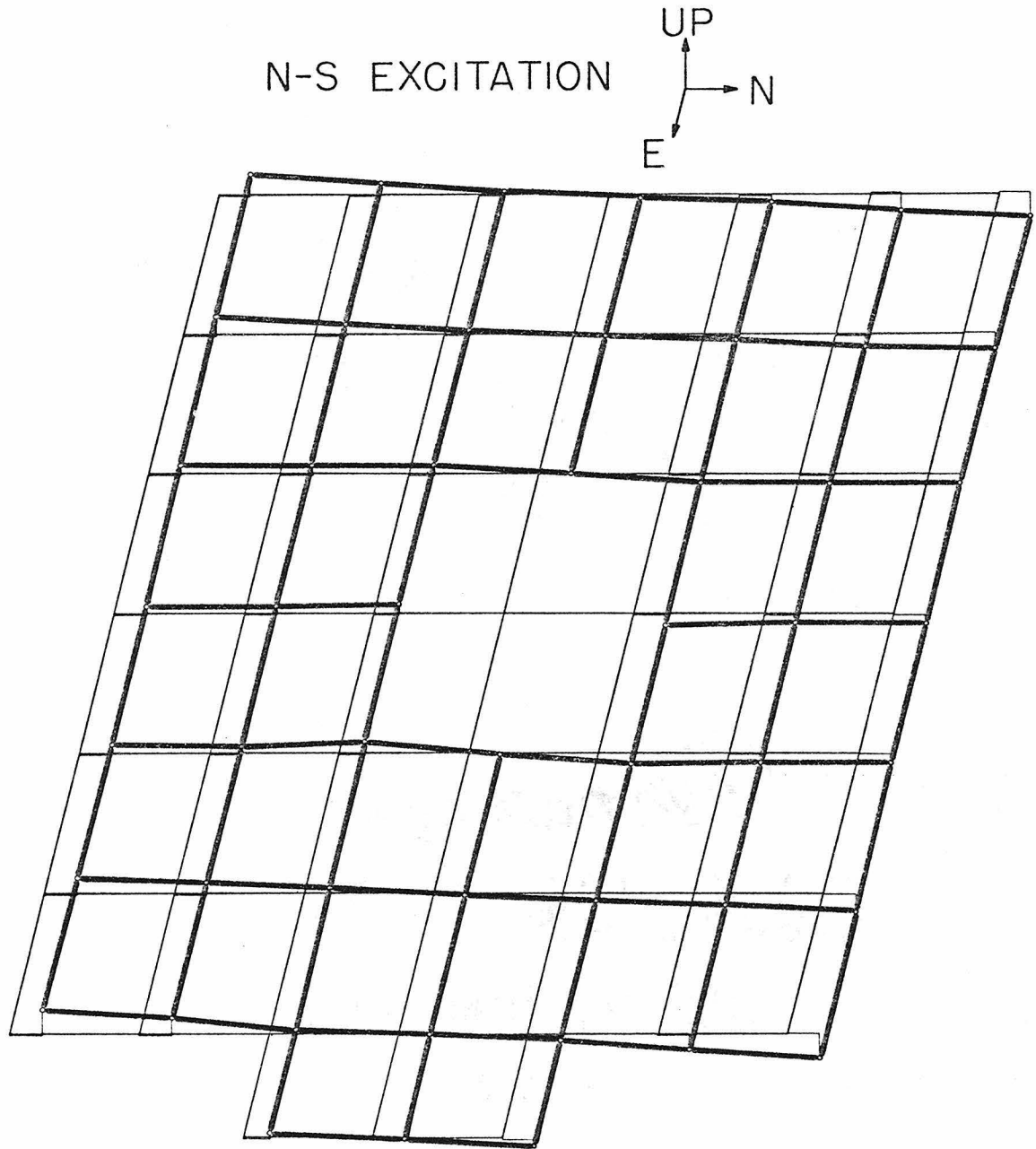


Figure A-2

DEFORMATION OF THE 4TH FLOOR  
OF MILLIKAN LIBRARY

N-S EXCITATION

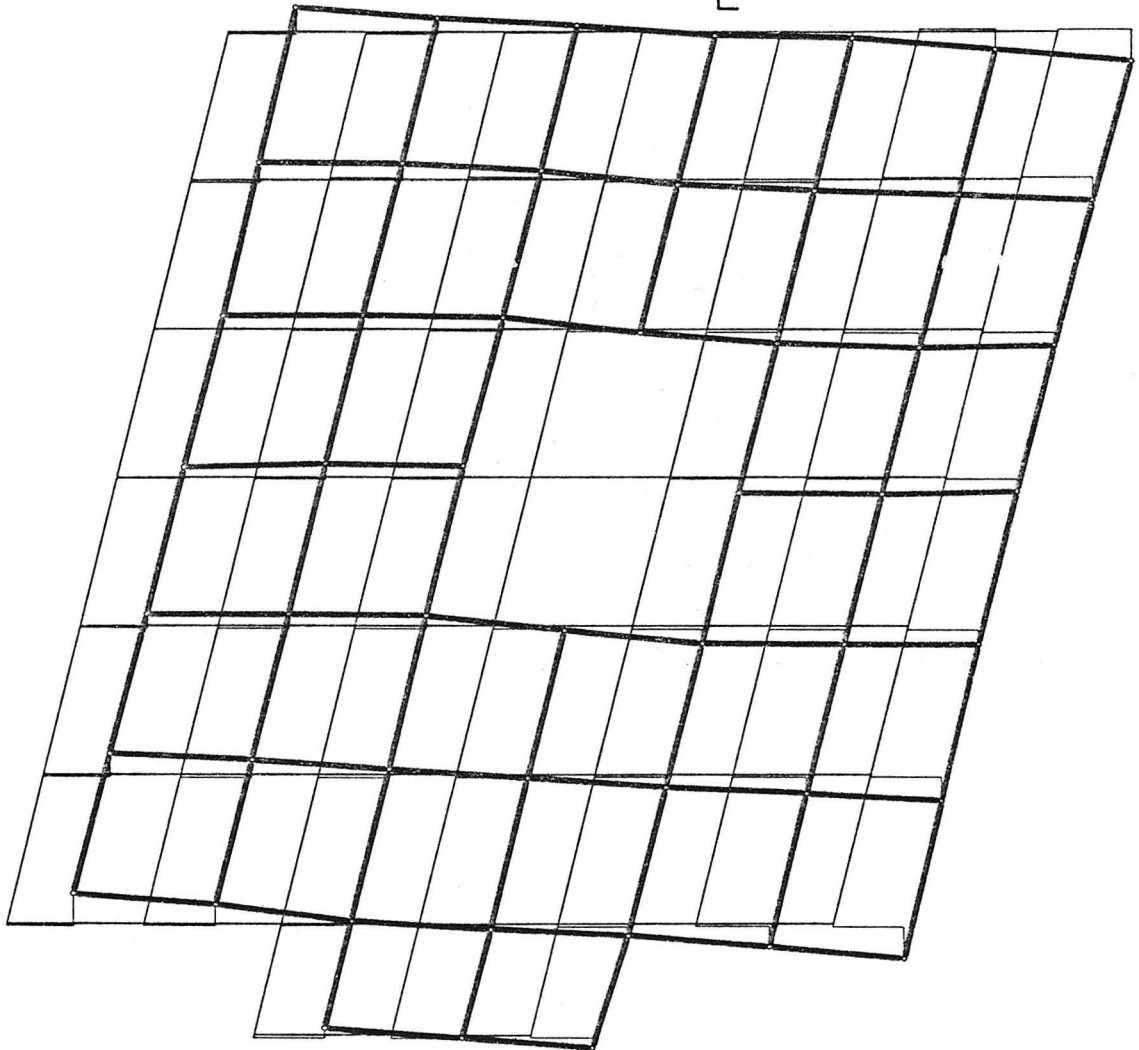
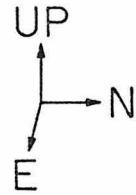


Figure A-3

DEFORMATION OF THE 6TH FLOOR  
OF MILLIKAN LIBRARY

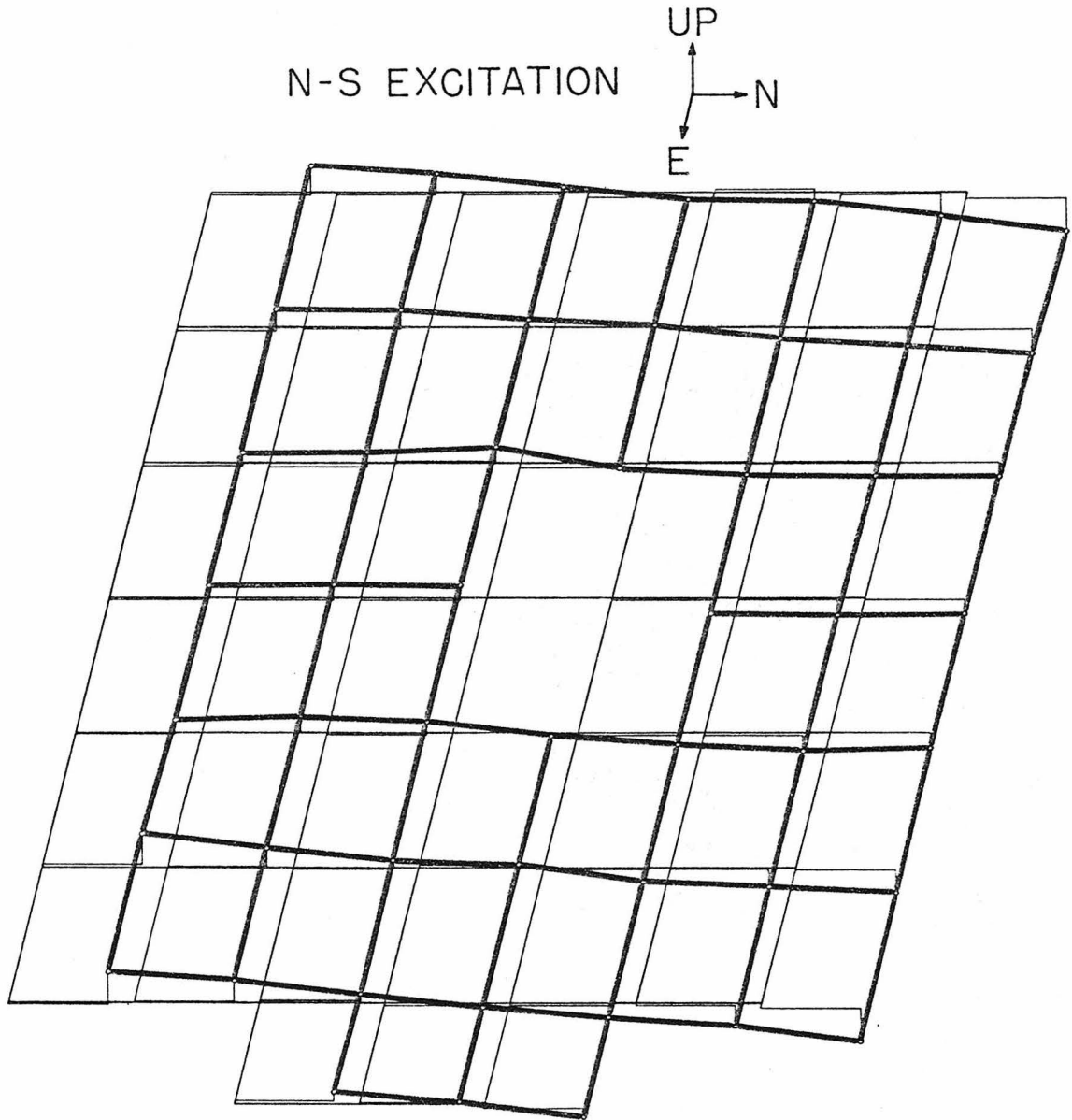


Figure A-4

DEFORMATION OF THE ROOF  
OF MILLIKAN LIBRARY

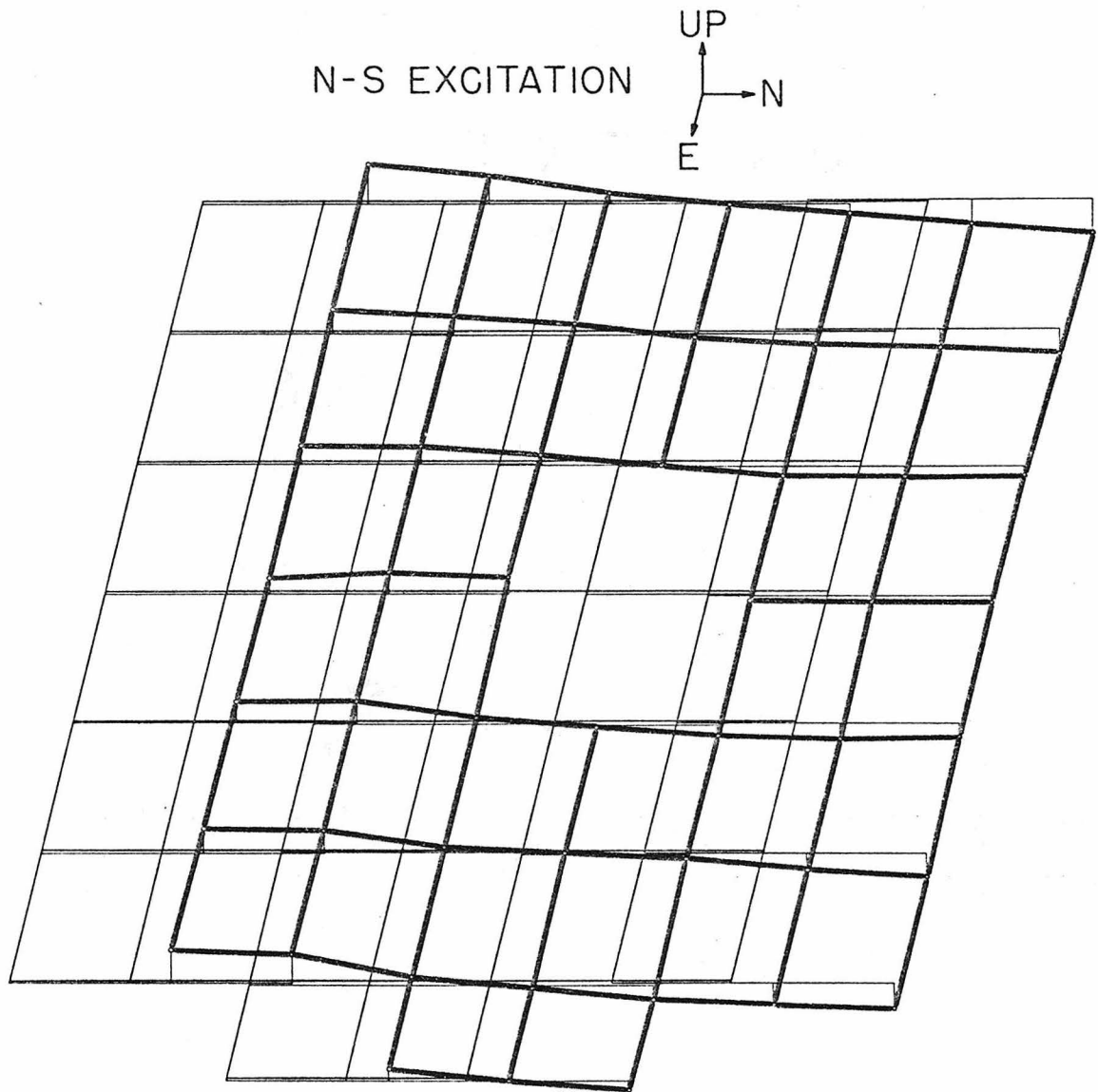


Figure A-5

FLOOR DEFORMATION IN THE BASEMENT  
OF MILLIKAN LIBRARY

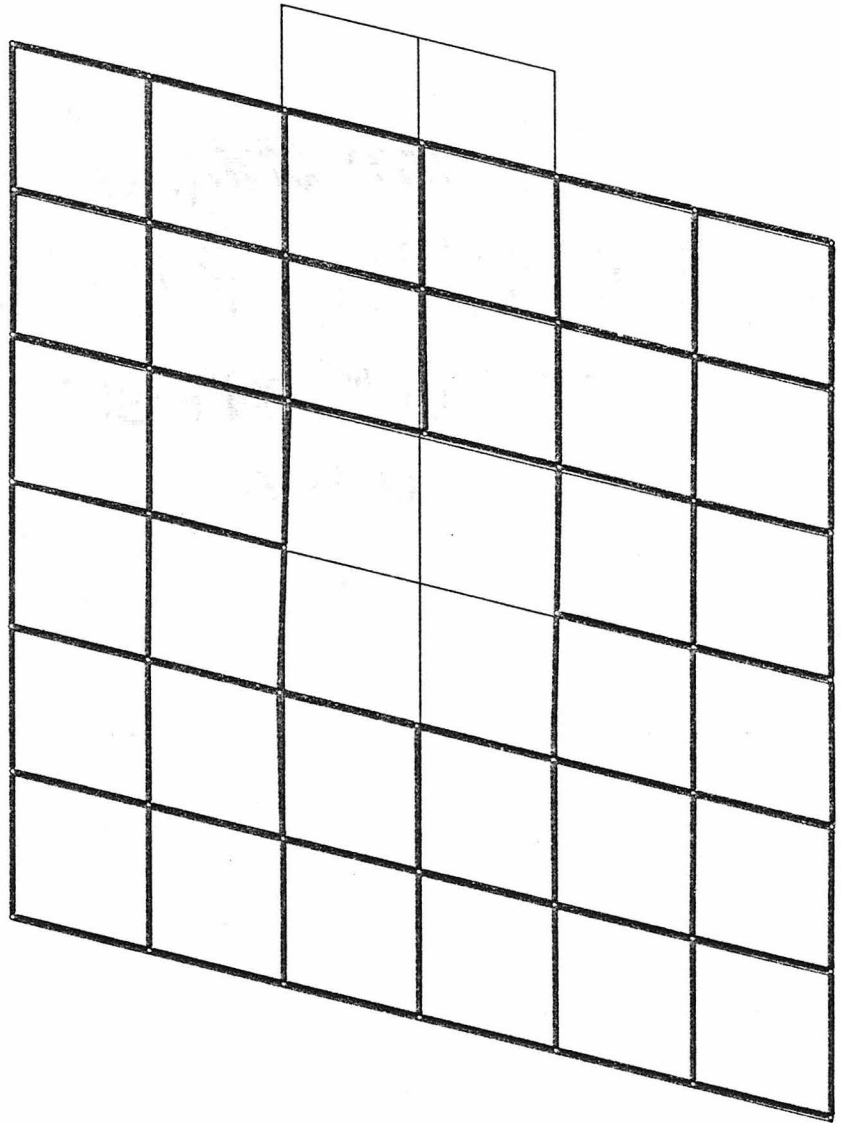


Figure A-6

DEFORMATION OF THE 2ND FLOOR  
OF MILLIKAN LIBRARY



E-W EXCITATION

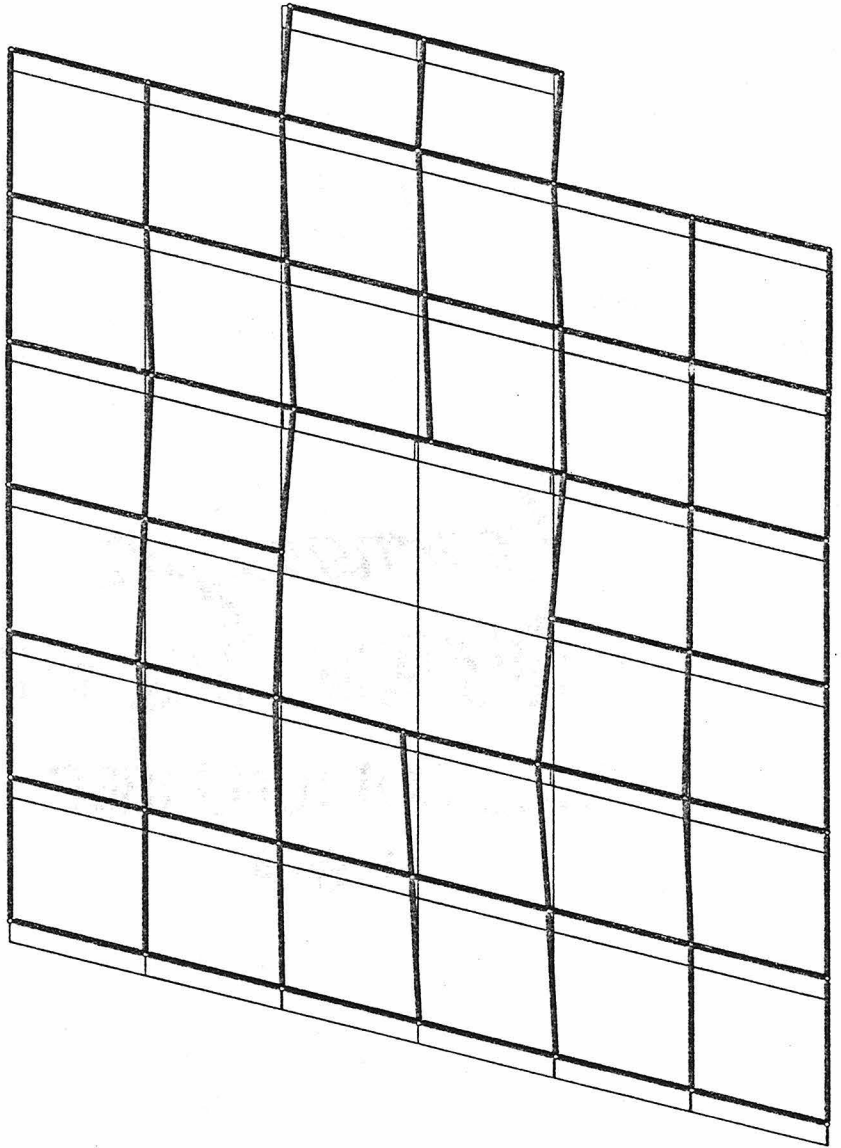


Figure A-7

DEFORMATION OF THE 4TH FLOOR  
OF MILLIKAN LIBRARY

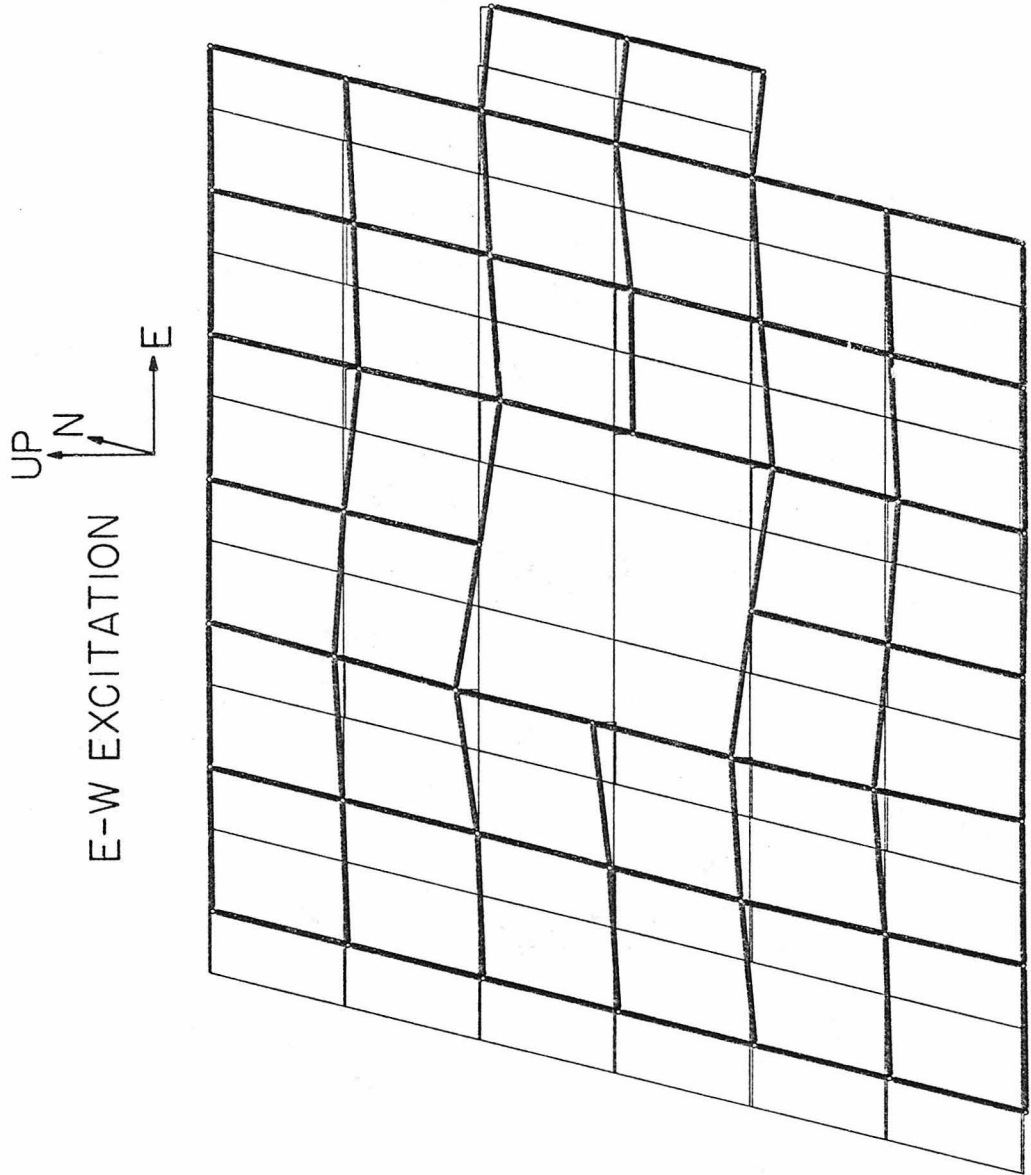


Figure A-8

DEFORMATION OF THE 6TH FLOOR  
OF MILLIKAN LIBRARY

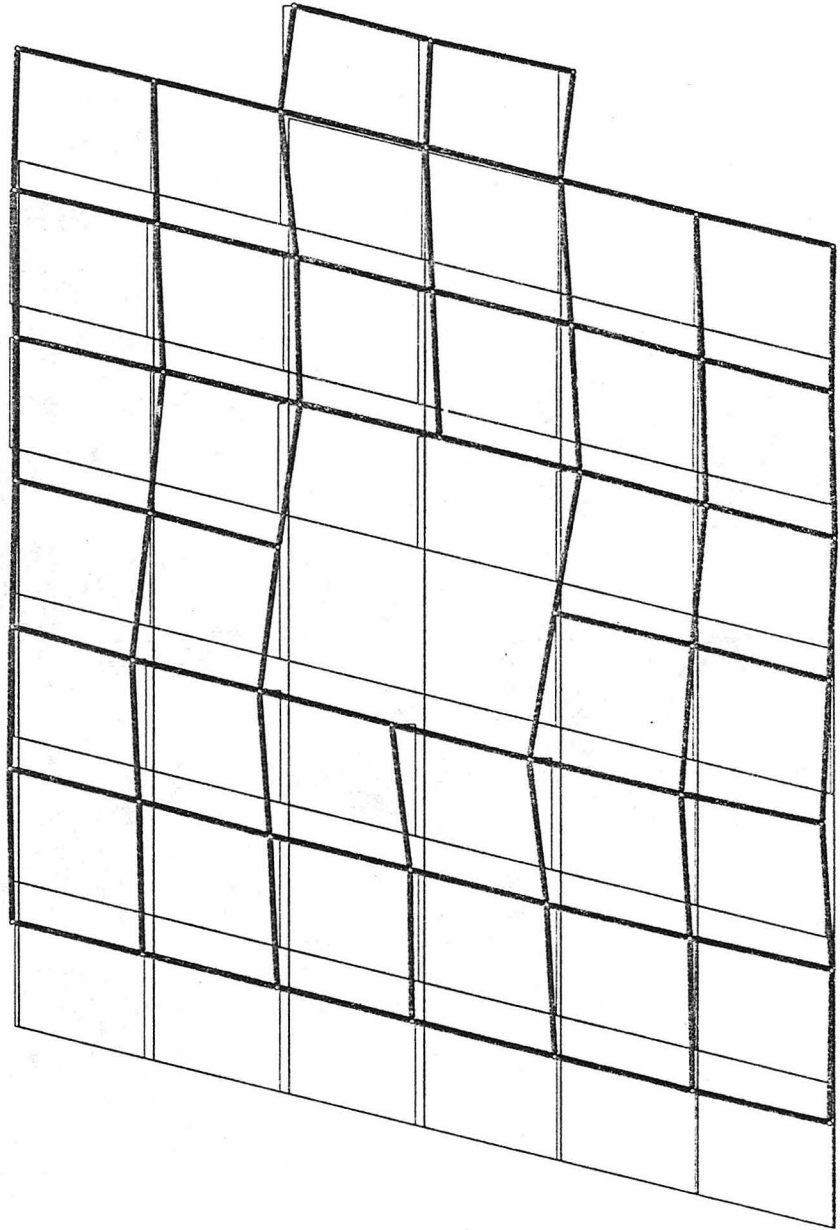


Figure A-9

DEFORMATION OF ROOF  
OF MILLIKAN LIBRARY

UP  
N  
E-W EXCITATION  
E

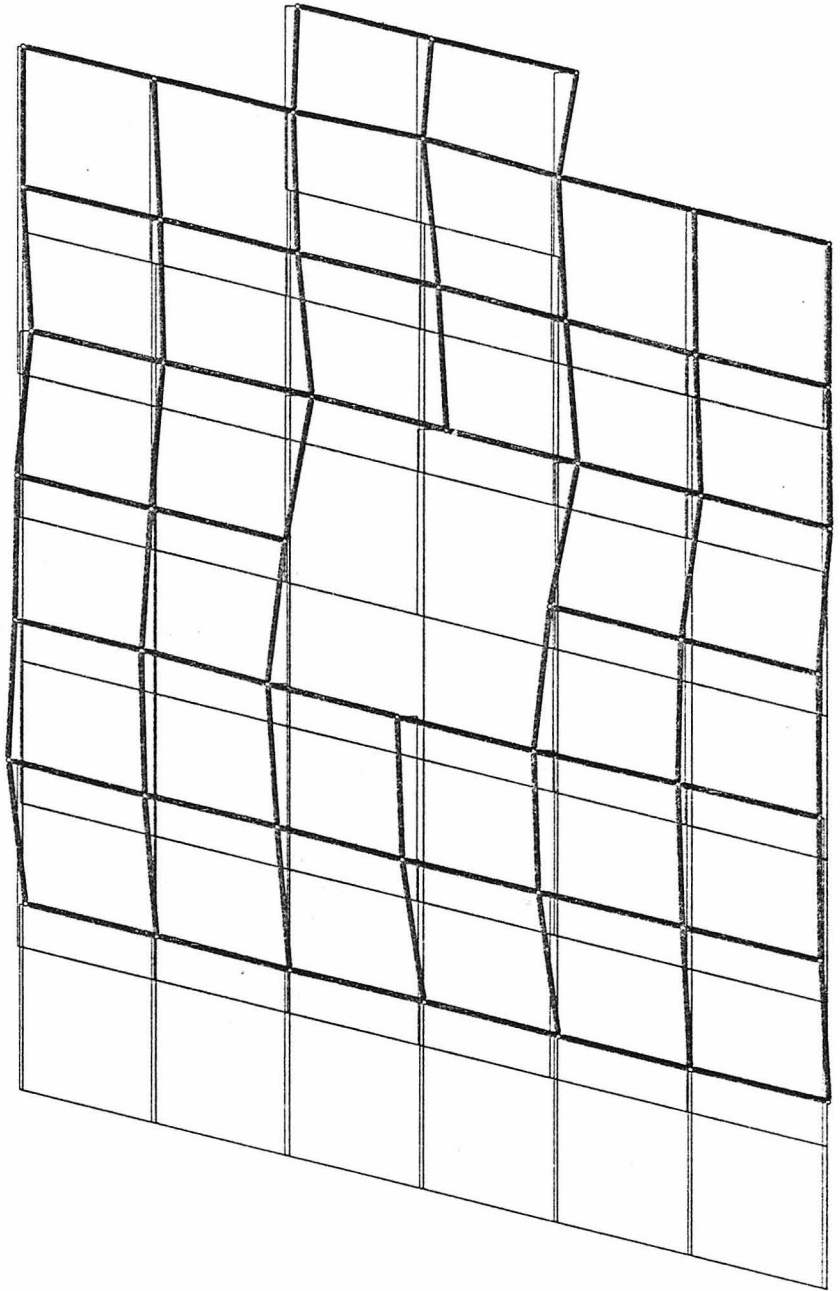


Figure A-10